Simulations of Watershed Response to Land Use and Climate Change in the Saugahatchee Creek Watershed using the WARMF Model

by

Sushban Shrestha

A thesis submitted to the Graduate Faculty of
Auburn University
in partial fulfillment of the
requirements for the Degree of
Master of Science

Auburn, Alabama
August 6, 2011

Keywords: watershed, hydrology, water quality,
land use, climate change, WARMF

Approved by

Xing Fang, Chair, Associate Professor of Civil Engineering
Jose G. Vasconcelos, Assistant Professor of Civil Engineering
Luke J. Marzen, Associate Professor of Geography

Abstract

During recent years, land surfaces have been markedly transformed with artificial land cover limiting natural forests, accompanied by urbanization. The atmospheric concentration of greenhouse gases is believed to be increasing, thereby leading to anthropogenic climate change. It is very important, from watershed management point of view, to know how these alterations would affect water resources. In this study, we have tested the ability of a watershed model WARMF to simulate flow and water quality in the Saugahatchee Creek Watershed in Alabama and applied the developed model to assess the impact due to historical land use change and potential future climate change. Surface water temperature, dissolved oxygen, total phosphorus, total nitrogen, and chlorophyll-a concentrations were simulated along with flow at the watershed outlet.

Based on model simulation, historical land use changes from 1991 to 2008 show rising pattern in nutrient levels and algal mass depleting water quality in the Saugahatchee Creek. Future climate for the 21st century, derived from HadCM3 A2 and B2 emission scenarios, were downscaled to local watershed scale for impact analysis. Surface water temperature is projected to increase, mostly in summer and dissolved oxygen concentration is projected to decrease. Both HadCM3 scenarios' output predicted decrease in flow in the 21st century. Nutrient concentration increased corresponding to low flow. These results under different land use and climate change scenarios can be useful information for watershed planning and management decision.

Acknowledgement

Two years have passed since I joined MS program at Auburn University. As I approach towards receiving my Master's Degree, I hereby take this opportunity to share my earnest gratitude to one and all for being part of this wonderful journey.

First and foremost, I owe my deepest gratitude to my advisor, Dr. Xing Fang, for his enthusiasm, inspiration, and unique ability to motivate. His mentorship has not only guided me during my graduate study, but also, to a greater extent, has sharpened the career path I am willing to follow. I would also like to extend my appreciation to my committee members Dr. Jose Vasconcelos and Dr. Luke Marzen, for their valuable insights and suggestions. I wish to especially thank Joel Herr of Systech for sharing his expertise in WARMF; Rajesh Sawant, Mac Martin, and Dr. Luke Marzen of AlabamaView for providing land cover data; Eric Reutebuch and Dr. William Deutsch of Alabama Water Watch for sharing water quality data. Thanks are due to Prof. Junqi Li for his valuable inputs to collaborated research work.

I do not want to miss this opportunity to thank all the colleagues in my department, who have contributed immensely to my professional and personal life at Auburn. A sincere thank to this great source of knowledge and friendship. Last but not least, I would like to thank my family and friends for their unwavering support throughout my education and life.

Table of Contents

List of Tables

List of Figures

List of Abbreviations

ADEM	Alabama Department of Environmental Management
ASCE	American Society of Civil Engineers
BASINS	Better Assessment Science Integrating Point and Nonpoint Sources
BMP	Best Management Practice
CASTNET	Clean Air Status and Trends Network
CCCSN	Canadian Climate Change Scenarios Network
CSTR	Continuously Stirred Tank Reactor
DEM	Digital Elevation Map
DO	Dissolved Oxygen
EISA	Energy Independence Security Act
GCM	General Circulation Model
GHG	Greenhouse Gas
GI	Green Infrastructure
GIS	Geographic Information System
GSOD	Global Summary of Day
HadCM3	Hadley centre Coupled Model, version 3
HSPF	Hydrological Simulation Program - Fortran
HUC	Hydrologic Unit Codes
IPCC	Intergovernmental Panel on Climate Change

LAI	Leaf Area Index
LID	Low Impact Development
METF	Maximum Extent Technically Feasible
NADP	National Atmospheric Deposition Program
NCAR	National Center for Atmospheric Research
NCDC	National Climatic Data Center
NCEP	National Centers for Environmental Prediction
NHD	National Hydrography Dataset
NLCD	National Land Cover Dataset
NOAA	National Oceanic and Atmospheric Administration
NRCS	National Resources Conservation Service
NSE	Nash-Sutcliffe's Efficiency
PBIAS	Percent Bias
RSR	RMSE - Standard Deviation Ratio
SCW	Saugahatchee Creek Watershed
SDSM	Statistical Downscaling Model
SRES	Special Report on Emission Scenarios
SSURGO	Soil Survey Geographic Database
SWAT	Soil and Water Assessment Tool
TMDL	Total Maximum Daily Load
TN	Total Nitrogen
TP	Total Phosphorus
USDA	United States Department of Agriculture

USEPA	United States Environmental Protection Agency
USGS	United States Geological Survey
WARMF	Watershed Analysis Risk Management Framework
WQV	Water Quality Volume
WWTP	Waste Water Treatment Plant

Chapter 1. Introduction

Background

A watershed, also referred as drainage basin or catchment, is the area of land where all of the water that is under it or drains off of it goes into a common waterway, such as a stream, reservoir, estuary, or even the ocean (USEPA 2009). A scientist geographer, John Wesley Powell defined watershed as “that area of land, a bounded hydrologic system, within which all living thing are inextricably linked by their common water course and where, as humans settled, simple logic demanded that they become part of a community.” The quantity and quality of water in a water body is directly impacted by natural or human activities in its watershed. During the recent years, rapid urbanization has lead to massive land use changes. With industrialization and population growth, the atmospheric concentrations of greenhouse gases and aerosols are believed to be increasing, thereby leading to anthropogenic climate change. Climate change, if it occurs, will cause increase in temperature, evaporation, evapotranspiration, and precipitation variability and extremes (Kundzewicz et al. 2007). These alterations will change the hydrological behavior of watershed ecosystem in physical, chemical, and biological terms.

To study the watershed response to land use change and future climate scenarios, a physically based watershed model WARMF (Watershed Analysis Risk Management

Framework; Chen et al. 2001) project was set up and applied to the Saugahatchee Creek Watershed (SCW) in Alabama. Saugahatchee Creek, which feeds on the parts of rapidly growing Auburn-Opelika metropolitan area, has been reported of two portions listed on Alabama's 303(d) list of impaired waters (discussed in Chapter 2) for nutrients and organic enrichment/dissolved oxygen according to ADEM (2009). This study focuses on simulating driving variables like flow and water temperature , together with nutrients, algal and dissolved oxygen concentrations for different land use and climate scenarios.

Scope and Objectives

Historical land use scenarios and potential future climate scenarios, inputs to the WARMF model, are not developed in this study. AlabamaView provided three Saugahatchee land use scenarios for the past decade for this study (AlabamaView 2009). Future projection of land use has not been addressed in this research study. The output from General Circulation Models (GCMs) future climate data, HadCM3 (Hadley Centre Coupled Model, version 3; Gordan et al. 2000; Pope et al. 2000) in this case, is used in this study and downscaled using SDSM (Statistical Downscaling Model; Wilby and Dawson 2007). The predictor variables derived from HadCM3 scenarios that are required for SDSM model are available for download on Canadian Climate Change Scenarios Network (CCCSN) website (CCCSN 2010).

The flow and water quality vary depending upon watershed characteristics, its geographical location, and climatic condition. The current study focuses on development of the WARMF model for the Saugahatchee Creek Watershed in Alabama. Although the quantitative results from this study may be represented for this particular watershed, the relevant knowledge about watershed processes and its response to land use change and climate change can be shared and compared with other watershed studies.

The main objectives of this study are as follows:

1. To develop the WARMF model project for the SCW, calibrate and validate flow and water quality parameters,

2. To apply the developed model to assess the impact due to historical land use change in the SCW, and

3. To apply the developed model to assess the impact due to future climate scenarios in the 21^{st} century

To accomplish the objective 1, the following tasks were completed:

1. Delineate land catchments, stream segments, and reservoirs in the SCW,

2. Prepare necessary input data, such as meteorological data, atmospheric deposition, etc. for WARMF simulation, and

3. Simulate flow and water quality, calibrate and validate the model

To accomplish the objective 2, the following tasks were completed:

1. Run the WARMF simulations using three land use scenarios as model inputs

2. Analyse the changes in modeled flow and water quality parameters using three land use change scenarios

To accomplish the objective 3, the following task were completed:

1. Downscale to local watershed scale, using statistical techniques, output from HadCM3 A2 and HadCM3 B2 future climate scenarios to generate meteorological inputs for the WARMF model,

2. Run the WARMF simulations for three allotted future time period of 2020s, 2050s, and 2080s to simulate flow and water quality based on downscaled climate scenario from (1).

3. Analyse the anomalies of the modeled flow and water quality parameters using climate change scenarios to baseline scenario (1981-2010)

In addition to these objectives, specific research questions were encountered and dealt with:

1. Is the WARMF model a viable tool to simulate flow and water quality in the SCW?

2. What difference it will bring to chlorophyll-a concentration, if we considered an impounded section as a stream instead as a reservoir?

3. What will be the effect of simulation time step on certain water quality parameters such as dissolved oxygen?

4. How will vertical stratification, if any, in a reservoir will affect dissolved oxygen concentration?

Thesis Organization

This thesis is divided into five chapters. Chapter 1 covers the background, scope, objectives, and overall thesis organization. Next three chapters, organized in journal paper format, are prepared for ASCE journal publication.

Chapter 2 documents the processes involved during WARMF project development of the Saugahatchee Creek Watershed that includes watershed delineation, preparation of model input data, model calibration and validation for flow and water quality constituents.

Next, Chapter 3 describes the application of the WARMF model developed in Chapter 2 to assess the impact on hydrology and water quality in the streams and reservoirs of the Saugahatchee Creek Watershed due to land use and climate change. In addition, development of future climate scenarios using statistical downscaling techniques are discussed in this chapter.

Chapter 4, accompanied by a preface, is a technical note submitted for publication in ASCE journal that reports 95th percentile 24-hour rainfall depths computed following the U.S. Environmental Protection Agency (USEPA) guidelines at 206 weather stations/ cities in the contiguous U.S. This chapter is independent of earlier studies in the thesis and is developed with a purpose of developing 95th percentile rainfall isohyetal map for the contiguous US. The result obtained herein may provide valuable information for engineers and designer to comply with Section 438 of EISA when federal agencies need to design, construct, and maintain stormwater management practices for development and redevelopment projects in the contiguous U.S

Lastly, Chapter 5 summarizes the project accomplishment against the set objectives. This chapter also outlines some related topics for future exploration.

References

Alabama Department of Environmental Management (ADEM). (2009). "2008 Alabama 303(d) List." *303(d) Information and Map*. <http://adem.alabama.gov/programs/water/wquality/2008AL303dList.pdf> (Aug. 12, 2009).

AlabamaView (2009). "Saugahatchee Watershed Landcover." *Saugahatchee Watershed Project,* <http://www.alabamaview.org/watershed_project.html> (Mar. 20, 2009).

Canadian Climate Change Scenarios Network (CCCSN). (2010). " HadCM3 predictors: A2(a) and B2(a) experiments." *Statistical Downscaling Input,* <http://cccsn.ca/?page=pred-hadcm3> (Sep. 21, 2010)

Chen, C. W., Herr, J. W., and Weintraub, L. (2001). "Watershed Analysis Risk Management Framework (WARMF): Update One–A decision support system for watershed analysis and total maximum daily load calculation, allocation and implementation." Publication No. 1005181. Electric Power Research Institute, Palo Alto, California.

Gordon, C., Cooper, C., Senior, C. A., Banks, H., Gregory, J. M., Johns, T. C., Mitchell, J. F. B., and Wood, R. A. (2000). "The simulation of SST, sea ice extents and ocean heat transports in a version of the Hadley Centre coupled model without flux adjustments." *Climate Dynamics*, 16(2), 147-168.

Kundzewicz, Z. W., Mata, L. J., Arnell, N. W., Doll, P., Kabat, P., Jimenez, B., Miller, K. A., Oki, T., Sen, Z., and Shiklomanov, I. A. (2007). "Freshwater resources and their management." Climate Change 2007: impacts, adaptation and vulnerability: contribution of Working Group II to the fourth assessment report of the Intergovernmental Panel on Climate Change, M. L. Parry, O. F. Canziani, J. P. Palutikof, P. J. v. d. Linden, and C. E. Hanson, eds., Cambridge Univ Press, Cambridge, UK, 173-210.

Pope, V., Gallani, M. L., Rowntree, P. R., and Stratton, R. A. (2000). "The impact of new physical paramterizations in the Hadley Centre climate model: HadAM3." *Climate Dynamics*, 16, 123-146.

U. S. Environmental Protection Agency (USEPA). (2009). "What is a watershed?" *Watersheds,* <http://water.epa.gov/type/watersheds/> (Nov. 17, 2009).

Wilby, R. L., and Dawson, C. W. (2007). "SDSM 4.2–A decision support tool for the assessment of regional climate change impacts." Lancaster University, UK.

Chapter 2. Development of WARMF Model to Study Hydrology and Water Quality in Streams and Reservoirs of the Saugahatchee Creek Watershed

Abstract

A physically based watershed model WARMF was set up for the Saugahatchee Creek Watershed in order to assess the impact on hydrology and water quality in streams and reservoirs due to land use and climate change. This paper deals with explaining the process involved during WARMF project development that includes watershed delineation, preparation of input data required for WARMF model, calibration and validation for flow and water quality constituents. Flow calibration (validation) performed using 10 years' observed daily flow displayed satisfactory model performance resulting Nash-Sutcliffe's efficiency (NSE) of 0.64 (0.56), ratio of the root mean square error to the standard deviation of measured data (RSR) of 0.60 (0.66) and percent bias (PBIAS) of -2.78% (-9.53%) . Water quality calibration and validation were performed using graphical comparison. Saugahatchee Creek WARMF project was then applied in the companion paper to assess the impact of land use change and climate change on hydrology and water quality in the watershed.

Introduction

Flow and water quality conditions in a stream or reservoir depend on not only in-stream and in-reservoir processes but also inputs of flow and water quality constituents from its surrounding and upstream watersheds. Various watershed-scale modeling efforts are made to mimic the physical, chemical, and biological processes involved during water transport from precipitation through canopy, land surfaces, soil layers, streams, and reservoirs. The output of these models under different meteorological, land use, and land management scenarios gives hydrological and water quality response of streams and reservoirs to these changes over time, and are useful for watershed management and planning.

Complex hydrological models such as AGNPS (Agricultural Nonpoint Source Pollution Model; Young et al. 1987); BASINS (Better Assessment Science Integrating point and Nonpoint Sources;(USEPA 2004); HSPF (Hydrological Simulation Program – Fortran; Johanson et al. 1980); GWLF (Generalized Watershed Loading Functions; Haith and Shoenaker 1987); SWAT (Soil and Water Assessment Tool; Arnold and Soil 1994); and WARMF (Watershed Risk Analysis Management Framework; Chen et al. 2001) have been frequently applied to study watershed hydrology in the United States (U.S.) and all over the world. A physically based, dynamic watershed model WARMF was applied in this study to the Saugahatchee Creek Watershed (SCW) for assessing hydrology and water quality impact due to land use and climate change. Although other models, discussed above, would yield similar results, WARMF was applied here for its integration of stream and one-dimensional (1-D) reservoir water quality models, user friendly graphical interface and ability to assess the impact of point and nonpoint sources with varying land use and meteorological scenarios. WARMF is also incorporated with decision support system designed to support the watershed approach analysis and Total Maximum Daily Load (TMDL) calculations. WARMF has undergone several peer reviews (Keller 2000; Keller 2001) and has been compared with other renowned models (Chen and Herr 2002; Chen et al. 2005; Neilson et al. 2003). WARMF has been applied for various practices over the years including TMDL study (Chen et al. 2000; Herr et al. 2002; Herr et al. 2003; McDonald et al. 2000; Stringfellow et al. 2009); nutrient management strategy development (NC DENR 2009; Wang et al. 2004); and watershed assessment and planning (RMC Water and Environment 2007). Very few studies have demonstrated the capacity of WARMF model for climate change and land use change impact study. Rich et al. (2005) enhanced WARMF with a module capable of constructing different climate and management scenarios and applied it to evaluate the effects of extended droughts and increased temperature on water budgets in the San Juan Basin.

In this study, WARMF project was developed for the Saugahatchee Creek Watershed in Alabama to assess land use and climate change impact. This paper deals with explaining the process involved during WARMF project development that includes watershed delineation using BASINS, preparation of model input data, model calibration and validation for flow and water quality constituents. The Saugahatchee Creek WARMF development was applied to the companion paper for assessing the impact on hydrology and water quality due to land use and climate change.

Study Area

The watershed of concern is the Saugahatchee Creek Watershed, located mostly in Piedmont region of eastern Alabama with an area of approximately 550 km^2 (Fig. 2.1). Beginning with its headwaters in Chamber and Lee counties, Saugahatchee Creek runs westward through parts of Macon and Tallapoosa counties until it enters Yates Reservoir and converges to Tallapoosa River. Two segments in the SCW are listed on the Alabama Department of Environmental Management (ADEM)'s 303 (d) list of impaired waters under the federal Clean Water Act (ADEM 2009). Pepperell branch, a tributary to Saugahatchee Creek is listed as impaired waters for nutrients and the portion of Saugahatchee Creek (Yates Reservoir Embayment) is listed for nutrients and organic enrichment/dissolved oxygen (Fig. 2.1). Table 2.1 specifies the causes and sources of impairment according to ADEM website (ADEM 2009).

Methods

Model Description

WARMF is an integrated watershed model and decision support system (DSS) having simulation models, databases, and decision support tools under one GIS-based graphical user interface, available as a public domain tool via U.S. Environmental Protection Agency (USEPA) website <http://www.epa.gov/athens/wwqtsc/html/warmf.html>. The algorithms embedded in WARMF are adapted from many well established codes such as ILWAS (Integrated Lake Watershed Acidification Study (Chen et al. 1983; Gherini et al. 1985)), ANSWERS (Areal Nonpoint Source Watershed Environmental Response Simulation (Beasley et al. 1980; Beasley and Huggins 1981)), SWMM (Storm Water Management Model (Huber et al. 1988)), and WASP (Water Quality Analysis Simulation Program (Ambrose et al. 1993)). WARMF is organized into five modules – Data, Engineering, Knowledge, TMDL and Consensus Module.

Data module provides data to engineering module for model simulations and for evaluation of model outputs. Engineering module performs mass balance, heat balance, reaction kinetics, chemical equilibrium and other calculations and returns model outputs. Knowledge module can be used to store technical documents or other useful information. Consensus module helps stakeholders make informed decisions by formulating and evaluating management alternatives. TMDL module provides a step-by-step process of calculating the total maximum daily load of pollutants entering from upstream of a water quality limited section (Chen et al. 2001; Herr et al. 2000).

WARMF represents a watershed by dividing it into a network of land catchments, stream segments, and reservoirs (Fig. 2.2). Major streams and their tributaries in a watershed are divided into different stream segments as model compartments in WARMF by land catchments. Land catchment is further divided into canopy layer, snowpack and soil layers (Fig. 2.2). Each compartment is considered as a seamlessly connected continuously stirred tank reactor (CSTR) for flow routing and mass balance calculation. WARMF simulates the hydrologic process of canopy interception, snowpack accumulation and snowmelt, infiltration through soil layers, evapotranspiration, surface runoff and groundwater exfiltration to stream segments. Canopy interception is determined as function of leaf area index (LAI), the maximum canopy interception, and available precipitation. LAI varies monthly for each land use category and is part of system coefficients of WARMF. When the precipitation is greater than canopy interception, the excess becomes throughfall. Throughfall and snowmelt fall onto the ground surface. Impervious surface will result in immediate runoff. On pervious surfaces, the water may infiltrate into the soil layers, remain on the surface (local depression storage), and flow as surface runoff. Infiltration is carried out based on physical processes in each soil layers depending upon the amount of water available for infiltration, the void space available in the layer below and the vertical infiltration rate. The lateral flow from the soil layers to adjacent catchment, river or reservoir is based on Darcy's law:

$$Q_j = K_{hj} S W Z_j \tag{2.1}$$

Where, Q_j is the lateral exfiltration from layer j; K_{hj} is the horizontal hydraulic conductivity of layer j; S is slope of the catchment; W is width of the catchment parallel to its receiving stream, or perpendicular to the direction of ground water flow; and Z_j is thickness of layer j. The final water balance is performed from the bottom layer to the top layer, one layer at a time. For each soil layer, the overall water balance is as follows,

$$V_j = V_{j0} + I_j - I_{j+1} + L_j - E_j - Q_j \tag{2.2}$$

Where, V_j is the volume of water in the soil layer j; V_{j0} is the initial volume of water in soil layer j; I_j is the infiltration to layer j; I_{j+1} is the percolation from layer j to layer $j+1$; L_j is the lateral inflow from an upstream segment; Ej is the evapotranspiration from layer j; and Q_j is lateral exfiltration from layer j. The surface water which does not infiltrate into the soil may be ponded on the surface as detention storage or it will runoff as sheet flow. The sheet flow is calculated by Manning's equation:

$$Q_s = \frac{W Z_0 S^{1/2}}{n \times 0.01^{1/3}} \tag{2.3}$$

Where, Q_s is runoff from the pervious areas (m^3/s); Z_0 is the water depth available for sheet flow; n is the Manning's roughness coefficient. Evapotranspiration depends on the available amount of water that can be transpired and the potential evapotranspiration calculated as a function of latitude according to Hargreaves (1974).

The water from the upstream stream segment is fully mixed with the water in the stream segment from previous time step and the point and nonpoint loads entering the stream segment during the time step. For each CSTR (canopy layer, soil layer, stream segment, reservoir layer, etc.), the flow continuity equation can be written based on conservation of mass:

$$\sum Q_{in} - \sum Q_{out} = \frac{dV}{dt} \tag{2.4}$$

Where, Q is the flow rate, V is the volume, subscripts *in* and *out* represents inflows and outflows respectively. The example of inflows to a stream segment will include flows from upstream stream segments, reservoirs, surrounding land catchment, soil layers, and point sources.

Heat budget and mass balance calculation are performed to calculate the water temperature and concentrations of various water quality constituents in each soil layer, stream segment, and reservoir layer (Chen et al. 2001). Dynamic mass balance and heat budget equation can be written as follows:

$$\frac{d(VC)}{dt} = \sum Q_{in} C_{in} - \sum Q_{out} C + \sum SS \tag{2.5}$$

$$\frac{d(VT)}{dt} = \sum Q_{in} T_{in} - \sum Q_{out} T + \sum SS \tag{2.6}$$

Where, V is the volume of each compartment (control volume), C is the constituent concentration, T is the temperature, Q is the flow rate, SS is the sources and sinks of the constituents, subscripts *in* and *out* represents inflows and outflows respectively.

A reservoir is further divided into about 30 horizontal layers along depth to simulate water quality in a stratified reservoir. Each layer is assumed to be horizontally mixed. When reservoir elevation rise and fall due to variations of inflow(s) and outflow(s), the model correspondingly add or delete layers. The model requires reservoir bathymetric data in the form of stage-area relationship for simulation. The reservoir flow balance is made according to the Equation (2.4).

Watershed Delineation using BASINS

The delineated watershed map with land catchments, stream segments, and reservoirs, is required for WARMF, to which input data can be given and simulation results can be viewed. The functionality of watershed delineation is available in original WARMF model (private version developed by Systech Water Resources Inc.) but deactivated in USEPA-distributed WARMF model. However, WARMF is compatible with data extraction and delineation tools of BASINS. The watershed delineation developed from BASINS 3.1 can be imported into WARMF (Systech 2005).

BASINS is a GIS-based software system developed by U. S. EPA to assist regional, states and local agencies in performing watershed analysis and examining management alternatives. It integrates a GIS, national watershed data, and state-of-the-art environmental assessment and modeling tools into one software package. The environmental assessment and modeling tool embedded in BASINS was not used here. Instead, watershed delineation tool in BASINS was utilized to delineate watershed based on digital elevation map (DEM) and river network. BASINS data download tool extracts nationally derived databases like boundaries for states and cataloging units, DEM, National Hydrography Dataset (NHD), and National Land Cover Dataset (NLCD). A BASINS project can be set up for USGS 8-digit HUC (Hydrologic Unit Codes) watershed by selecting the geographic area of interest from among the entire 48 contiguous United States.

In this study, BASINS 3.1 was utilized to delineate watershed and prepare necessary GIS layers for the WARMF model. We selected the Lower Tallapoosa Watershed which is an 8-digit HUC 03150110 watershed that contains Saugahatchee Creek Watershed (Fig. 2.3). BASINS watershed delineation tool divided the Lower Tallapoosa Watershed into 279 subwatersheds (catchments) when threshold area of 850 hectares was used. Out of 279 subwatersheds, 44 subwatersheds that drain to the Saugahatchee Creek were selected and clipped to generate catchment layer and river layer for the study watershed (Fig. 2.3). Systech (2005) provides detailed instructions and procedures of creating WARMF application using BASINS delineation tools.

The stream segments were cut off and replaced with reservoir segment where 171 ha Lake Saugahatchee and 83 ha Yates Reservoir Embayment existed. Three stream segments in place of Lake Saugahatchee and one stream segment in place of Yates Reservoir Embayment had to be deleted before these reservoir segments were imported into WARMF. The reservoir segments are shown along with 44 land catchments and 40 remaining stream segments in Fig. 2.4. Table 2.2 provides the statistical summary for areas of 44 catchments and 40 stream segments of the SCW imported to WARMF model. The catchment area was ranged from 62.0 ha (0.24 mile^2) to 4035.5 ha (15.6 mile^2). The length of stream segments was ranged from 419.8 m to 11,694.1 m. Each stream segment is a model compartment or CSTR in WARMF, therefore, large length of stream segments may prevent us to mimic variation of water quality constituents along a stream.

WARMF Model Input

WARMF requires preparation of series of input data before it can be used to simulate the watershed hydrology and water quality. The model inputs can be divided into two categories: model coefficients and time series data. Model coefficients are those parameters that describe physical, chemical and biological characteristics of the watershed. The model coefficients are further classified as catchment, river, reservoir, and system coefficients. Model coefficients are adjusted during model calibration. Time varying data such as rainfall data is time-series data. Data module manages and stores time-series data. The major time-series input data are meteorology, atmospheric deposition, and point source discharges data. Observed flow and water quality data are required for model calibration and validation. The major meteorological input categories to the model are described as follows:

Meteorological Data:

WARMF requires meteorological variables such as precipitation, minimum and maximum temperatures, mean station pressure, dew point temperature, wind speed and cloud cover for hydrology simulation. The meteorological data can be downloaded from National Climatic Data Center (NCDC) website. The daily precipitation records for a station closer to the study watershed were available since 1996 in the station near Auburn, AL (Auburn No. 2). The meteorological variables other than precipitation required for WARMF input were downloaded and extracted from the Class I weather station in Montgomery, AL (Montgomery Dannelly Field) except cloud cover data which was calculated using the formula suggested by Systech (2005):

$$dT = ABS\left[\frac{(T_{\min} + T_{\max})}{2} - T_{dew}\right] \tag{2.7}$$

(2.8)

```
If Precip = 0 then
    If dT < 4 then
        Cloud = 0.6
    Else If dT < 6 then
        Cloud = 0.3
    Else
        Cloud = 0
Else If Precip > 2 then
    Cloud =1
Else If Precip > 1 then
    Cloud = 0.9
Else
    Cloud = 0.8
End If
```

Where, T_{min} is the minimum temperature in °C , T_{max} is the maximum temperature in °C, T_{dew} is the dewpoint temperature °C, *Precip* is the precipitation in centimeters, and *Cloud* is the cloud cover. Table 2.3 shows the monthly average, standard deviation, maximum and minimum values of precipitation (from Auburn No. 2 station) along with minimum and maximum temperatures (from Montgomery Dannelly Field station) for 1997-2009 used for this study.

Land Use:

Land use describes surface characteristics of the watershed. NLCD 2001 land use data was available for Tallapoosa Basin from Alabama Cooperative Extension System (ACES) website (ACES 2009). The portion of Saugahatchee Creek Watershed was cropped using GIS tools from Tallapoosa Basin (Fig. 2.5). SCW's land use is dominated by forest, cropland, pasture and urban areas.Fig. 2.5 illustrates the distribution of land use categories in the watershed according to NLCD 2001.

GIS shapefile of land use can be imported directly into WARMF after it has been unprojected to decimal degrees (Systech 2005). When the land use shapefile is imported, WARMF automatically calculates the percentage of land use categories in each catchment. Table 2.4 shows examples of the variations in land use distributions in three catchments (catchment 11, 22, and 42 in WARMF associated with three monitoring stations) within the watershed (Fig. 2.4). Catchment 11, one of the upstream urban catchments, has higher percentage (42%) of residential area whereas Catchment 22 and Catchment 42 are mostly forest area comprising about 62% and 88% forestland (Table 2.4).

Land Application:

Nitrogen and phosphate fertilizers usage rate for cotton was used to calculate the fertilizer application rate for cropland using the following equation (NC DENR 2009):

$$A = 1.12085 \times Q \times P \quad (2.9)$$

where, A is the average annual nitrogen or phosphate application rate in kg/ha; Q is the average annual nitrogen or phosphate application rate in lbs/acre, 1.12085 being conversion factor; and P is the percentage of fertilizer used crops area from total cropland. United States Department of Agriculture (USDA) provides annual nitrogen and phosphate fertilizers usage rate (lbs/acre) for different crops including cotton in Alabama (USDA 2011). Cotton is the major crop, which makes 22% of cropland in Lee County in

Alabama, 71% are forages and rest 7% are other crops according to 1997 US Census of Agriculture (CropMAP 2010). The fertilizer application rate for cotton and other crops were considered to be equal and that from forages was assumed to be half of the rate for cotton.

The annual average fertilizer application rate for phosphate was broken down into monthly application rate with 4 kg/ha during the growing season (April - October) and 3 kg/ha for rest of the period. For nitrogen fertilizer, the total annual value was equally shared between ammonia and nitrate usage rate. Both ammonia and nitrate fertilizer application rate were used as 2.5 kg/ha during growing season and 2 kg/ha for rest of the period. The monthly fertilizer application rate for urban areas was calibrated to attain good fit between the modeled and observed nutrient concentration during water quality calibration.

Soils Data:

USDA's National Resources Conservation Service (NRCS) Soil Data Mart provides Soil Survey Geographic Database (SSURGO) soils data for each county. Lee County soils data were downloaded and three prominent soil coverage based on larger percentage coverage were Pacolet sandy loam, Cecil sandy loam and Marvyn loamy sand. Based on these soil types, soil parameters such as soil thickness, field capacity, saturation moisture, horizontal conductivity and vertical conductivity were estimated. The soil parameters were adjusted during model calibration to generate good match between modeled and observed data. The soil parameters along with other adjusted parameters for calibration are listed in Table 2.5.

Atmospheric Deposition:

WARMF requires dry and wet chemical constituents' concentration in air (μg/m^3) and rain water (mg/l) respectively. The Clean Air Status and Trends Network (CASTNET) provides dry deposition of particles over 55 site locations mostly in the eastern United States. The National Atmospheric Deposition Program (NADP) provides wet deposition concentration over 200 sites in the United States, Puerto Rico, Virgin Island, Samoa and Islands. CASTNET station GAS153 (Georgia Station, GA) is the best source for weekly dry deposition concentration and NADP station AL10 (Black Belt Research & Extension Center, AL) is the most appropriate source for weekly wet deposition concentration. The dry and wet atmospheric deposition data from these stations were extracted, processed and imported into WARMF.

Point Sources Data:

The major point source dischargers in the SCW were Auburn Northside Waste Water Treatment Plant (WWTP), Opelika Westside WWTP and West Point Stevens (Table 2.6). The loading from these point discharges for the time period 2000-2002 were available from data collected by ADEM and Auburn University (ADEM 2008) and presented in the appendices. These point sources were included as input to respective streams in the catchment map.

To extend the point sources data for the time period other than 2000-2002, 90th percentile of the loadings were calculated and used as the constant rate. The 90th percentile loading and the observed loading for three major point source dischargers during 2001-2002 period are shown in Fig. 2.6.

Observed flow:

The daily flow data can be obtained from USGS water data web site <http://waterdata.usgs.gov/nwis/sw>. For the SCW, the only available USGS station with continuous daily data is USGS 02418230 in the Saugahatchee Creek at County Road 188 near Loachapoka. The USGS daily data available from 2000 through 2009 were used for model calibration and validation. The monthly summary of daily flow data is provided in the box and whisker plot with monthly average, maximum, minimum, median, first and third quartiles (Fig. 2.7).

Observed Water Quality:

ADEM and Auburn University collected water quality data throughout the Saugahatchee Creek Watershed in 2000-2002 (ADEM 2008). The stations in the Pepperell Branch downstream of West Point Stevens (Station-16), in the Saugahatchee Creek near Loachapoka (Station-8) and in the portion of the Saugahatchee Creek entering Yates Reservoir (Yates-2 Station) were used in the study for the purpose of model calibration and validation for water quality constituents. The surface water temperature, dissolved oxygen (DO), total phosphorus (TP) and total nitrogen (TN) concentrations were the water quality parameters sampled in Station-16 and Station-8, used in our study for model calibration and validation. From Yates-2 station, the surface water temperature, DO and chlorophyll-a concentration were derived for our study.

WARMF Simulation

After completing all of the setup and importing necessary input data outlined in the previous sections, WARMF model is ready to run and simulate hydrology and water quality in the streams and reservoirs of the watershed. The simulation was performed from 1997 through 2009. The model simulation was run three years prior to the calibration period (2000 - 2009) to minimize the effect of initial unknown parameters used in the model. A daily time step was used for calibration and validation of the model. WARMF can also simulate using desired hourly time step. Hourly time step simulation can be useful to predict diurnal phenomenon. For example, in an aquatic system with high algal concentration, dissolved oxygen largely varies during day and night. Simulation using daily time steps may not be able to catch the extreme values which are very critical in context of stream and reservoir ecology. But at the same time, it should be accounted with change in model coefficients, as simulation using hourly and daily time steps do not yield identical results. If we use daily time step, constant moderate amount of light is in effect all day which is favorable for algal growth whereas if we simulate using hourly time step, during night time there is no light and during some part of day there is too much light hindering algal growth. The model coefficients can be adjusted separately for simulation using hourly or daily time steps during calibration process. The maximum algal growth rate, which is expressed “per day” was used to be 1 per day. For hourly time step, higher growth rate might have to be used to match it with observed algal concentration taking into consideration that algal growth requires ideal light condition which occur only few hours of the day. We used maximum growth rate of 2.8 per day for simulation using 1-hour time step.

Results and Discussions

Calibration Criteria

The performance of the WARMF model was evaluated using both graphical and statistical measures. Moriasi et al. (2007) recommends performance of the model can be evaluated based on three quantitative statistics, Nash-Sutcliffe efficiency (NSE), ratio of the root mean square error to the standard deviation of measured data (RSR), and percent bias (PBIAS) in addition to the graphical techniques. The recommended quantitative statistics between simulated (Y_i^{sim}) and observed (Y_i^{obs}) were computed as follows:

$$NSE = 1 - \left[\frac{\sum_{i=1}^{n} (Y_i^{obs} - Y_i^{sim})^2}{\sum_{i=1}^{n} (Y_i^{obs} - Y^{mean})^2} \right] \tag{2.10}$$

$$RSR = \frac{\sqrt{\sum_{i=1}^{n} (Y_i^{obs} - Y_i^{sim})^2}}{\sqrt{\sum_{i=1}^{n} (Y_i^{obs} - Y^{mean})^2}} \tag{2.11}$$

$$PBIAS = \left[\frac{\sum_{i=1}^{n} (Y_i^{obs} - Y_i^{sim}) \times 100}{\sum_{i=1}^{n} (Y_i^{obs})} \right] \tag{2.12}$$

The simulation of watershed model can be judged satisfactory if NSE > 0.5 and RSR ≤ 0.7 and if PBIAS is within ±25% for flow (Moriasi et al. 2007).

Saugahatchee Creek Watershed was divided into 44 catchments, 40 stream segments and 2 reservoirs. The hydrologic and water quality parameters can be assigned to these segments individually, referred as catchment coefficients, river coefficients, and reservoir coefficients in WARMF manual (Herr et al. 2000). There are another set of parameters, known as system coefficients that apply to all catchments in the watershed.

During the calibration, some of catchment, river, reservoir and system coefficients were adjusted to obtain a best fit. Although WARMF includes auto-calibration tool, manual calibration was performed prioritizing the critical parameters that are sensitive to flow and water quality. Zheng and Keller (2006) and Geza et al. (2009) have listed sensitive parameters during WARMF simulation. The adjusted model parameters for our study are listed in Table 2.5.

Flow Calibration and Validation

The observed flow daily data is available for USGS gage station in the Saugahatchee Creek near Loachapoka since 2000. The flow was calibrated for the period 2000-05 and validated for the period 2006-09 (Fig. 2.8). WARMF simulated the flow well in the Saugahatchee Creek although there are few underestimations of higher peaks. The simulation of flow resulted in NSE, RSR and PBIAS value for calibration (validation) as 0.64, 0.60 and -2.78 % (0.56, 0.66 and -9.53 %) respectively (Table 2.7).

Water Quality Calibration and Validation

Auburn University and ADEM collected water quality data in the SCW in 2000-2002 (ADEM 2008). Simulated surface water temperature, dissolved oxygen (DO), algal and nutrients concentrations from WARMF were compared to the observed data at Station 16, Station 8, and Yates-2 Station. The calibration was performed for the year 2000/01 and validation for the year 2002. As the water quality data were not collected in daily basis, water quality calibration and validation was performed based on visual comparison of simulated and observed data. Time series plots are used for visual and graphical representation. The calibration and validation results are listed according to the water quality stations as follows:

At Pepperell Branch downstream of West Point Stevens (Station 16):

Fig. 2.9 shows the time series plots of the observed and modeled surface water temperature, DO, TP and TN concentrations at Pepperell branch downstream of West Point Stevens (Station 16). The simulated surface temperature closely followed the observed temperature pattern, but seemed to overpredict temperature periodically, especially in the summer. The match between the modeled and observed DO shows few extreme observed values missing out during simulation. Fig. 2.9 shows satisfactory fit between the modeled and observed nutrient (TP and TN) concentrations.

At USGS 02418230 Station in the Saugahatchee Creek near Loachapoka:

Fig. 2.10 illustrates the time series plot of the observed and modeled surface water temperature, DO, TP and TN concentrations at USGS 02418230 Station in the Saugahatchee Creek near Loachapoka. The simulated surface water temperature closely followed the observed water temperature. For DO simulation, there were few extreme observed values, which were not well predicted. But, the overall pattern of observed and modeled values was very similar. Fig. 2.10 depicts satisfactory time series plot of observed and modeled nutrients concentration.

At Yates Reservoir Embayment:

Fig. 2.11 shows the time series plot of the observed and modeled surface DO, TP and chlorophyll-a concentrations. Chlorophyll-a and TN concentrations were well simulated. DO concentration seemed to be over predicted, which could be partly due to diurnal variation in dissolved oxygen and partly due to vertical stratification.

Chlorophyll-a and DO Simulation in Yates Reservoir Embayment

The WARMF model developed for the SCW provides two alternatives to model Yates Reservoir Embayment: (1) as a reservoir containing about 30 horizontal layers along depth and (2) a stream segment. Other popular watershed models, e.g., SWAT (Arnold and Soil 1994) and HSPF (Johanson et al. 1980), do have a pond model component but treat it as well-mixed pond and cannot simulate stratification of any water quality parameters. The modeled chlorophyll-a concentrations when Yates Reservoir Embayment is treated as a stream segment got to very low values as compared to treated as a reservoir. Reservoir, as opposed to stream segment, has calm water (slow velocities) and higher nutrient enrichment/ organic deposition that support algal growth. When Yates Reservoir Embayment was treated as a reservoir, the modeled chlorophyll-a concentration, though slightly overpredicted few observed values, showed comparable outputs whereas when treated as a stream segment the modeled chlorophyll hugely under-predicted the observed values (Fig. 2.12).

Still, model predicted DO values at Yates-2 station are very high compared to the observed values. During growing season, the modeled and observed chlorophyll-a concentration in Yates Reservoir Embayment showed higher concentration. With chlorophyll-values greater than 15 μg/l, water body is regarded eutrophic (Carlson 1977).

The studies have shown that, for eutrophic water bodies, the fluctuation of DO concentration within a day is larger (Ansa-Asare et al. 2000). DO level are increased during day time when algal photosynthesis adds oxygen to the system. When there is no light for photosynthesis during night time, algal respiration and decomposition reduces oxygen levels from the system. For long-term future analysis, the model was simulated on daily time step, from which diurnal fluctuation is not observable.

To better understand DO diurnal fluctuation at Yates-2 station, the WARMF model was set up and run using hourly time step. Fig. 2.13 shows standard deviation of surface DO from daily mean for each day for the year 2000 and 2002 simulated at Yates Reservoir Embayment using hourly time step. Surface DO standard deviation, corresponding to higher chlorophyll-a concentration in growing season, has higher values (Fig. 2.13). Simulated surface DO fluctuation during a day for five days for which observed DO values were less than 5 mg/l show the fluctuation of 2.7 mg/l at most.(Fig. 2.14) However, the modeled values at reservoir surface layer were greater than 5 mg/l.

The observed values of DO were measured at mid-depth if depth < 10ft and at 5 ft if depth ≥ 10 ft by ADEM and Auburn University (ADEM 2008). WARMF outputs the modeled time step values only at the reservoir surface for time-series plots (e.g., Fig. 2.13). Therefore, the vertical stratification, if any, may provide better understanding for DO simulation. Unlike stream segment as a CSTR, reservoir is divided into about 30 horizontal layers in WARMF to simulate stratification. Usually, the upper layers known as epilimnion, close to surface have tendency to be mixed and get aerated but the deeper hypolimnion, in case of stratified reservoir, possess diminished oxygen levels. For the same five days (observed DO<5mg/l), the vertical profiles of simulated DO were plotted with 5 ft line drawn to scale (Fig. 2.15). Simulated DO at 5 ft are all less than surface DO except on September 26, 2002 when fall overturn resulted well mixed profile. Simulated DO values got the lowest as 2.6 mg/l near reservoir bottom.

These results show that temporal variation of DO during a day in algal abundance (Fig. 2.13 and Fig. 2.14) and spatial (vertical) variation of DO (Fig. 2.15) in a stratified reservoir could be reason for DO mismatch between observed and modeled values at Yates-2 station (Fig. 2.11).

Summary

Saugahatchee Creek WARMF project was set up in order to assess the impact due to land use and climate change on hydrology and water quality in the watershed. The calibration and validation was performed based on the best available data in the watershed. The flow calibration was done using 2000-2005 observed flow, and validated using data from 2006-2009 available at the USGS gauge station located in the Saugahatchee Creek near Loachapoka. The water quality parameters were calibrated and validated at three stations where ADEM and Auburn University collected water quality data for 2000-2002. By evaluating model performance criteria and visual inspection of time series plot, the calibration and validation results were observed to be satisfactory enough for its further application.

As with all watershed models, there are inherent model limitations associated with WARMF. The simplistic ground-water approach in WARMF does not thoroughly simulate complex ground-water aquifers. Each stream segment is a model compartment or CSTR in WARMF, therefore, large length of stream segments may prevent us to mimic variation of water quality constituents along a stream.

References

Alabama Cooperative Extension System (ACES). (2009). “Land Use and Land Cover Data”. *Alabama GIS Data Distribution*. Alabama Cooperative Extension System. < http://www.aces.edu/waterquality/gis_data/>. (Apr. 30, 2009).

Alabama Department of Environmental Management (ADEM). (2008). "Final total maximum daily load: Nutrients & OE/DO. Pepperell branch AL03150110-0201-700 Nutrients; Sougahatchee Creek Embayment (Yates Reservoir) AL03150110-0204-101 Nutrients & OE/DO.", Alabama Department of Environmental Management, Montgomery, AL.

Alabama Department of Environmental Management (ADEM). (2009). “2008 Alabama 303(d) List.” *303(d) Information and Map*. Alabama Department of Environmental Management <http://adem.alabama.gov/programs/water/wquality/2008AL303dList.pdf> (Aug. 12, 2009).

Ambrose, R., Wool, T., and Martin, J. (1993). "WASP 5, The Water Quality Analysis Simulation Program Version 5.00." *ASCI Corporation, Athens, Georgia*.

Ansa-Asare, O. D., Marr, I. L., and Cresser, M. S. (2000). "Evaluation of modelled and measured patterns of dissolved oxygen in a freshwater lake as an indicator of the presence of biodegradable organic pollution." *Water Research*, 34(4), 1079-1088.

Arnold, J. G., and Soil, G. (1994). *SWAT (Soil and Water Assessment Tool)*, Grassland, Soil and Water Research Laboratory, USDA, Agricultural Research Service.

Beasley, D., Huggins, L., and Monke, E. J. (1980). "ANSWERS: A model for watershed planning."

Beasley, D. B., and Huggins, L. F. (1981). "ANSWERS, areal nonpoint source watershed environment response simulation: user's manual."

Carlson, R. E. (1977). "A trophic state index for lakes." *Limnology Oceanography*, 22(2), 361-369.

Chen, C. W., Gherini, S. A., Hudson, R., and Dean, J. (1983). "The Integrated Lake-Watershed Acidification Study. Volume 1: Model principles and application procedures." *Electric Power Research Institute report EA-3221, Palo Alto, California, USA*.

Chen, C. W., and Herr, J. W. (2002). "Comparison of BASINS and WARMF models: Mica Creek watershed." *Technial Rep. No. 1005344*, Electric Power Research Institute, Palo Alto, CA.

Chen, C. W., Herr, J. W., Goldstein, R. A., Ice, G., and Cundy, T. (2005). "Retrospective comparison of watershed analysis risk management framework and hydrologic simulation program Fortran applications to Mica Creek watershed." *Journal of Environmental Engineering*, 131, 1277.

Chen, C. W., Herr, J. W., and Weintraub, L. (2001). "Watershed Analysis Risk Management Framework (WARMF): Update One–A decision support system for watershed analysis and total maximum daily load calculation, allocation and implementation. Publication No. 1005181." *Electric Power Research Institute, Palo Alto, California*.

Chen, C. W., Loeb, C., and Herr, J. W. (2000). "Adaptation of WARMF to Calculate TMDL for Chartiers Creek Watershed in Pennsylvania." Final Rep. to USEPA Region 3, Philadelphia, PA and The Chartiers Creek Watershed TMDL Stakeholder Group, Pittsburgh, PA.

CropMAP (2010). "Alabama Cropmap Lee County." *A New Crop Information System for Alabama*. Purdue University. Center for New Corps & Plants Products. <http://www.hort.purdue.edu/newcrop/cropmap/alabama/counties/lee.html> (Mar. 2, 2011).

Geza, M., Poeter, E. P., and McCray, J. E. (2009). "Quantifying predictive uncertainty for a mountain-watershed model." *Journal of Hydrology,* 376,(1-2), 170-181.

Gherini, S., Mok, L., Hudson, R., Davis, G., Chen, C., and Goldstein, R. (1985). "The ILWAS model: formulation and application." *Water, Air, & Soil Pollution*, 26(4), 425-459.

Haith, D. A., and Shoenaker, L. L. (1987). "Generalized watershed loading functions for stream flow nutrients." *JAWRA Journal of the American Water Resources Association*, 23(3), 471-478.

Hargreaves, G. H. (1974). "Estimation of potential and crop evapotranspiration." *Transcations ASAE,* Vol. 17, 701-704.

Herr, J., Weintraub, L., and Chen, C. (2000). "User's Guide to WARMF: Documentation of Graphical User Interface." *EPRI. Palo Alto, CA. Report EP-P2346/ C*, 1054.

Herr, J. W., Chen, C. W., Goldstein, R. A., and and, J. N. B. "A Tool for Sediment TMDL Development on Oostanaula Creek." *Total Maximum Daily Load (TMDL) Environmental Regulations: Proceedings of the March 11-13, 2002 Conference*, Fort Worth, TX.

Herr, J. W., Chen, C. W., Goldstein, R. A., Herd, R., and Brown, J. M. (2003). "Modeling acid mine drainage on a watershed scale for TMDL calculations." *JAWRA Journal of the American Water Resources Association*, 39(2), 289-300.

Huber, W. C., Dickinson, R. E., and Barnwell Jr, T. O. (1988). "Storm water management model; version 4." *Environmental Protection Agency, United States*.

Johanson, R. C., Imhoff, J. D., and Davis, H. H., Jr. (1980). "Users manual for hydrological simulation program - Fortran (HSPF)." Environmental Research Laboratory, US Environmental Protection Agency, Athens, GA.

Keller, A. (2000). "Peer Review of the Watershed Analysis Risk Management Framework (WARMF)–An evaluation of WARMF for TMDL applications by independent experts using USEPA guidelines." *EPRI, Palo Alto, CA., Report*, 1000252.

Keller, A. (2001). "Peer Review of the Acid Mine Drainage Module of the Watershed Analysis Risk Management Framework (WARMF)–An evaluation of WARMF/AMD using USEPA guidelines." *Electric Power Research Institute, Palo Alto, CA, Technical Report*.

McDonald, S., Bhimani, S., Weintraub, L., Herr, J., Chan, C., and Dennis, G. (2000). "Decision Support Process for Truckee River Watershed Management." Watershed Management & Operations Management 2000, ASCE, Fort Collins, CO.

Moriasi, D. N., Arnold, J. G., Van Liew, M. W., Bingner, R. L., Harmel, R. D., and Veith, T. L. (2007). "Model Evaluation Guidelines for Systematic Quantification of Accuracy in Watershed Simulations." *Transactions of the ASABE*, 50(3), 885-900.

NC DENR. (2009). "Falls Lake Watershed Analysis Risk Management Framework (WARMF) Development: Final Report." N. C. Department of Environment and Natural Resources, Raleigh, NC.

Neilson, B., Horsburgh, J., Stevens, D., Matassa, M., Brogdon, J., and Spackman, A. (2003). "Comparison of Complex Watershed Models ‘Predictive Capabilities: EPRI‘s Watershed Analysis Risk Management Framework WARMF vs. USEPA‘s Better Assessment Science Integrating Point and Nonpoint Sources BASINS/WinHSPF." *Final Rep. Prepared for Utah Water Research Laboratory, Utah State Univ., Logan, Utah*.

Rich, P. M., Weintraub, L. H., Chen, L., and Herr, J. "Climate Change Impacts on Hydrology and Water Management of the San Juan Basin." *American Geophysical Union, Fall Meeting 2005*, 1054.

RMC Water and Environment. (2007). "Upper Mokelumne River Watershed Assessment and Planning Project." Upper Mokelumne River Watershed Authority, Oakland, CA.

Stringfellow, W., Herr, J., Litton, G., Brunell, M., Borglin, S., Hanlon, J., Chen, C., Graham, J., Burks, R., and Dahlgren, R. (2009). "Investigation of river eutrophication as part of a low dissolved oxygen total maximum daily load implementation." *Water Science & Technology*, 59(1), 9-14.

Systech (2005). "Creating a WARMF 6.1 Application Using a BASINS 3.1 Delineation: A User's Guide." Systech Water Resources, Inc., Walnut Creek, CA.

USDA (2011). “Fertilizer use - cotton.” *Fertilizer Use and Price*. U.S. Department of Agriculture. <http://www.ers.usda.gov/Data/FertilizerUse/> (Mar. 2, 2011).

USEPA. (2004). "Better Assessment Science Integrating point and Nonpoint Sources (BASINS) Version 3.1: User's Manual." *EPA-823-C-04-004*, United States Environmental Protection Agency.

Wang, P., Shariq, L., Montague, L., Kwaan, R., and Kella, V. (2004). "Developing a Nutrient Management Plan for the Napa River Watershed." Donald Bren School of Environmental Science and Management, University of California, Santa Barbara, CA.

Young, R. A., Onstad, C. A., Bosch, D. D., and Anderson, W. P. (1987). *AGNPS, agricultural non-point-source pollution model: A watershed analysis tool*, U.S. Department of Agriculture (USDA), Agricultural Research Service, Report No. 35. Washington, D.C.

Zheng, Y., and Keller, A. A. (2006). “Understanding parameter sensitivity and its management implications in watershed-scale water quality modeling.” *Water Resources Research,* 42(5), W05402.

Table 2.1 2008 ADEM 303(d) List of Impaired Waters in the Saugahatchee Creek Watershed

Water body name	County	Size	Uses	Causes	Sources
Pepperell Branch	Lee	6.67 miles (10.73 km)	Fish & Wildlife	Nutrients	Industrial
Saugahatchee Creek (Yates Reservoir Embayment)	Tallapoosa	203.78 acres (82.47 ha)	Public Water Supply, Swimming, Fish & Wildlife	Nutrients, Organic Enrichment	Industrial, Municipal, Non-irrigated crop production, Pasture grazing

Table 2.2 Statistical Summary for Areas of 44 Catchments and Lengths of 40 Stream Segments of the Saugahatchee Creek Watershed Imported to WARMF Model

	Catchment Area (ha)	Stream Segments Length (m)
Average	1263.9	3616.4
Standard Deviation	942.8	2820.6
Maximum	4035.5	11694.1
Minimum	62.0	419.8
75th percentile	1866.2	4922.4
50th percentile	1120.0	2753.1
25th percentile	268.1	1483.6

Table 2.3 Monthly Average, Standard Deviation, Maximum, and Minimum Values of Meteorological Variables for 1997-2009 Period Imported into WARMF Model for the Saugahatchee Creek Watershed

	Precipitation[1]				Minimum Temperature[2]				Maximum Temperature[2]			
	Ave	Stdev	Max	Min	Ave	Stdev	Max	Min	Ave	Stdev	Max	Min
J	3.35	8.09	50.80	0	2.59	6.40	17.20	-11.10	16.30	5.82	28.30	1.10
F	4.27	10.48	63.50	0	3.97	5.46	17.80	-8.90	18.19	5.17	27.20	5.60
M	5.06	14.85	136.14	0	7.58	5.24	20.60	-7.80	22.53	4.87	31.70	4.40
A	3.89	11.80	104.65	0	10.85	4.62	21.70	-0.60	25.82	3.68	34.40	13.00
M	3.10	8.91	83.57	0	15.66	3.78	23.30	5.60	29.66	2.83	35.00	21.70
J	4.77	11.44	76.20	0	20.04	2.44	26.70	11.70	32.77	2.76	38.30	23.90
J	3.70	9.64	103.12	0	21.83	1.51	25.60	15.00	33.82	2.21	40.00	26.70
A	3.37	9.23	89.92	0	21.66	1.90	26.10	14.40	33.98	2.58	41.10	26.10
S	2.98	8.87	84.58	0	18.80	3.77	25.00	6.00	31.35	2.76	37.20	21.10
O	2.85	9.80	71.12	0	12.02	5.74	23.00	-1.00	26.72	4.13	33.30	12.80
N	3.73	11.52	115.57	0	6.25	5.62	21.10	-6.10	21.62	4.49	31.10	7.80
D	4.00	9.85	82.55	0	2.70	5.86	18.30	-9.40	16.85	5.26	27.80	2.80

[1] derived from Auburn No. 2 Station
[2] derived from Montgomery Dannelly Field Station

Table 2.4 Land Use Distribution in Percentage for Three Catchments Containing Flow/Water Quality Monitoring Stations in the Saugahatchee Creek Watershed

Land Use Categories	Catchment 11 (Station-16)	Catchment 22 (Station-8)	Catchment 42 (Yates-2)
Deciduous Forest	18.75	32.20	23.05
Coniferous Forest	14.08	26.53	64.29
Mixed Forest	2.29	2.86	0.47
Cropland/Pasture	5.41	15.56	2.26
Rangeland	3.79	17.90	4.13
Wetland	0.20	3.07	0.73
Barren	0.91	0.09	0.11
Residential	42.31	1.22	1.17
Comm./Industrial	11.78	0.05	0.00
Water	0.49	0.54	3.79
TOTAL	100.00	100.00	100.00

Table 2.5 Calibrated Parameters of WARMF Model for the Saugahatchee Creek Watershed

Parameters	Units	Literature Range[1]	Calibrated Value
Precipitation Weighting Factor	-	0.5 - 1.5	0.74
Evaporation Magnitude	-	0.6 - 1.4	0.91
Evaporation Skewness	-	0.6 - 1.4	0.9
Number of Soil Layers	-	1 - 5	3
Thickness of Soil Layers	cm	> 0	8 – 79
Saturation Moisture	-	0.2 - 0.6	0.35 – 0.45
Field Capacity	-	0 - 0.4	0.18 - 0.31
Initial Moisture	-	0 - 0.6	0.25
Horizontal Conductivity	cm/day	> 0	3600 – 5600
Vertical Conductivity	cm/day	> 0	1800 – 2800
Aeration Factor	/day	0.2 - 1	0.5
Sediment Oxygen Demand	$g/m^2/day$	0.1 – 2	0.8 – 2

[1] From Herr et al. (2001)

Table 2.6 List of Major Point Source Dischargers in the Saugahatchee Creek Watershed

	Facility Name	Type	Latitude	Longitude	Discharge (MGD)
1	Auburn Northside	Sewerage System	32.6306	-85.5426	1.6 (0.07 m^3/s)
2	Opelika Westside	Sewerage System	32.6607	-85.4505	4.0 (0.18 m^3/s)
3	West Point Stevens	Process Water (Industrial)	32.6294	-85.4181	1.6 (0.07 m^3/s)

Table 2.7 Model Performance for Flow Simulation during Calibration and Validation Period

Statistical Measure	Recommended Values[1]	Calibration (2000-2005)	Validation (2006-2009)
NSE	> 0.5	0.64	0.56
RSR	≤ 0.7	0.60	0.66
PBIAS	± 25%	-2.78%	-9.53%

[1] Based on Moriasi et al. (2007)

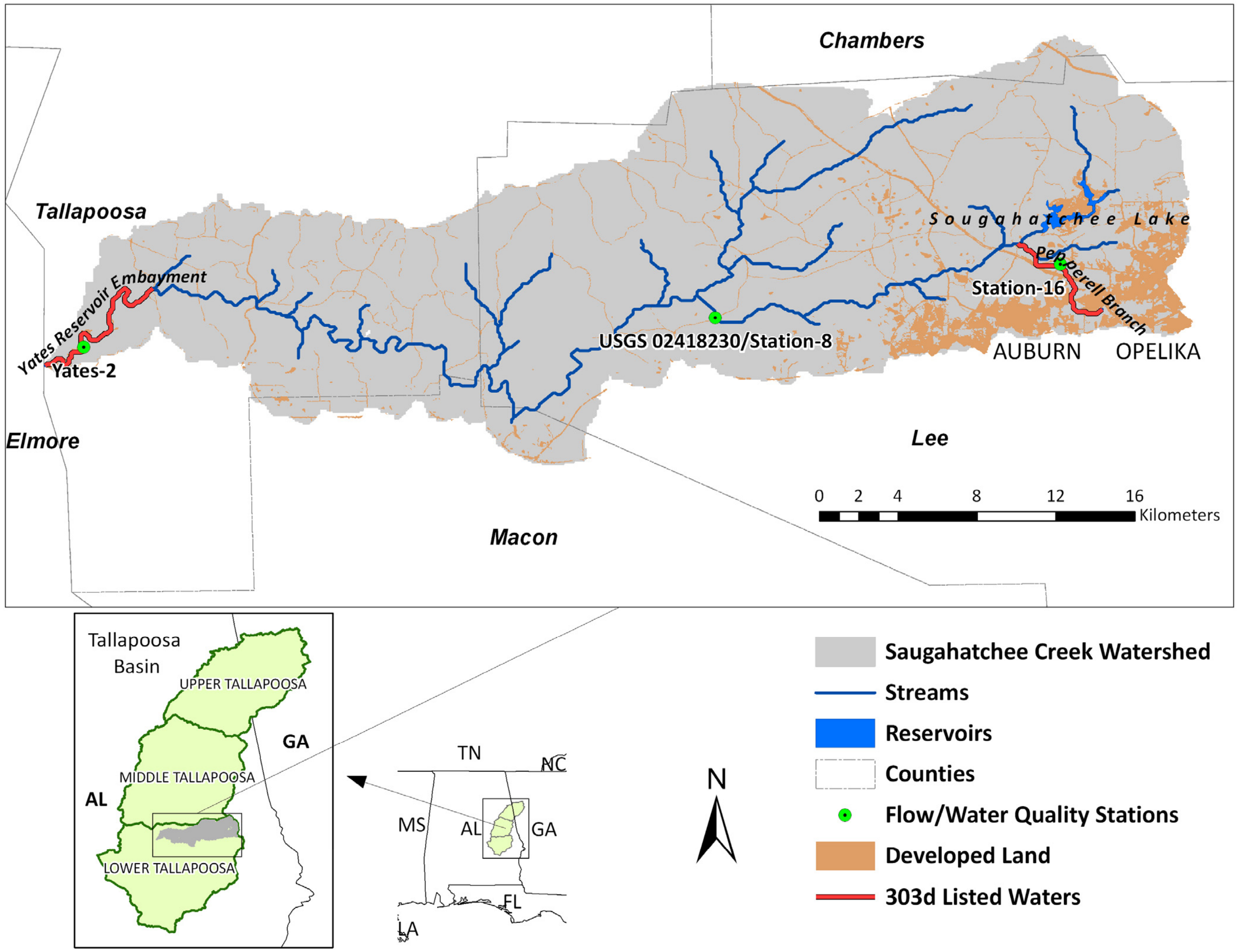

Fig. 2.1 Location map of the Saugahatchee Creek Watershed including surrounding counties and locations of three flow and water quality stations

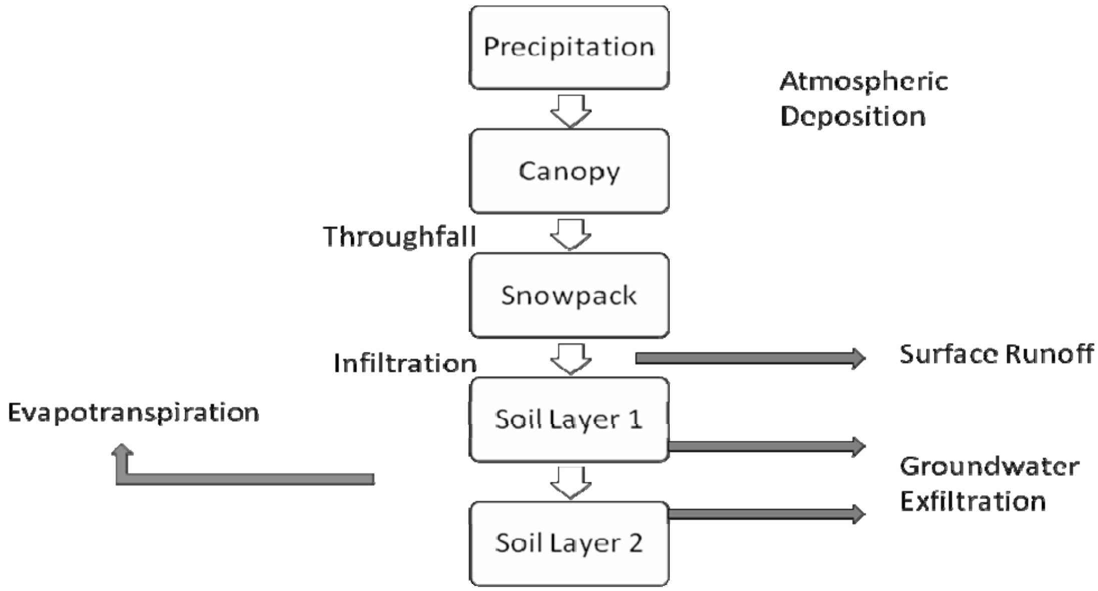

Fig. 2.2 Definition sketch for the compartments of a catchment in WARMF model (Chen et al. 2001)

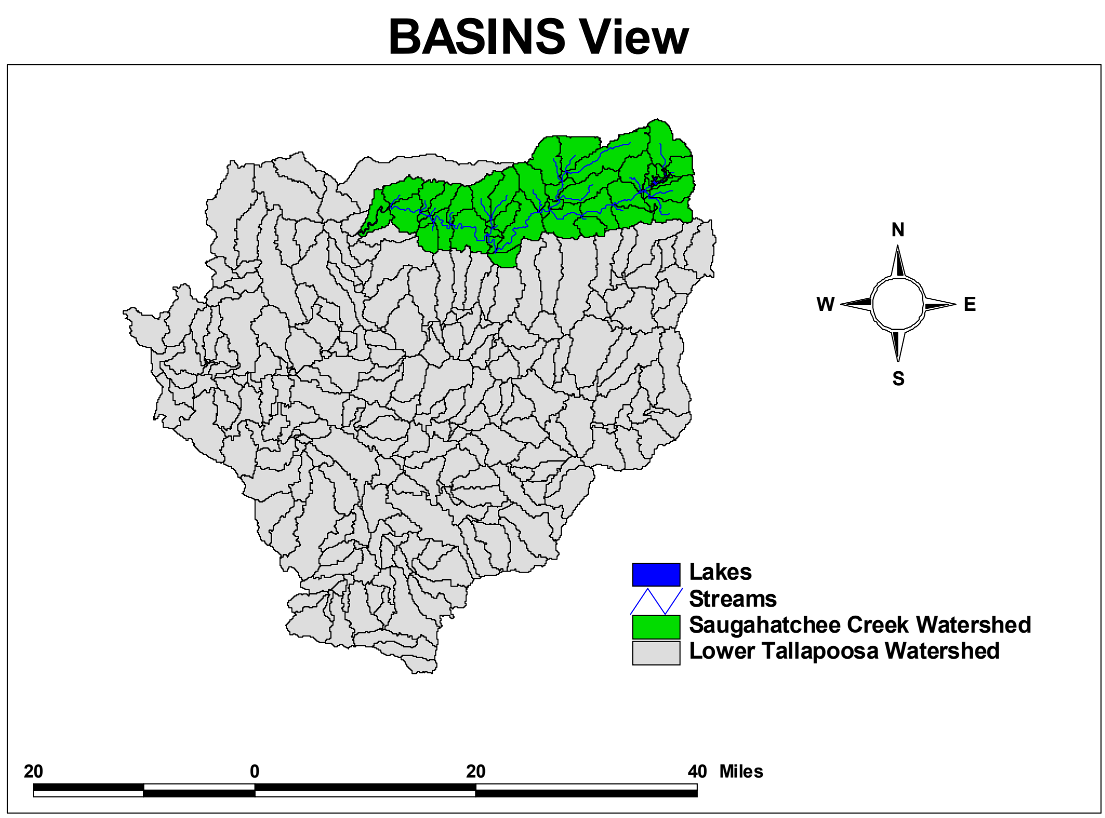

Fig. 2.3 Selection of the Saugahatchee Creek Watershed from the Lower Tallapoosa Watershed (HUC 03150110) in BASINS

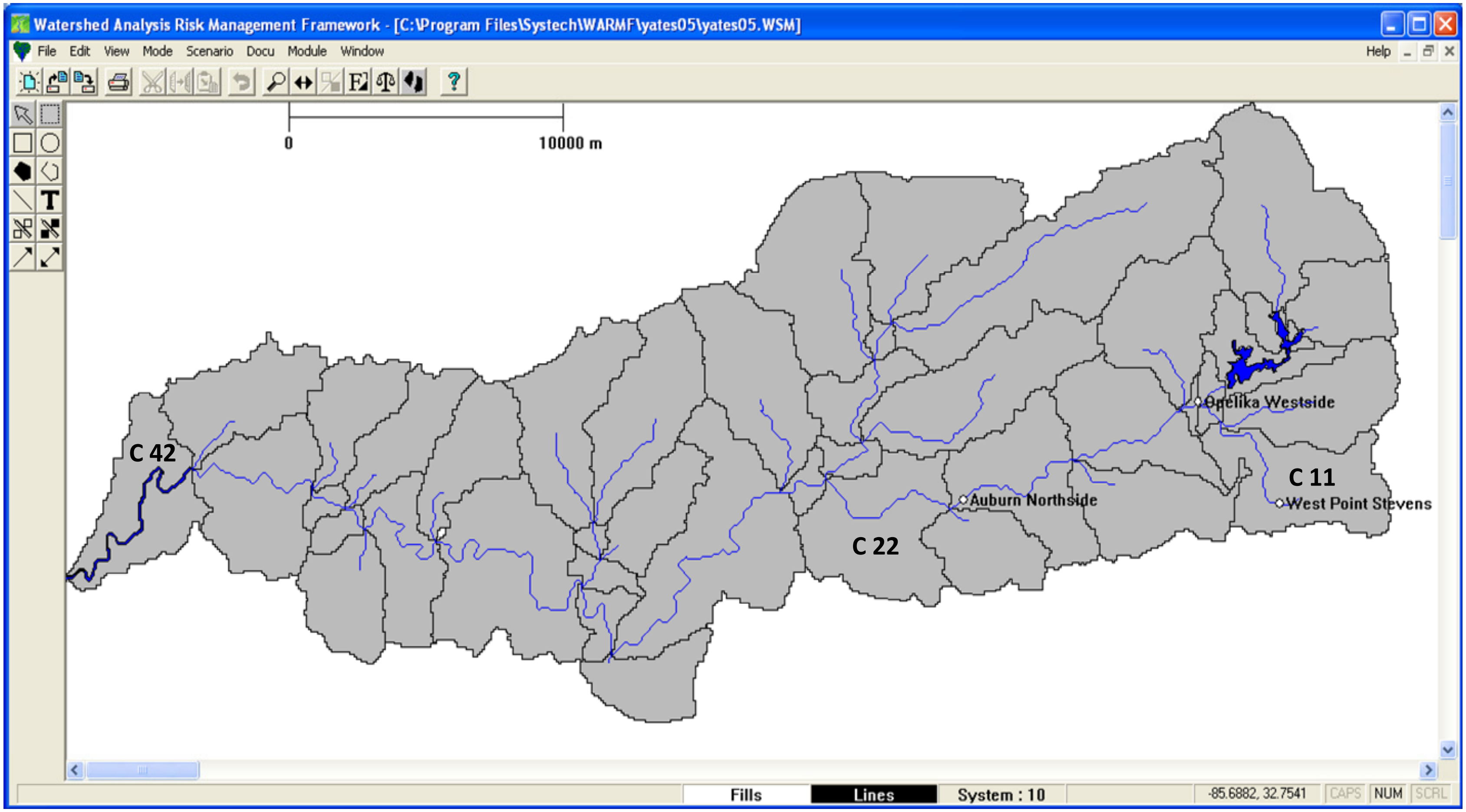

Fig. 2.4 Land catchments, stream segments, and reservoirs of the Saugahatchee Creek Watershed imported into WARMF including three major point source dischargers (Table 2.6)

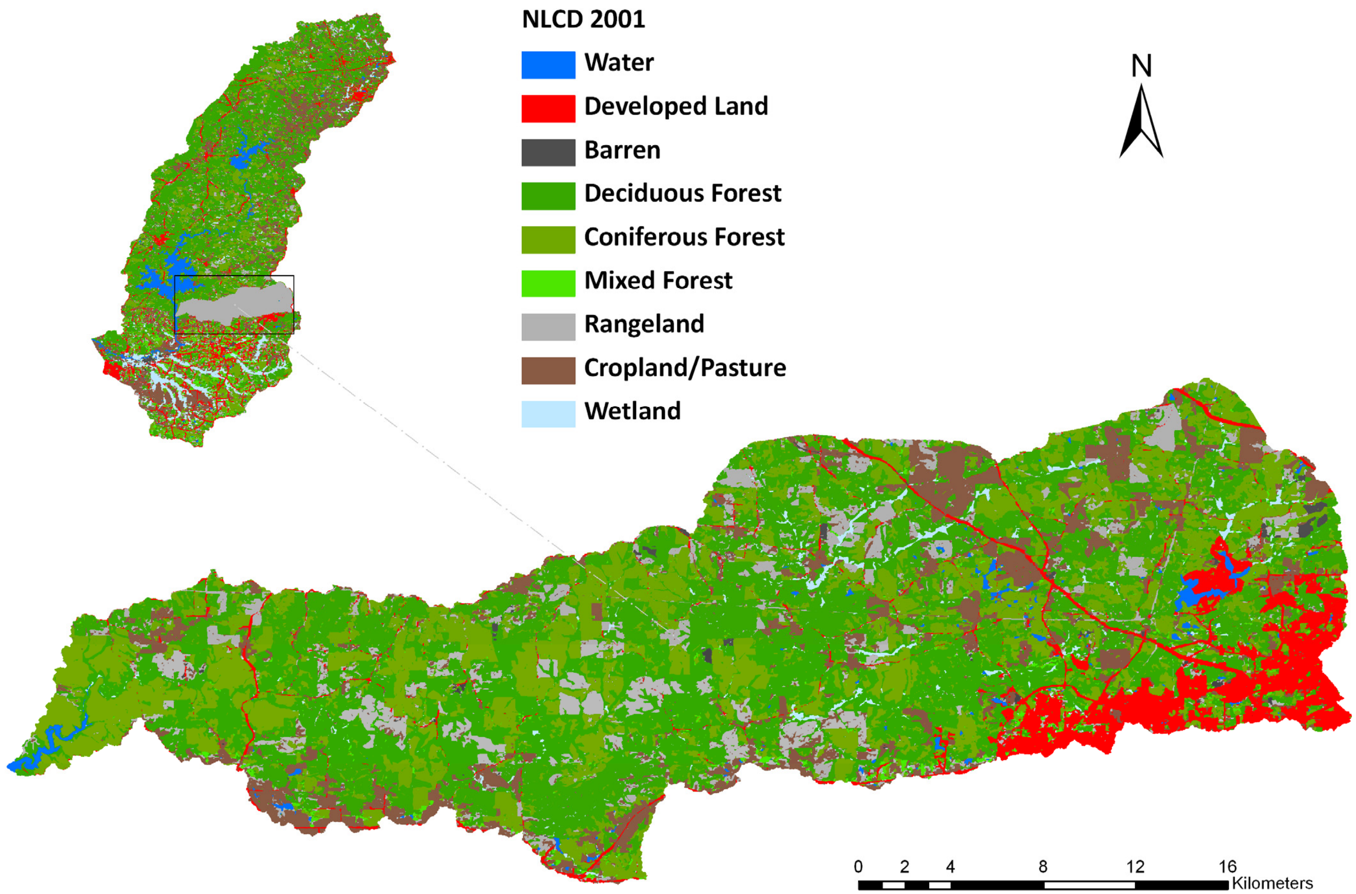

Fig. 2.5 NLCD 2001 land use of the Saugahatchee Creek Watershed clipped from Tallapoosa Basin

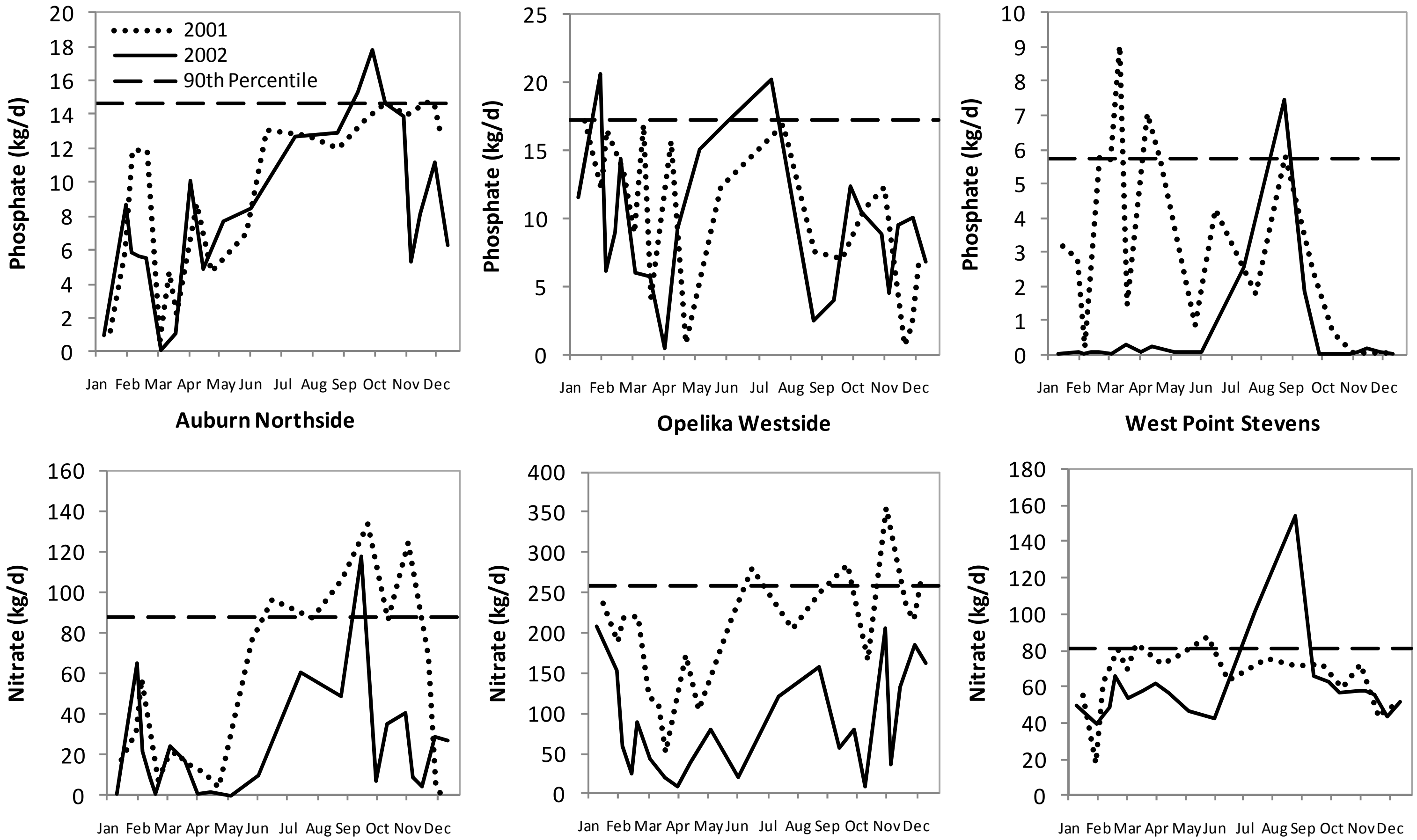

Fig. 2.6 Observed phosphate and nitrate loadings in 2001, 2002 and 90th percentile for Auburn Northside WWTP, Opelika Westside WWTP, and West Point Stevens Finishing Plant, respectively

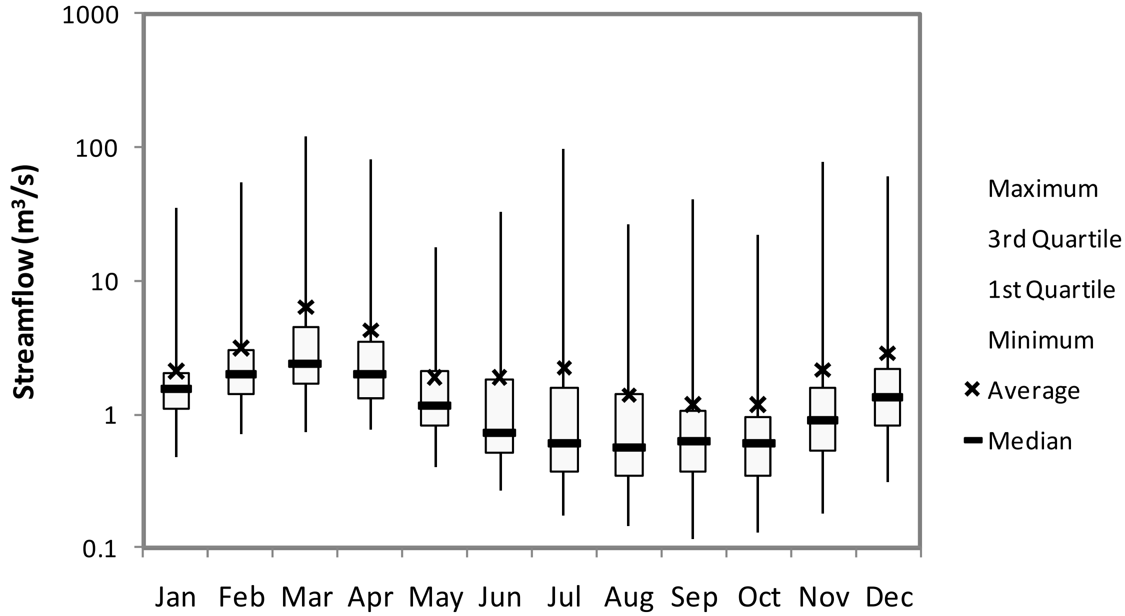

Fig. 2.7 Monthly summary of observed daily flow from 2000-2009 at USGS 02418230 station in the Saugahatchee Creek near Loachapoka

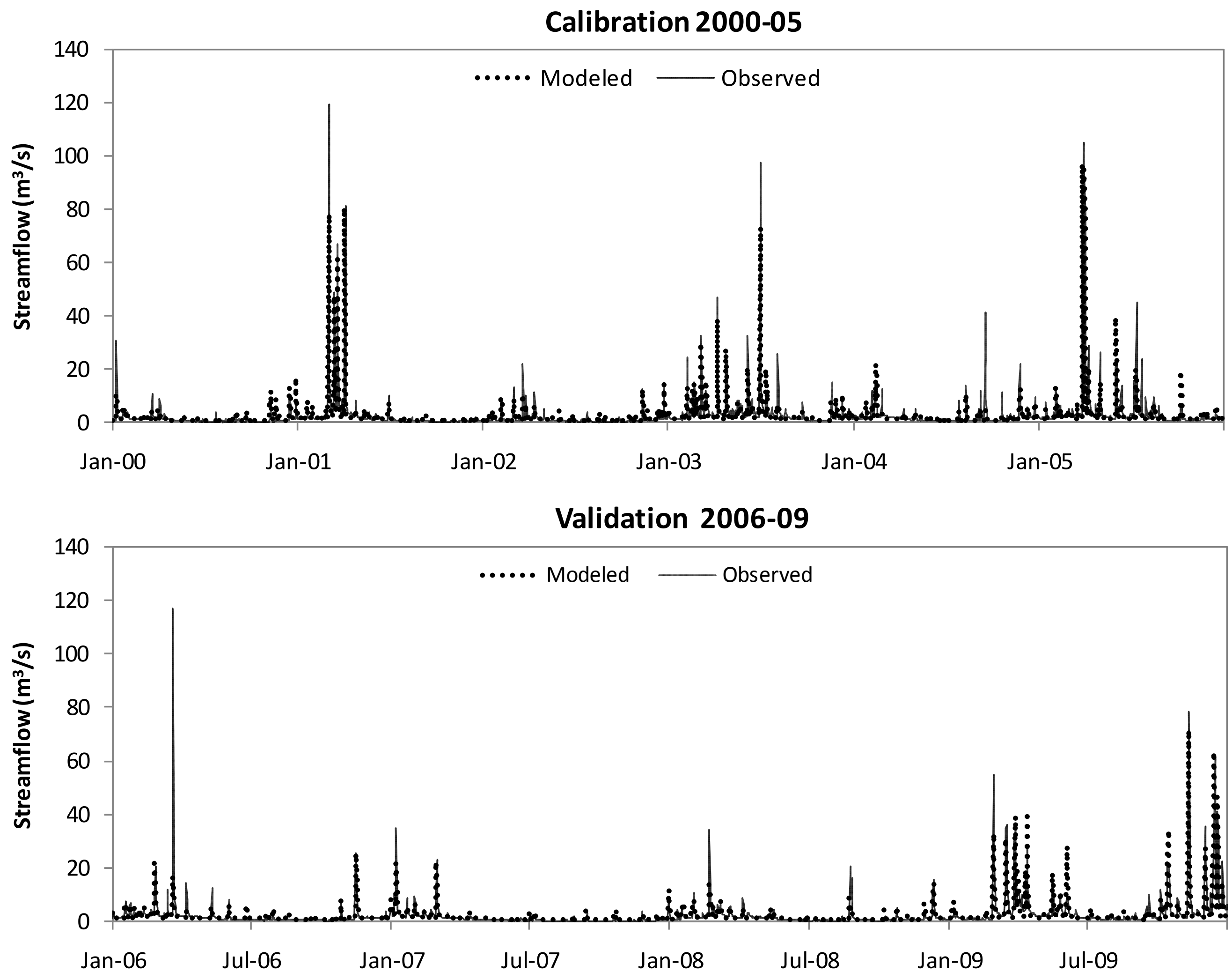

Fig. 2.8 Flow calibration (2000-05) and validation (2006-09) at USGS 02418230 station in the Saugahatchee Creek near Loachapoka

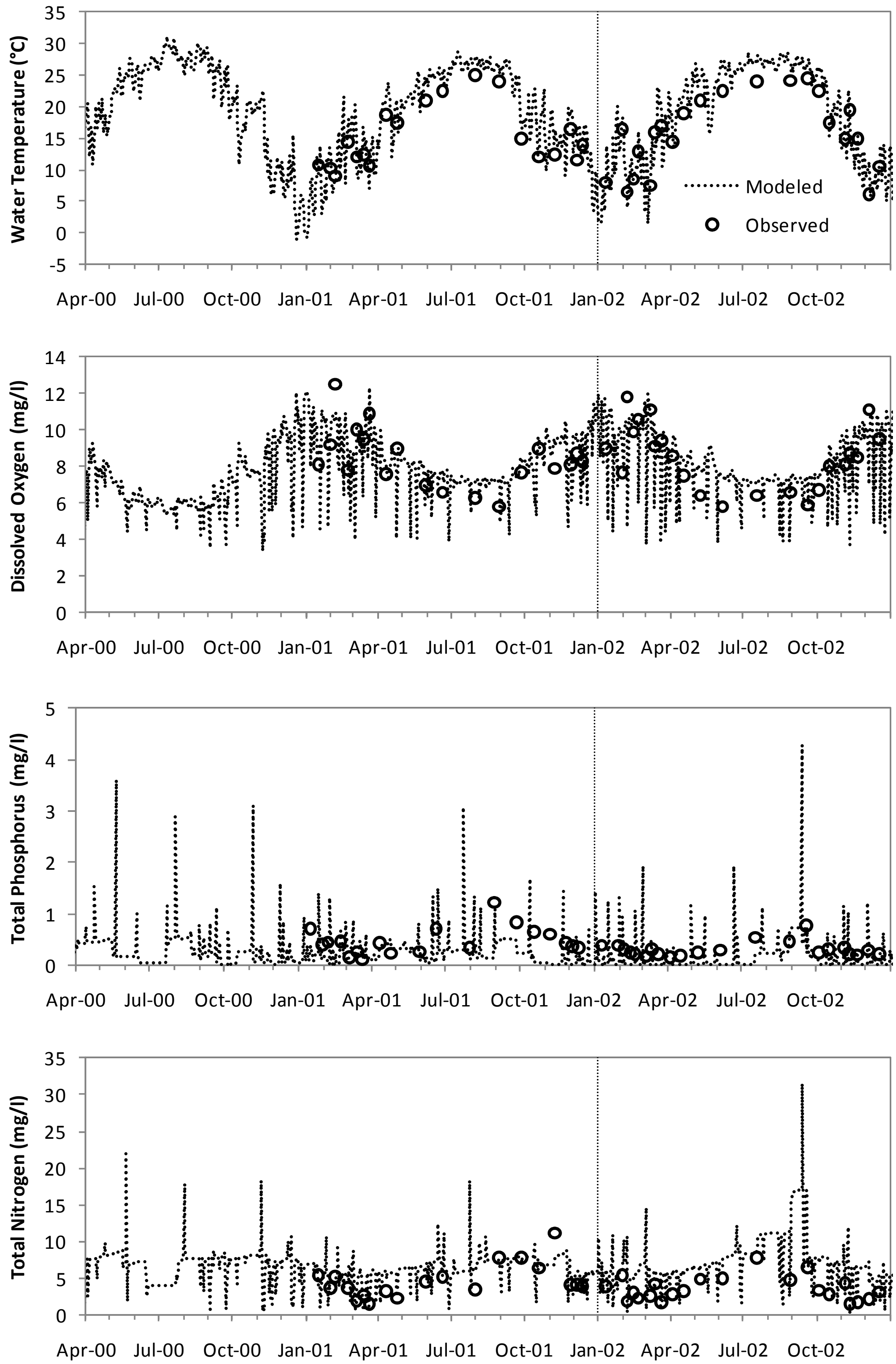

Fig. 2.9 Observed and modeled water temperature, DO, TP, and TN concentration during calibration and validation period at Station-16 in the Pepperell Branch

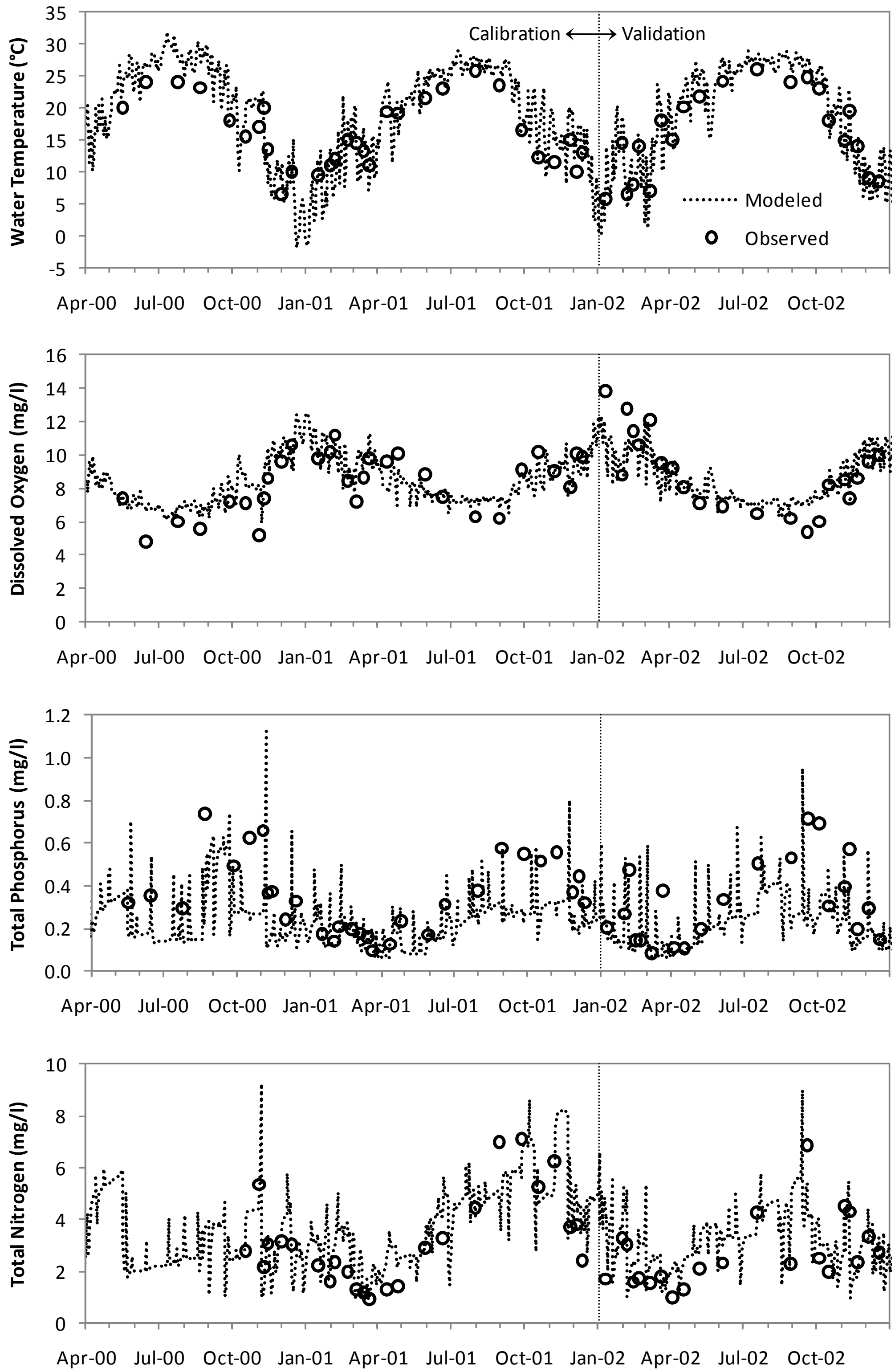

Fig. 2.10 Observed and modeled water temperature, DO, TP, and TN concentration during calibration and validation period at Station-8 in the Saugahatchee Creek near Loachapoka

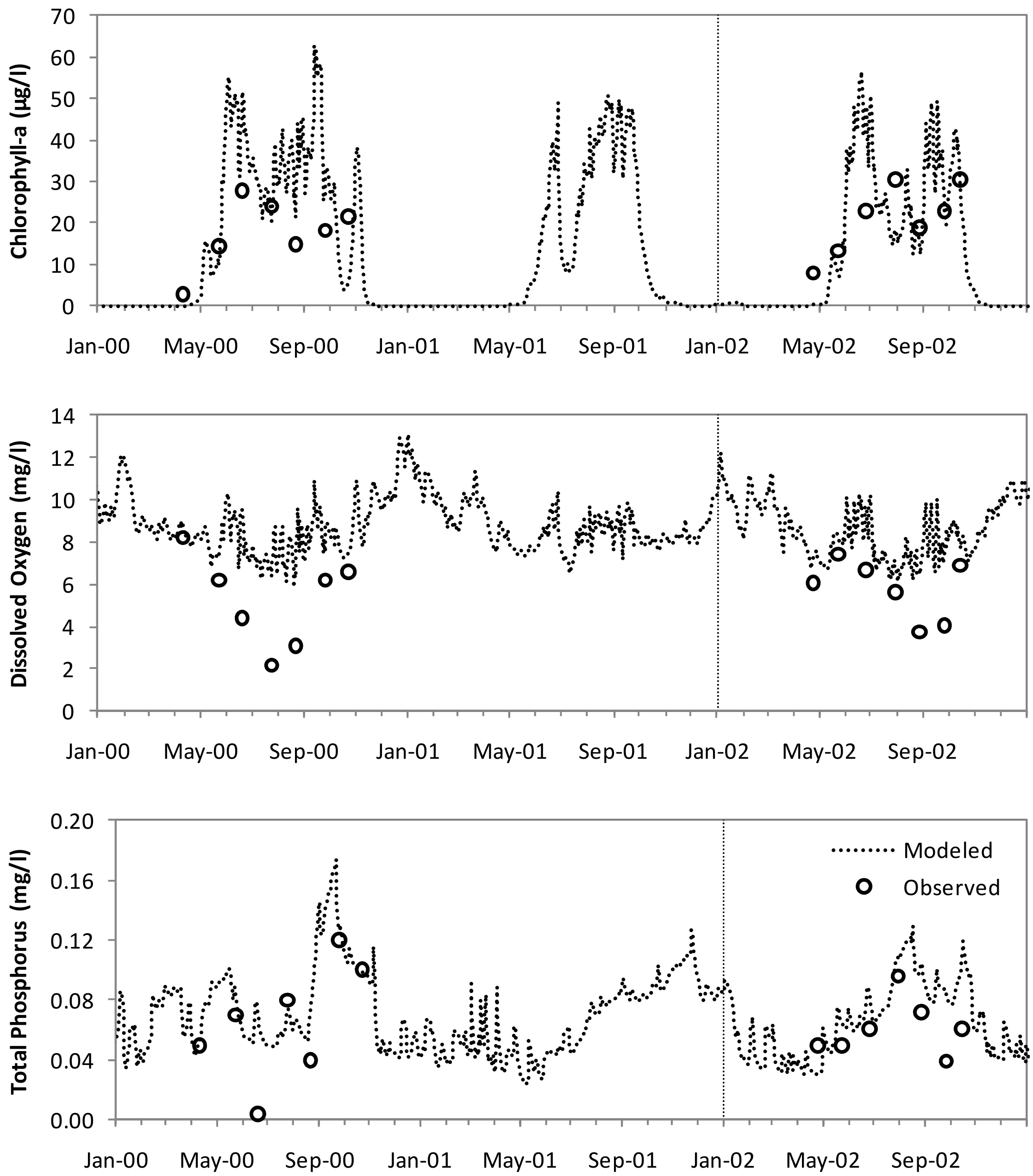

Fig. 2.11 Observed and modeled chlorophyll-a, DO, and TP concentration during calibration and validation period at Yates-2 station in the Saugahatchee Creek (Yates Reservoir Embayment)

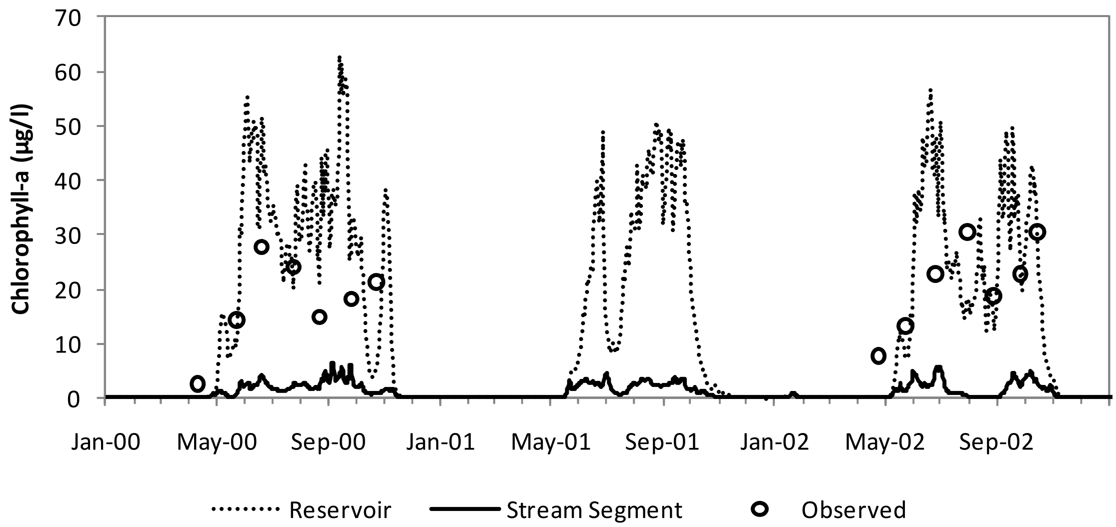

Fig. 2.12 Chlorophyll-a concentration in Yates Reservoir Embayment modeled as a reservoir and as a stream segment with observed values (2000-02)

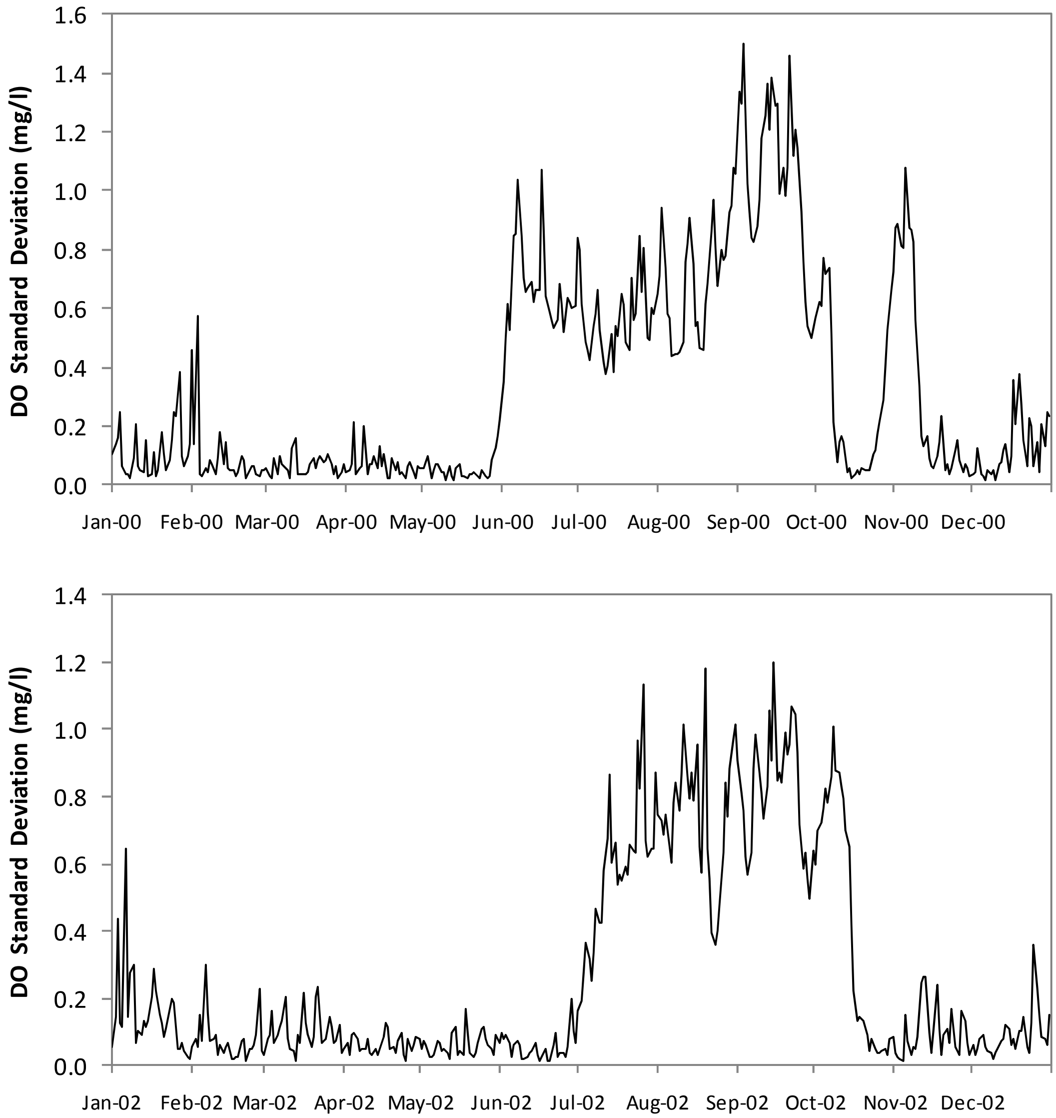

Fig. 2.13 Daily standard deviation of dissolved oxygen simulated using hourly time step at Yates Reservoir Embayment for the year 2000 and 2002

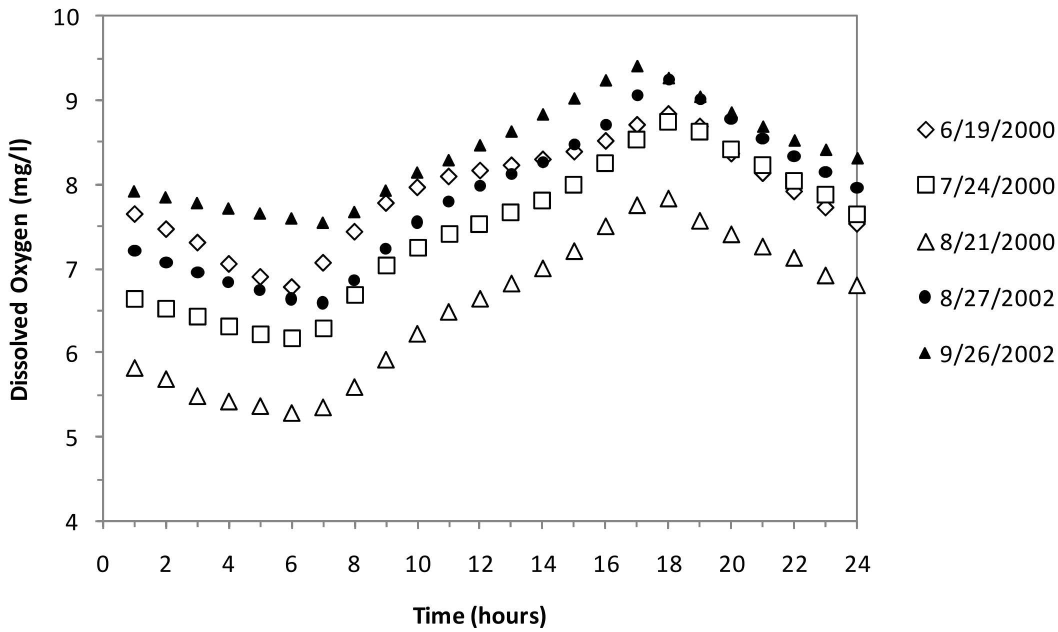

Fig. 2.14 Diurnal variation of DO simulated using hourly time step for days with observed DO less than 5 mg/l at Yates Reservoir Embayment

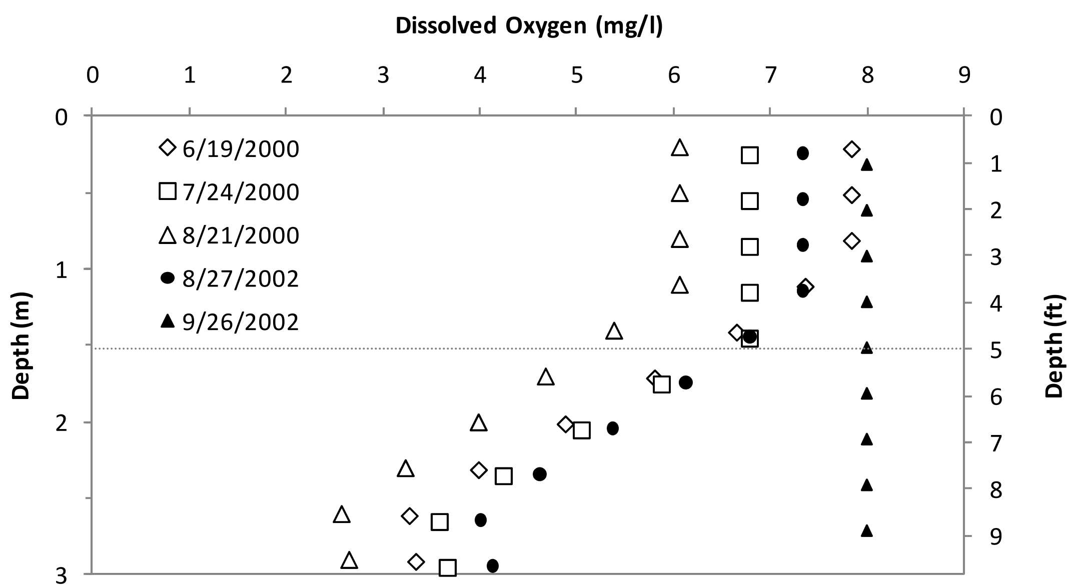

Fig. 2.15 Vertical profiles of DO for days with observed DO less than 5 mg/l

Chapter 3. Assessing the Impact on Hydrology and Water Quality in the Saugahatchee Creek due to Land Use Change and Climate Change using the WARMF Model

Abstract

The hydrology and water quality of a stream or a reservoir gets affected due to human activities and land use change in its watershed. Similarly, climate change, if it occurs, is likely to have significant impacts on local watershed system. In this study, a physically based watershed model WARMF was applied to the Saugahatchee Creek Watershed to investigate hydrologic and water quality response to historical land use scenarios and statistically downscaled future climate scenarios derived from HadCM3 A2 and B2 scenarios. Based on monthly average of daily predicted values, nutrients levels increased for recent land use scenarios of 2001 and 2008 compared to that of 1991. Based on model results, monthly average of daily water temperature is predicted to rise with warmer and drier future climate projections. Accordingly, flow will likely decrease, nutrient concentration are expected to increase. Algal concentration are predicted to increase up to mid 21st century and then decline thereafter. DO concentration are predicted to fall, especially in summer. The results of this study can be incorporated into watershed management and planning strategies after careful evaluation of uncertainties associated with future climate predictions, downscaling, and watershed model output.

Introduction

During the recent years, rapid urbanization has lead to massive land use changes, pervious forest soils have been reduced and industrial and residential areas have been increased. Similarly, the atmospheric concentrations of greenhouse gases and aerosols are believed to be increasing, thereby leading to climate change. Climate change, if it happens, will cause increase in temperature, evaporation, evapotranspiration, precipitation variability and extremes (Kundzewicz et al. 2007)). These alterations will change the hydrological behavior of watershed ecosystem in physical, chemical, and biological terms. The potential effects of land use and climate change are not limited to quantity; it can have serious impacts on water quality of streams and reservoirs in the watershed. In this study, we utilized the Watershed Analysis Risk Management Framework (WARMF) (Chen et al. 2001; Herr et al. 2000) to develop a regional-specific modeling framework to systematically assess the impact on hydrology and water quality in streams and reservoirs of the Saugahatchee Creek Watershed (SCW) using land use and future climate scenarios as model inputs.

The Intergovernmental Panel on Climate Change (IPCC) Fourth Assessment Report summarized that the linear trend over the last 50 years is warming of 0.13 (0.10 to 0.16) °C per decade, nearly twice that for the last 100 years, and it is projected to further increase by 0.2 °C per decade for the next two decades (IPCC 2007). The IPCC (Kundzewicz et al. 2007) summarized the impact of climate change on freshwater systems are mainly due to increases in temperature and precipitation variability. Higher water temperatures, increased precipitation intensity, and longer periods of low flows exacerbate water pollution, with impacts on ecosystems, human health, water system reliability and operating cost (Kundzewicz et al. 2007).

The outputs from various General Circulation Models (GCMs) like Hadley Centre Coupled Model, version 3 (HadCM3) are available to generate future climate scenarios. However, the GCMs were not designed to analyze the hydrologic impact at the watershed scale and therefore have coarser spatial resolution as compared to what is required for watersheds impact studies. GCMs are inherently unable to represent watershed scale feature and dynamics for hydrologic impact studies (Samuels et al. 2010; Wigley et al. 1990). To bridge this gap, the techniques have been developed to downscale GCMs output into local meteorological variables required for hydrological modeling, usually referred to as downscaling techniques. The downscaling techniques can be statistical or dynamic. The statistical downscaling model was used in this study, considering its advantages over dynamic method because statistical method is computationally undemanding and provides station-scale climate information based on GCM-scale output (Wilby and Dawson 2007).

Hydrological impact of land use change has been investigated in a variety of studies using modeling methods (Breuer et al. 2009; Choi et al. 2003; Choi and Deal 2008; Kim et al. 2002). The water quality in a watershed is affected directly by vegetative cover and agricultural and other land management practices (Bhattarai et al. 2008). Bhattarai et al. (2008) used BASINS-SWAT model to estimate the effect of land use change on nitrogen and phosphorus runoff and sediment deposition in a small watershed in the Alabama Wiregrass Region. Similarly, many researchers have pointed out adverse effect of increasing urban land use on water quality (Ouyang et al. 2006; Schoonover et al. 2005; Sliva and Williams 2001; Tu et al. 2007).

Many previous studies have assessed the impact of climate change on hydrology (Chang et al. 2002; Gleick and Chalecki 1999; Liu et al. 2011; Novotny and Stefan 2007; Xu et al. 2009; Zhang et al. 2007). Dibike and Coulibaly (2005) applied statistical downscaling techniques to generate future climate scenarios in the Saguenay watershed in Canada at local watershed scale and simulated the corresponding flow based on the downscaled future climate data as input to hydrological models. Rich et al. (2005) applied watershed model (WARMF) to assess impacts of extended droughts and increased temperature due to climate change on hydrology of the San Juan Basin in Colorado and New Mexico. Simulations showed that drought and increased temperature impact water availability and lead to increased frequency of critical shortages. The assessment of impact of climate change on water quality in the southeastern United States revealed that watersheds are likely to have higher nitrogen levels and lower dissolved oxygen problems (Cruise et al. 1999). However, very few have conducted the climate change impact study for water quantity as well as quality (Bouraoui et al. 2002; Cruise et al. 1999; Neff et al. 2000; Tu 2009). Wang (2010) investigated the individual and combined impact of future land use and climate change in the Wolf Bay Watershed using SWAT. USEPA is evaluating the impacts of land use and climate change on hydrology and water quality in major river basins throughout the United States using watershed models, HSPF and SWAT (Butcher et al. 2010). Limited water quality parameters such as total nitrogen, total phosphorus concentration, etc. are considered in previous impact studies.

To the best of authors' knowledge, no studies have been conducted using a physically based complex watershed model and downscaling 100 years' future climate data to evaluate the impact on flow and water quality parameters including water temperature, dissolved oxygen, total nitrogen, total phosphorus and algal concentration, due to land use and climate change, in streams of a local watershed in Alabama. The objective of this study was to assess the impact of historical land use change and potential climate change downscaled to local watershed scale based on HadCM3 future climate projections, on flow and above mentioned five water quality parameters in the streams of the Saugahatchee Creek Watershed in Alabama. The WARMF model for the SCW was set up, calibrated, and validated for the observed flow and water quality, and then it was run for land use change and future climate scenarios, and their potential impacts were evaluated.

Study Watershed

The watershed of concern is the Saugahatchee (otherwise known as Sougahatchee) Creek Watershed, located mostly in Piedmont region of eastern Alabama with an area of approximately 550 km^2 (Fig. 3.1). Beginning with its headwaters in Chamber and Lee counties, Saugahatchee Creek runs westward through parts of Macon and Tallapoosa counties until it enters Yates Reservoir and converges to Tallapoosa River. Two segments in the SCW are listed on the State of Alabama's 303 (d) list of impaired waters under the federal Clean Water Act (ADEM 2009). Pepperell branch, a tributary to Saugahatchee Creek is listed as impaired waters for nutrients and the portion of Saugahatchee Creek entering Yates Reservoir (Yates Reservoir Embayment) is listed for nutrients and organic enrichment/dissolved oxygen.

Models, Data, and Methods

WARMF is an integrated watershed model with simulation models and databases under one GIS-based graphical user interface (GUI). The algorithms embedded in WARMF are adapted from many well established codes such as ILWAS (Integrated Lake Watershed Acidification Study; Chen et al. 1983; Gherini et al. 1985), ANSWERS (Areal Nonpoint Source Watershed Environmental Response Simulation; Beasley et al. 1980; Beasley and Huggins 1981), SWMM (Storm Water Management Model; Huber et al. 1988), and WASP (Water Quality Analysis Simulation Program; Ambrose et al. 1993).

WARMF represents a watershed by dividing it into a network of land catchments, river segments, and reservoirs. Land catchment is further divided into a canopy layer, a snowpack, and (up to five) soil layers. Each compartment is considered as a seamlessly connected continuously stirred tank reactor (CSTR) for flow routing and mass balance calculation. WARMF simulates the process of canopy interception, snowpack accumulation and snowmelt, infiltration through soil layers, evapotranspiration, surface runoff, and groundwater exfiltration to river segments. The water from the upstream river segment is mixed with the water in the river segment from previous time step and the point and nonpoint loads entering the river segment during the time step. Heat budget and mass balance calculation are performed to calculate the temperature and concentrations of various water quality constituents in each soil layer, river segment, and reservoir (Chen et al. 2001).

The delineated watershed map with land catchments, stream segments, and reservoirs , is required for WARMF, to which input data can be given and simulation results can be viewed. BASINS (Better Assessment Science Integrating point and Nonpoint Sources; USEPA 2004) provides watershed delineation tool which helps to delineate watershed based on DEM (Digital Elevation Map) and river network. To delineate watershed, BASINS Data Download tool extracts nationally derived databases like States boundaries, cataloging unit boundaries, DEM, National Hydrography Dataset (NHD), and National Land Cover Dataset (NLCD). A BASINS project can be set up for 8-digit HUC (Hydrologic Unit Codes) watershed by selecting the geographic area of interest from among the entire 48 contiguous United States. The watershed delineation developed from BASINS can be imported into WARMF (Systech 2005). The SCW is a subset watershed of the Lower Tallapoosa Watershed in Alabama (HUC 03150110). BASINS project for HUC 03150110 was built and only those catchments layers were selected which drains into Saugahatchee Creek for the WARMF model.

To run the simulation, WARMF requires land use data, meteorological data, atmospheric deposition, and soil data. Observed hydrology and water quality data are required for model calibration and validation. WARMF uses readily available data from online sources to predict hydrology and water quality in streams and reservoirs. Land use data can be directly imported into WARMF as a GIS shapefile. Land use shapefile was obtained for the SCW for 2001 from NLCD website (Fig. 3.2). The meteorological data required for WARMF includes precipitation, dew point, minimum and maximum temperature, cloud cover, air pressure and wind speed. National Climatic Data Center (NCDC) Global Summary of Day (GSOD), online climate dataset was used to download the necessary weather data for station in Montgomery, AL (Montgomery Dannelly Field). The dry and wet deposition for air quality was obtained from National Atmospheric Deposition Program (NADP) and USEPA Clean Air Status and Trends Network (CASTNET) website for GAS153 and AL10 station, respectively. There are three major point source dischargers, which contribute to the Saugahatchee Creek. The average flow discharge from these point source dischargers and constituent loadings were obtained from data collected by Alabama Department of Environmental Management (ADEM) and Auburn University (ADEM 2008).

Model Calibration/ Validation

The SCW was divided into 44 land catchments, 40 stream segments and 2 lake layers. The hydrologic and water quality parameters can be assigned to these segments individually, referred as catchment coefficients, river coefficients, and reservoir coefficients in WARMF manual (Herr et al. 2000). There are another set of parameters known as system coefficients that apply to all catchments in the watershed. During the calibration, some of catchment, river, reservoir, and system coefficients were adjusted to obtain a best fit. Table 3.1 list the adjusted parameters, with their literature range, for model calibration.

The model evaluation techniques to compare simulated and observed data are based on graphical and statistical methods. Moriasi et al. (2007) recommended, in addition to the graphical techniques, following quantitative statistics to be used for model evaluation:

Nash-Sutcliffe efficiency (NSE; Nash and Sutcliffe, 1970):

$$NSE = 1 - \left[\frac{\sum_{i=1}^{n} (Y_i^{obs} - Y_i^{sim})^2}{\sum_{i=1}^{n} (Y_i^{obs} - Y^{mean})^2} \right] \tag{3.1}$$

RMSE-observations standard deviation ratio (RSR; Moriasi et al. 2007):

$$RSR = \frac{\sqrt{\sum_{i=1}^{n} (Y_i^{obs} - Y_i^{sim})^2}}{\sqrt{\sum_{i=1}^{n} (Y_i^{obs} - Y^{mean})^2}} \tag{3.2}$$

Percent bias (PBIAS; Gupta et al. 1999):

$$PBIAS = \left[\frac{\sum_{i=1}^{n} (Y_i^{obs} - Y_i^{sim}) \times 100}{\sum_{i=1}^{n} (Y_i^{obs})} \right] \tag{3.3}$$

Where, Y_i^{obs} is the i^{th} observed value, Y_i^{sim} is the i^{th} simulated value, Y^{mean} is the mean of the observed values, and *n* is the total number of observed values. The simulation of watershed model can be judged satisfactory if NSE > 0.5 and RSR ≤ 0.7 and if PBIAS is within ±25% for flow (Moriasi et al. 2007).

The observed flow daily data is available at USGS 02418230 station in the Saugahatchee Creek near Loachapoka since 2000. The flow was calibrated for the period 2000–2005 and validated for the period 2006–2009 (Fig. 3.3). The model simulation was run three years prior to the calibration period starting from 1997 to minimize the effect of initial unknown parameters used in the model. The simulation of flow resulted in satisfactory values of NSE, RSR and PBIAS for calibration (validation) to be 0.64, 0.60, and 9.21 % (0.56, 0.66, and 3.79 %), respectively (Table 3.2).

ADEM and Auburn University collected water quality data in the SCW in 2000–2002 (ADEM 2008). The observed water quality data such as water temperature, dissolved oxygen (DO), total phosphorus (TP), and total nitrogen (TN) were available for the same station but not in daily basis. Therefore, water quality calibration was performed based on graphical techniques, which include visual comparison of simulated and observed data such as time series plots (Fig. 3.4).

Historical Land Use Change Scenarios

There have been significant changes in land use pattern of Saugahatchee watershed over the last two centuries, particularly in recent years (AWW, 2005). The upper watershed is undergoing rapid transition from forest to urban/developed land. The changes in land use distribution are expected to bring changes in water quality, including surface flow, nutrient runoff, and sedimentation levels (Bhattarai et al. 2008). For land use change scenarios, we used land use shapefiles downloaded from AlabamaView website (AlabamaView 2009) for the SCW for 1991, 2001 and 2008 (Fig. 3.5). From 1991 to 2008, forest areas decreased from 80% to 72%, while urban land increased from 4% to 8% and cropland increased from 7% to 9% (

Table 3.3).

Climate Change Scenarios and Downscaling

Hadley Centre Coupled Model, version 3 (HadCM3):

HadCM3 is a coupled atmospheric-ocean general circulation model (AOGCM) developed at the Hadley Centre in the United Kingdom for IPCC Third Assessment

Report use (Gordan et al. 2000; IPCC 2001; Pope et al. 2000) . The spatial resolution of HadCM3, which is 2.5° latitude by 3.75° longitude, represents a global grid of 96 × 73 grid cells. This is equivalent to a surface resolution of about 417 km × 278 km at the Equator, reducing to 295 km × 278 km at 45 degrees of latitude (IPCC 2001).

SRES Emission Scenarios:

IPCC published a set of future climate scenarios in Special Report on Emission Scenarios (SRES) to explore the uncertainties behind potential trends in global development and GHG emissions (Nakivenovic et al. 2000). Four SRES storylines and scenario families were developed, which assumes a distinctly different direction for future developments. Each storyline represents different demographic, social, economic, technological, and environmental developments. The major scenario families are discussed below (Nakivenovic et al. 2000):

- A1: The A1 storyline and scenario family describes a future world of very rapid economic growth, global population that peaks in mid-century and declines thereafter, and the rapid introduction of new and more efficient technologies. Major underlying themes are convergence among regions, capacity building and increased cultural and social interactions, with a substantial reduction in regional differences in per capita income.
- A2: The A2 storyline and scenario family describes a very heterogeneous world with high population growth. The underlying theme is self-reliance and preservation of local identities. Economic development is primarily regionally

oriented and per capita economic growth and technological change are more fragmented and slower than in other storylines.

- B1: The B1 storyline and scenario family describes a convergent world with the same low population growth as in the A1 storyline, but with rapid changes in economic structures toward a service and information economy, with reductions in material intensity, and the introduction of clean and resource-efficient technologies. The emphasis is on global solutions to economic, social, and environmental sustainability, including improved equity, but without additional climate initiatives.
- B2: The B2 storyline and scenario family describes a world in which the emphasis is on local solutions to economic, social, and environmental sustainability. It is a world with moderate population growth, intermediate levels of economic development, and less rapid and more diverse technological change than in the B1 and A1 storylines. While the scenario is also oriented toward environmental protection and social equity, it focuses on local and regional levels.

The outputs derived from HadCM3 A2 and HadCM3 B2 were downscaled to local watershed scale using statistical techniques and applied to the WARMF model for the SCW.

Downscaling:

Future climate projected using GCMs have coarser spatial resolution than what is required for hydrologic impact study. For hydrologic and water quality impact studies, local or station scale meteorological variables are required, which can be derived using large-scale atmospheric variables available from GCM outputs. Future climate change scenarios are downscaled for the SCW at daily time scales, using large-scale GCM outputs. SDSM (Statistical DownScaling Model; Wilby and Dawson 2007) was used for the purpose of downscaling meteorological variables to the local watershed.

In statistical downscaling techniques, the quantitative relationships are established between large-scale atmospheric variables (known as predictors) and local or station surface variables (known as predictands). The National Centers for Environmental Prediction (NCEP) and the National Center for Atmospheric Research (NCAR) worked together in a reanalysis project to produce a physically consistent retroactive record of more than 50 years of global analyses of atmospheric fields to support the needs of research and climate monitoring communities (Kalnay et al. 1996). Reanalysis project involved the recovery of data from many observed and measurement systems, quality controlled and assimilated with a data assimilation system kept unchanged over the reanalysis period. The main objective of reanalysis is to eliminate perceived climate jumps associated with changes in data assimilation system and provide consistent records of temperature, precipitation, winds and many other variables that describe climatic conditions from the past to the present. The daily NCEP/NCAR reanalysis data was selected to represent the large-scale predictors in the SDSM model. NCEP/NCAR data has been used in several downscaling studies in different regions over the world (Dibike and Coulibaly 2005; Tatli et al. 2004).

Using SDSM, the appropriate large-scale predictor variables were selected from the list of predictors obtained from NCEP/NCAR reanalysis data for the period of 1961-1990, based on regression techniques, to downscale predictands (such as station precipitation, maximum and minimum temperature). Table 3.4 lists the predictor variables (from NCEP/NCAR) screened for downscaling and the predictands. SDSM constructs a downscaling model with parameters of the model based on multiple regression equations, given observed daily weather data (predictand) and the selected large-scale NCEP predictors for the same time period. The observed daily weather data at Montgomery Dannely Field station from 1961–1990 was downloaded from NOAA's NCDC web site. The data from 1961–1975 was used to develop the regression model and the model regression weights produced as a parameter file was then used to validate for the period from 1976–1990. The process of selecting predictors, calibration results, parameter file generation, and validation for downscaling precipitation in Montgomery Dannelly Field station are listed in Appendix A.

The parameter file was then used to downscale future climate to local watershed scale based on predictor derived from HadCM3. The GCM predictor data, derived from the HadCM3 A2 and B2 experiments, can be obtained for any global land area through data portal maintained by the CCCSN along with the daily observed predictor data, which is derived from NCEP/NCAR reanalyses and interpolated to the same grid as HadCM3 (CCCSN 2010). Given the latitude and longitude of the SCW, GCM and NCEP/NCAR predictors were extracted for the nearest grid. The future climate projection scenarios are organized into allotted three time frames and termed as 2020s (2011-2040), 2050s (2041-2170), and 2080s (2071-2099).

Fig. 3.6 and Fig. 3.7 show the patterns of downscaled precipitation, maximum and minimum temperatures for the study watershed along with standard deviation corresponding to HadCM3 A2 and HadCM3 B2 scenarios, respectively. The monthly mean of daily maximum and minimum temperatures are projected to increase whereas that of precipitation are projected to decrease, especially in summer. Table 3.5 shows the statistical summary of maximum temperature, minimum temperature, and precipitation for allotted time period of 2020s, 2050s, and 2080s for HadCM3 A2 and B2 scenarios.

Results and Discussions

For comparing results of land use change scenarios and future climate scenarios, flow and water quality parameters were simulated at the watershed outlet. The monthly average of daily values over the 30 years' period of baseline and different scenarios were calculated. The anomalies of the monthly average of daily outputs to the baseline scenario were computed and plotted.

Impact of Land Use Change on Hydrology and Water Quality

The hydrological and water quality response of the model corresponding to three land use scenarios were analysed using 30 years (1981-2010) simulation results. The baseline scenario corresponding to land use of 1991and the other two land use change scenarios corresponding to land use of 2001 and 2008 were run to investigate the land use change effect. The anomalies of flow and other water quality parameters corresponding to land use of 2001 and 2008 to the baseline were further computed.

Fig. 3.8 shows the relative change from the baseline, of monthly average of daily flow, for land use scenarios of 2001 ranged between -0.03 to 0.07 m^3/s and for 2008 ranged between -0.09 to 0.16 m^3/s. The increase or decrease in the flow corresponding to land use scenarios of 2001 and 2008 were not more than 1.76% and 3.89%, respectively.

Similarly, for surface water temperature, there was very little or no change in simulated results between three land use scenarios (Fig. 3.8). The increase or decrease in the surface water temperature corresponding to land use scenarios of 2001 and 2008 were less than 0.08% and 0.18%, respectively. Therefore, land use change from 1991 to 2008 did not have significant impact on flow and surface water temperature for the simulation period.

Surface dissolved oxygen concentration in the Yates Reservoir Embayment, in terms of monthly average of daily values, did not experience the expected change due to land use change, partly because the simulation was performed on daily time step. The water body with predominance of algae shows a larger fluctuations in dissolved oxygen than less productive water with low algal concentration (Ansa-Asare et al. 2000). The water bodies with algal concentration higher than 15 μg/l are categorized as eutrophic and higher than 40 μg/l as hypereutrophic waterbodies (Carlson 1977). Higher eutrophic level implies algal abundance and hence exhibit higher rate of photosynthesis, respiration, and decomposition. For eutrophic and hypereutrophic systems, the dissolved oxygen concentration tends to increase during day time due to algal photosynthesis dominating over respiration and decomposition; whereas the system will have less dissolved oxygen concentration during night as there is no sunlight for photosynthesis (O'Connor and Di Toro 1970; Odum 1956). Due to limited data availability, the simulation was run on daily time steps in the model, which doesn't model diurnal phenomenon. The diurnal fluctuation in the Saugahatchee Creek (Yates Reservoir Embayment) is discussed elsewhere (Chapter 2). Fig. 3.8 shows the relative change in monthly average of daily DO concentration to the baseline corresponding to land use scenarios of 2001 and 2008 was 0.14 mg/l at most. The relative change in DO concentration for 2001 and 2008 were not more than 1.66%.

In the SCW, forest areas have been transformed into cropland and urban areas (Table 3.3). Consequently, fertilizer inputs, livestock and cattle manure, sewage, industrial waste, and other sources of nutrients are increased. Therefore, the major impact that land use change has on the watershed, is to the nutrient concentration in the streams and reservoirs. Land use scenario of 2001 produced TP concentration to be 3.87 to 5.87% greater whereas that of 2008 produced TP concentration to be 11.18 to 15.37% greater than baseline scenario (Fig. 3.9). The relative change in monthly average of daily TN concentration to the baseline corresponding to land use scenario of 2001 ranged between -3.71 to 15.04% and that of 2008 ranged between -16.05 to 27.75%, respectively (Fig. 3.9).

The algal growth in streams and reservoirs are seasonal. The growing season for the SCW has been identified as April through October (ADEM 2008). Monthly chlorophyll-a concentration under 1991 land use varied from 1.6 to 33.2 μg/L during growing season. Fig. 3.9 shows the relative change in monthly average of daily algal concentration corresponding to land use scenario of 2001 ranged between -0.03 to 1.54 μg/l and and that of 2008 ranged between -0.09 to 2.39 μg/l, respectively. The increase in algal concentration reached as high as 15.04% and 27.75% for land use scenarios of 2001 and 2008, respectively.

Impact of Climate Change on Hydrology and Water Quality

The impact on flow and other water quality parameters due to future climate was analyzed under HadCM3 A2 and HadCM3 B2 future climate scenarios. Each GCMs output was further categorized into three time frames: 2020s (2011-2040), 2050s (2041-2070), and 2080s (2071-2099). The simulated results for these time frames were compared with baseline scenario (1981-2010). Fig. 3.10 - Fig. 3.13 show the monthly average of daily values of simulated flow and water quality parameters under future climate scenarios and the relative changes in the future projected values from the baseline scenario.

The monthly average of daily flow is projected to decrease corresponding to HadCM3 A2 and B2 scenarios. The flow is projected to decrease by 6.8 m^3/s and 6.5 m^3/s at most for HadCM3 A2 and B2 scenarios, respectively (Fig. 3.10 and Fig. 3.12). The surface water temperature is projected to increase, especially in summer having increment in monthly average of daily surface water temperature reached as high as 5.5 °C, and 4.7 °C for HadCM3 A2 and B2 scenarios, respectively (Fig. 3.10 and Fig. 3.12). The monthly average of daily surface DO decreased by 1.9 mg/l, and 1.2 mg/l at most corresponding to HadCM3 A2 and B2 scenarios, respectively (Fig. 3.10 and Fig. 3.12). The decrease in DO concentration is partly because of increased water temperature as dissolved oxygen solubility is inversely proportional to water temperature (APHA 1992).

For HadCM3 A2 and B2 scenarios, nutrient concentrations are projected to increase in the stream. It corresponds to the flow, as low flow tends to have higher concentration of nutrients. The total phosphorus increased as high as 87.4% and 83.2% for HadCM3 A2 and B2, respectively (Fig. 3.11 and Fig. 3.13). The total nitrogen increased as high as 80.0% and 57.5% for HadCM3 A2 and B2, respectively (Fig. 3.11 and Fig. 3.13).

The algal concentration is significant only during the growing season (April through October). For HadCM3 A2 and B2 scenarios, algal concentrations are projected to increase most of the time except during late-summer of 2080s when it decreases (Fig. 3.11 and Fig. 3.13). The algal growth rate increases with the increase in temperature up to the optimum level and then decreases with further increase in temperature (Chen et al. 2001).

Fig. 3.14 and Fig. 3.15 are the flow duration curves that compare low-flow and high-flow conditions, of daily flows, for future scenarios' time period and baseline period. A lower probability of exceedance (< 0.1) represent a high flow that has been exceeded by only 10% of the values in that period. On the contrary, a higher probability of exceedance represents low flow conditions. Both low flows and high flows for future climate scenarios are expected to decrease. However, in the later part of 21st century, it is predicted to have increased high flows (Fig. 3.14 and Fig. 3.15).

Conclusions

In this study, WARMF model was applied to assess the impact on hydrology and water quality in streams and reservoirs of the SCW due to historical land use change and projected future climate change. Land use change scenarios for 1991, 2001, and 2008 revealed that forest areas have been reduced and urban and agricultural areas have been increased in the watershed. The simulation over the period of 30 years (1981-2010) predicted the nutrient (TP and TN) concentrations for land use scenarios of 2001 and

2008 to be higher than the baseline land use scenario of 1991. The algal growth was predicted to increase during the growing seasons due to increased level of nutrients.

The downscaled results derived from the output of HadCM3 future climate model showed the climate will become warmer and drier in the 21st century. Temperature rise in these future climate scenarios are higher especially in summer. The watershed response to these changes, based on monthly average of daily values, resulted rise in water temperature, which was expected with rise in air temperatures. Accordingly, flow was expected to decrease corresponding to decreasing pattern of precipitation in the 21st century. Future climate scenarios predicted higher nutrient (TP and TN) concentration. Algal concentration are predicted to increase up to mid 21st century and then decline thereafter, most probably due to too much heat. DO concentration were expected to fall, especially in summer, with the mixed effect of rising temperature and increasing algal mass.

We should not discard possible uncertainties that output of future climate models, downscaling, and complex watershed model could bring to the results. However, the impact study under different scenarios of land use and climate change, in general, gives us better understanding how management alternatives can be launched during watershed planning.

References

Alabama Department of Environmental Management (ADEM). (2008). "Final total maximum daily load: Nutrients & OE/DO. Pepperell branch AL03150110-0201-700 Nutrients; Sougahatchee Creek Embayment (Yates Reservoir) AL03150110-0204-101 Nutrients & OE/DO.", Alabama Department of Environmental Management, Montgomery, AL.

Alabama Department of Environmental Management (ADEM). (2009). "2008 Alabama 303(d) List." 303(d) Information and Map. Alabama Department of Environmental Management <http://adem.alabama.gov/programs/water/wquality/2008AL303dList.pdf> (Aug. 12, 2009).

AlabamaView (2009). "Saugahatchee Watershed Landcover." Saugahatchee Watershed Project. <http://www.alabamaview.org/watershed_project.html> (Mar. 20, 2009).

Alabama Water Watch (AWW). (2005). "Saugahatchee Creek Watershed: Past, Present, & Future."Saugahatchee Creek Watershed Management Plan.

Ambrose, R., Wool, T., and Martin, J. (1993). "WASP 5, The Water Quality Analysis Simulation Program Version 5.00." *ASCI Corporation, Athens, Georgia*.

American Public Health Association (APHA). (1992). Standard methods for the examination of water and wastewater, 18 ed. Washington, DC.

Ansa-Asare, O. D., Marr, I. L., and Cresser, M. S. (2000). "Evaluation of modelled and measured patterns of dissolved oxygen in a freshwater lake as an indicator of the presence of biodegradable organic pollution." *Water Research*, 34(4), 1079-1088.

Beasley, D., Huggins, L., and Monke, E. J. (1980). "ANSWERS: A model for watershed planning."

Beasley, D. B., and Huggins, L. F. (1981). "ANSWERS, areal nonpoint source watershed environment response simulation: user's manual."

Bhattarai, G., Srivastava, P., Marzen, L., Hite, D., and Hatch, U. (2008). "Assessment of economic and water quality impacts of land use change using a simple bioeconomic model." *Environmental Management*, 42(1), 122-131.

Bouraoui, F., Galbiati, L., and Bidoglio, G. (2002). "Climate change impacts on nutrient loads in the Yorkshire Ouse catchment (UK)." *Hydrology and Earth System Sciences*, 6(2), 197-209.

Breuer, L., Huisman, J. A., Willems, P., Bormann, H., Bronstert, A., Croke, B. F. W., Frede, H. G., Gräff, T., Hubrechts, L., Jakeman, A. J., Kite, G., Lanini, J., Leavesley, G., Lettenmaier, D. P., Lindstrom, G., Seibert, J., Sivapalan, M., and Viney, N. R. (2009). "Assessing the impact of land use change on hydrology by ensemble modeling (LUCHEM). I: Model intercomparison with current land use." *Advances in Water Resources*, 32(2), 129-146.

Butcher, J. B., Parker, A., Johnson, T., and Weaver, C. P. (2010). "Nationwide Watershed Modeling to Evaluate Potential Impacts of Climate and Land Use Change on Hydrology and Water Quality." Proceedings of the 2010 Watershed Management Conference, K. W. Potter and D. K. Frevert, eds., Madison, WI.

Carlson, R. E. (1977). "A trophic state index for lakes." *Limnology Oceanography*, 22(2), 361-369.

Chang, H., Knight, C. G., Staneva, M. P., and Kostov, D. (2002). "Water resource impacts of climate change in southwestern Bulgaria." *GeoJournal*, 57(3), 159-168.

Chen, C., Gherini, S., Hudson, R., and Dean, J. (1983). "The Integrated Lake-Watershed Acidification Study. Volume 1: Model Principles and Application Procedures." *Electric Power Research Institute report EA-3221, Palo Alto, California, USA*.

Chen, C. W., Herr, J. W., and Weintraub, L. (2001). "Watershed Analysis Risk Management Framework (WARMF): Update One–A decision support system for watershed analysis and total maximum daily load calculation, allocation and implementation. Publication No. 1005181." *Electric Power Research Institute, Palo Alto, California*.

Choi, J. Y., Engel, B. A., Muthukrishnan, S., and Harbor, J. (2003). "GIS based long term hydrologic impact evaluation for watershed urbanization." *Journal of the American Water Resources Association*, 39(3), 623-635.

Choi, W., and Deal, B. M. (2008). "Assessing hydrological impact of potential land use change through hydrological and land use change modeling for the Kishwaukee River basin (USA)." *Journal of Environmental Management*, 88(4), 1119-1130.

Cruise, J. F., Limaye, A. S., and Al-Abed, N. (1999). "Assessment of impacts of climate change on water quality in the southeastern United States." *Journal of the American Water Resources Association*, 35(6), 1539-1550.

Dibike, Y. B., and Coulibaly, P. (2005). "Hydrologic impact of climate change in the Saguenay watershed: comparison of downscaling methods and hydrologic models." *Journal of Hydrology*, 307(1-4), 145-163.

Gherini, S., Mok, L., Hudson, R., Davis, G., Chen, C., and Goldstein, R. (1985). "The ILWAS model: formulation and application." *Water, Air, & Soil Pollution*, 26(4), 425-459.

Gleick, P. H., and Chalecki, E. L. (1999). "The impacts of climatic changes for water resources of the Colorado and Sacramento San Joaquin River Basins." *Journal of the American Water Resources Association*, 35(6), 1429-1441.

Gordon, C., Cooper, C., Senior, C. A., Banks, H., Gregory, J. M., Johns, T. C., Mitchell, J. F. B., and Wood, R. A. (2000). "The simulation of SST, sea ice extents and ocean heat transports in a version of the Hadley Centre coupled model without flux adjustments." *Climate Dynamics*, 16(2), 147-168.

Gupta, H. V., Sorooshian, S., and Yapo, P. O. (1999). "Status of automatic calibration for hydrologic models: Comparison with multilevel expert calibration." *Journal of Hydrologic Engineering*, 4(2), 135-143.

Herr, J., Weintraub, L., and Chen, C. (2000). "User's Guide to WARMF: Documentation of Graphical User Interface." *EPRI. Palo Alto, CA. Report EP-P2346/ C*, 1054.

Huber, W. C., Dickinson, R. E., and Barnwell Jr, T. O. (1988). "Storm water management model; version 4." *Environmental Protection Agency, United States*.

IPCC. (2001). *Climate Change 2001: Synthesis Report*. Contribution of Working Group I to the Third Assessment Report of the Intergovernmental Panel on Climate Change, [Houghton, J. T., Y. Ding, D. J. Griggs, M. Noguer, P. J. van der Linden, X. Dai, K. Maskell, and C. A. Johnson (eds.)], Cambridge University Press, Cambridge, United Kingdom and New York, NY, USA.

IPCC. (2007). *Climate Change 2007: The Physical Science Basis*. Contribution of Working Group I to the Fourth Assessment Report of the Intergovernmental Panel on Climate Change, [S. Solomon, D. Qin, M. Manning, Z. Chen, M. Marquis, K. B. Averyt, M. Tignor, and H. L. Miller (eds.)], Cambridge University Press, Cambridge, United Kingdom and New York, NY, USA.

Kalnay, E., Kanamitsu, M., Kistler, R., Collins, W., Deaven, D., Gandin, L., Iredell, M., Saha, S., White, G., and Woollen, J. (1996). "The NCEP/NCAR 40-Year Reanalysis Project." *Bulletin of the American Meteorological Society*, 77(3), 437-471.

Kim, Y., Engel, B. A., Lim, K. J., Larson, V., and Duncan, B. (2002). "Runoff impacts of land-use change in Indian River Lagoon watershed." *Journal of Hydrologic Engineering*, 7(3), 245-251.

Kundzewicz, Z. W., Mata, L. J., Arnell, N. W., Doll, P., Kabat, P., Jimenez, B., Miller, K. A., Oki, T., Sen, Z., and Shiklomanov, I. A. (2007). "Freshwater resources and their management." Climate Change 2007: impacts, adaptation and vulnerability: contribution of Working Group II to the fourth assessment report of the Intergovernmental Panel on Climate Change, M. L. Parry, O. F. Canziani, J. P.

Palutikof, P. J. v. d. Linden, and C. E. Hanson, eds., Cambridge Univ Press, Cambridge, UK, 173-210.

Liu, L., Liu, Z., Ren, X., Fischer, T., and Xu, Y. (2011). "Hydrological Impacts of Climate Change in the Yellow River Basinfor the 21st Century Using Hydrological Model and Statistical Downscaling Model." *Quaternary International., in press*.

Moriasi, D. N., Arnold, J. G., Van Liew, M. W., Bingner, R. L., Harmel, R. D., and Veith, T. L. (2007). "Model Evaluation Guidelines for Systematic Quantification of Accuracy in Watershed Simulations." *Transactions of the ASABE*, 50(3), 885-900.

Nakicenovic, N., Alcamo, J., Davis, G., de Vries, B., Fenhann, J., Gaffin, S., Gregory, K., Grubler, A., Jung, T.Y., Kram, T., La Rovere, E.L., Michaelis, L., Mori, S., Morita, T., Pepper, W., Pitcher, H., Price, L., Riahi, K., Roehrl, A., Rogner, H.-H., Sankovski, A., Schlesinger, M., Shukla, P., Smith, S., Swart, R., van Rooijen, S., Victor, N., and Dadi, Z. (2000): *IPCC Special Report on Emissions Scenarios*. Cambridge University Press, Cambridge, United Kingdom and New York, NY, USA.

Nash, J. E., and Sutcliffe, J. V. (1970). "River flow forecasting through conceptual models: Part 1. A discussion of principles." *Journal of Hydrology*, 10(3), 282-290.

Neff, R., Chang, H., Knight, C. G., Najjar, R. G., Yarnal, B., and Walker, H. A. (2000). "Impact of climate variation and change on Mid-Atlantic Region hydrology and water resources." *Climate Research*, 14(3), 207-218.

Novotny, E. V., and Stefan, H. G. (2007). "Stream flow in Minnesota: Indicator of climate change." *Journal of Hydrology*, 334(3-4), 319-333.

O'Connor, D. J., and Di Toro, D. M. (1970). "Photosynthesis and oxygen balance in streams." *Journal of the Sanitary Engineering Division*, 96(2), 547-571.

Odum, H. T. (1956). "Primary production in flowing waters." *Limnology and Oceanography*, 1(2), 102-117.

Ouyang, T., Zhu, Z., and Kuang, Y. (2006). "Assessing impact of urbanization on river water quality in the Pearl River Delta Economic Zone, China." *Environmental Monitoring and Assessment*, 120(1), 313-325.

Pope, V., Gallani, M. L., Rowntree, P. R., and Stratton, R. A. (2000). "The impact of new physical paramterizations in the Hadley Centre climate model: HadAM3." *Climate Dynamics*, 16, 123-146.

Rich, P. M., Weintraub, L. H., Chen, L., and Herr, J. "Climate Change Impacts on Hydrology and Water Management of the San Juan Basin." *Amerecan Geophysical Union, Fall Meeting 2005*, 1054.

Samuels, R., Rimmer, A., Hartmann, A., Krichak, S., and Alpert, P. (2010). "Climate change impacts on Jordan River flow: Downscaling application from a regional climate model." *Journal of Hydrometeorology*, 11(4), 860-879.

Schoonover, J. E., Lockaby, B. G., and Pan, S. (2005). "Changes in chemical and physical propertiesof stream water across an urban-rural gradient in western Georgia." *Urban Ecosystems*, 8(1), 107-124.

Sliva, L., and Williams, D. D. (2001). "Buffer zone versus whole catchment approaches to studying land use impact on river water quality." *Water Research*, 35(14), 3462-3472.

Systech (2005). "Creating a WARMF 6.1 Application Using a BASINS 3.1 Delineation: A User's Guide." Systech Water Resources Inc., Walnut Creek, CA.

Tatli, H., Nüzhet Dalfes, H., and Sibel Mente (2004). "A statistical downscaling method for monthly total precipitation over Turkey." *International Journal of Climatology*, 24(2), 161-180.

Tu, J. (2009). "Combined impact of climate and land use changes on streamflow and water quality in eastern Massachusetts, USA." *Journal of Hydrology*, 379(3-4), 268-283.

Tu, J., Xia, Z. G., Clarke, K. C., and Frei, A. (2007). "Impact of urban sprawl on water quality in eastern Massachusetts, USA." *Environmental Management*, 40(2), 183-200.

U.S. Environmental Protection Agency (USEPA). (2004). "Better Assessment Science Integrating point and Nonpoint Sources (BASINS) Version 3.1: User's Manual." *EPA-823-C-04-004*, United States Environmental Protection Agency.

Wang, R. (2010). "Modeling hydrologic and water quality responses to changing climate and land use/cover in the Wold Bay Watershed, South Alabama," M.S. thesis, Auburn University, Auburn, AL.

Wigley, T., Jones, P., Briffa, K., and Smith, G. (1990). "Obtaining sub-grid-scale information from coarse-resolution general circulation model output." *Journal of Geophysical Research*, 95(D2), 1943-1953.

Wilby, R. L., and Dawson, C. W. (2007). "SDSM 4.2–A decision support tool for the assessment of regional climate change impacts." Lancaster University, UK.

Xu, Z. X., Zhao, F. F., and Li, J. Y. (2009). "Response of streamflow to climate change in the headwater catchment of the Yellow River basin." *Quaternary International*, 208(1-2), 62-75.

Zhang, X., Srinivasan, R., and Hao, F. (2007). "Predicting hydrologic response to climate change in the Luohe River basin using the SWAT model." *Transactions of the ASABE*, 50(3), 901-910.

Table 3.1 Key Parameter Values after WARMF Calibration

Parameters	Units	Literature Range	Calibrated Value
Precipitation Weighting Factor	-	0.5 – 1.5	0.74
Evaporation Magnitude	-	0.6 – 1.4	0.91
Evaporation Skewness	-	0.6 – 1.4	0.9
Number of Soil Layers	-	1 – 5	3
Thickness of Soil Layers	cm	> 0	8 – 79
Saturation Moisture	-	0.2 – 0.6	0.35 – 0.45
Field Capacity	-	0 – 0.4	0.18 – 0.31
Initial Moisture	-	0 - 0.6	0.25
Horizontal Conductivity	cm/day	> 0	3600 – 5600
Vertical Conductivity	cm/day	> 0	1800 – 2800
Aeration Factor	/day	0.2 – 1	0.5
Sediment Oxygen Demand	$g/m^2/day$	0.1 – 2	0.8

Table 3.2 WARMF Performance during Calibration and Validation Periods for Daily Flow at USGS 02418230

Statistical Measure	Recommended Values[1]	Calibration (2000-2005)	Validation (2006-2009)
NSE	> 0.5	0.64	0.56
RSR	≤ 0.7	0.60	0.66
PBIAS	± 25%	-2.78%	-9.53%

[1] Recommended values are based on Moriasi et al. (2007) for flow simulation

Table 3.3 Land Use Change in the Saugahatchee Creek Watershed from 1991 to 2008

Land Use Categories	LU 1991	LU 2001	LU 2008
Water	0.92%	1.56%	1.22%
Forest	80.08%	71.41%	72.42%
Urban	3.56%	5.41%	7.92%
Rangeland	8.49%	14.29%	10.42%
Cropland	6.94%	7.32%	8.02%

Table 3.4 List of Predictands (Station Climate Parameters) and Corresponding Predictors used in SDSM Model to Downscale GCMs Output

Station Parameters	Predictors from NCEP/NCAR and HadCM3[1]
Precipitation	500 hPa divergence (p5zh), Relative humidity at 500 hPa (r500), Specific humidity at 500 hPa (s500), Relative humidity at 850 hPa (r850), and Specific humidity at 850 hPa (s850)
Maximum temperature	Mean temperature (temp), and 500 hPa geopotential height (p500)
Minimum temperature	Mean temperature (temp), and Near surface specific humidity (shum)

[1] variable name used in SDSM is given inside parenthesis

Table 3.5 Statistical Summary of Maximum Temperature, Minimum Temperature, and Precipitation Downscaled Based on HadCM3 A2 and B2

	Baseline	HadCM3 A2			HadCM3 B2		
	1961-1990	2020s	2050s	2080s	2020s	2050s	2080s
			Maximum Temperature (°C)				
Average	25.0	25.4	26.5	28.2	25.4	26.2	26.9
St. Dev.	7.7	8.0	8.3	8.7	8.1	8.1	8.5
Maximum	40.0	43.7	44.8	47.3	43.8	44.6	45.4
Minimum	-5.0	3.3	4.7	5.7	0.0	1.8	4.1
			Minimum Temperature (°C)				
Average	12.1	13.5	14.4	15.8	13.5	14.3	15.0
St. Dev.	8.5	8.6	8.8	9.1	8.6	8.7	9.1
Maximum	26.7	28.3	29.3	31.1	26.8	28.5	28.7
Minimum	-17.8	-5.8	-5.3	-4.0	-7.0	-6.2	-5.0
			Precipitation (mm)				
Average	3.7	3.3	3.1	2.8	3.1	2.9	3.1
St. Dev.	10.8	9.5	9.1	8.4	9.1	8.4	8.9
Maximum	199.1	170.0	152.5	176.6	137.0	168.2	140.1
Minimum	0.0	0.0	0.0	0.0	0.0	0.0	0.0

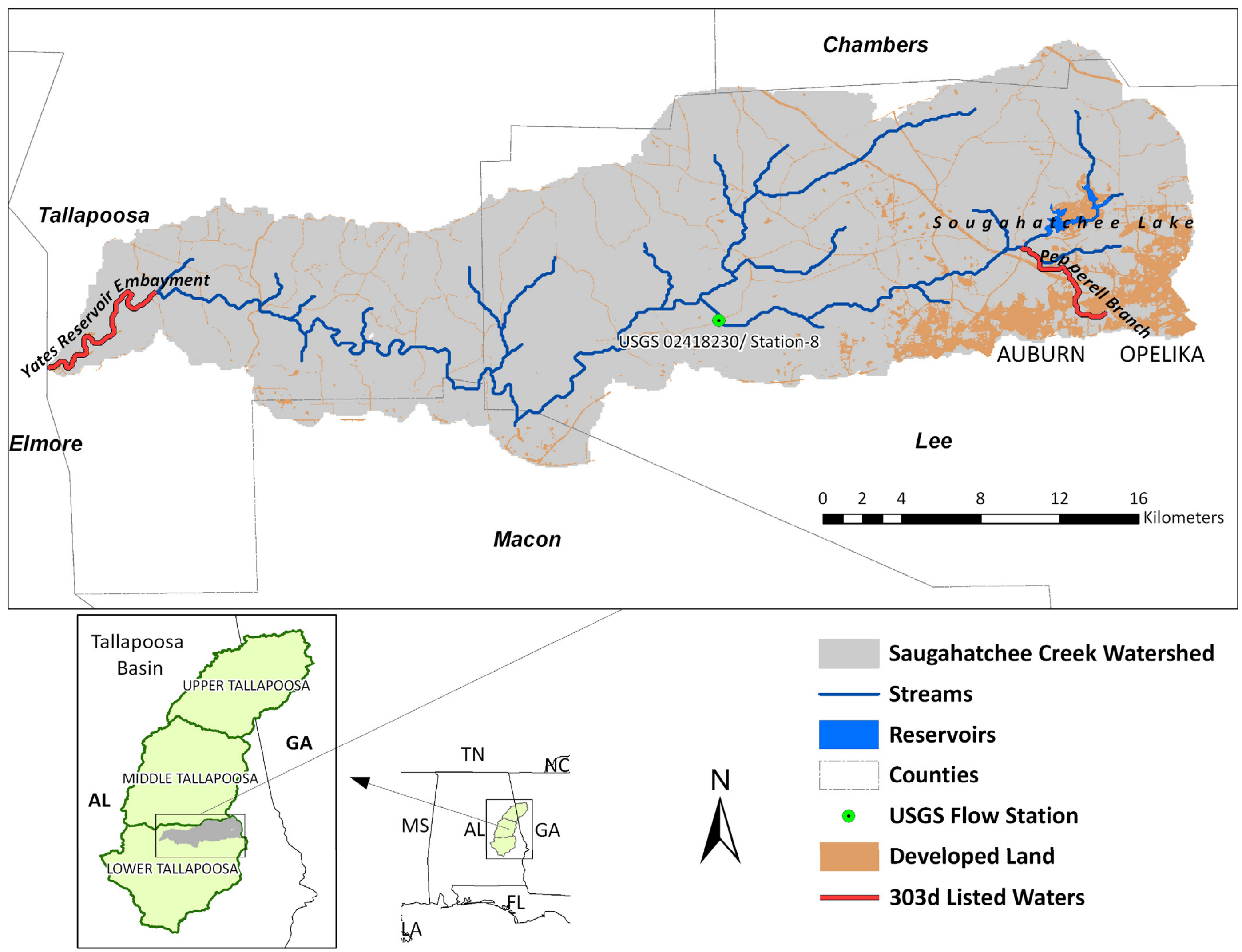

Fig. 3.1 Location map of the Saugahatchee Creek Watershed in the Tallapoosa Basin including surrounding counties in Alabama

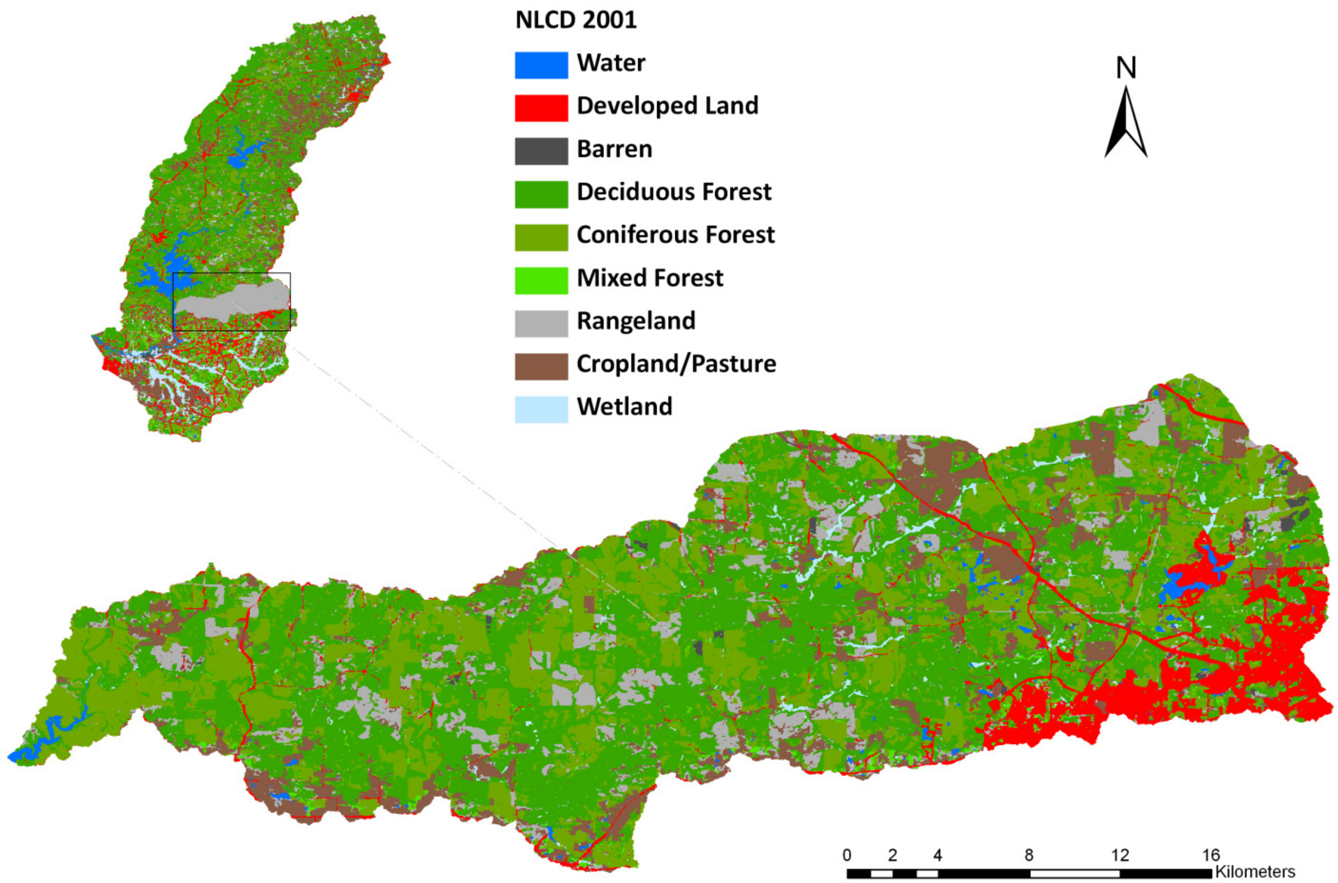

Fig. 3.2 2001 NLCD land use map of the Saugahatchee Creek Watershed

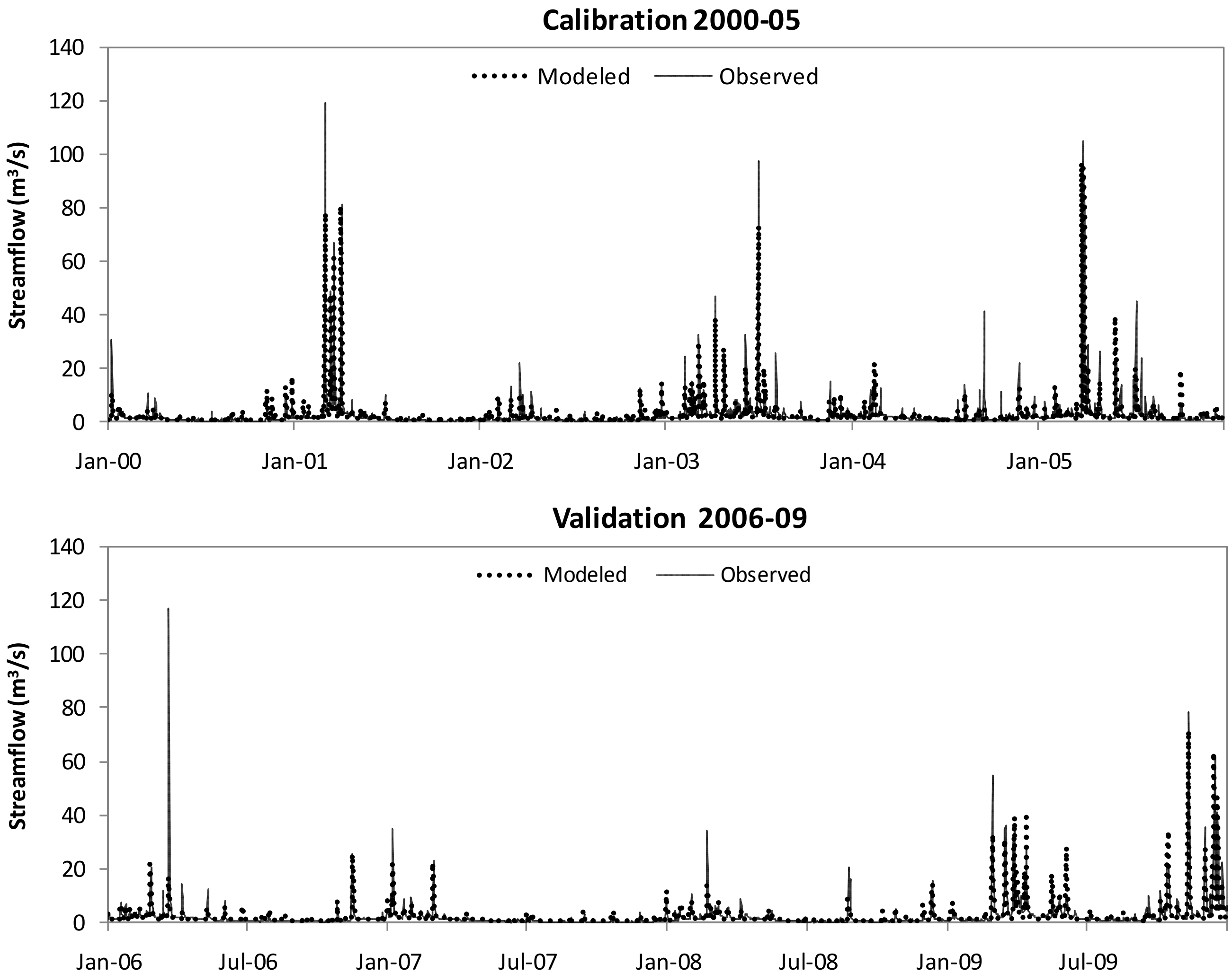

Fig. 3.3 Flow calibration (2000-05) and validation (2006-09) at USGS 02418230 station in the Saugahatchee Creek near Loachapoka

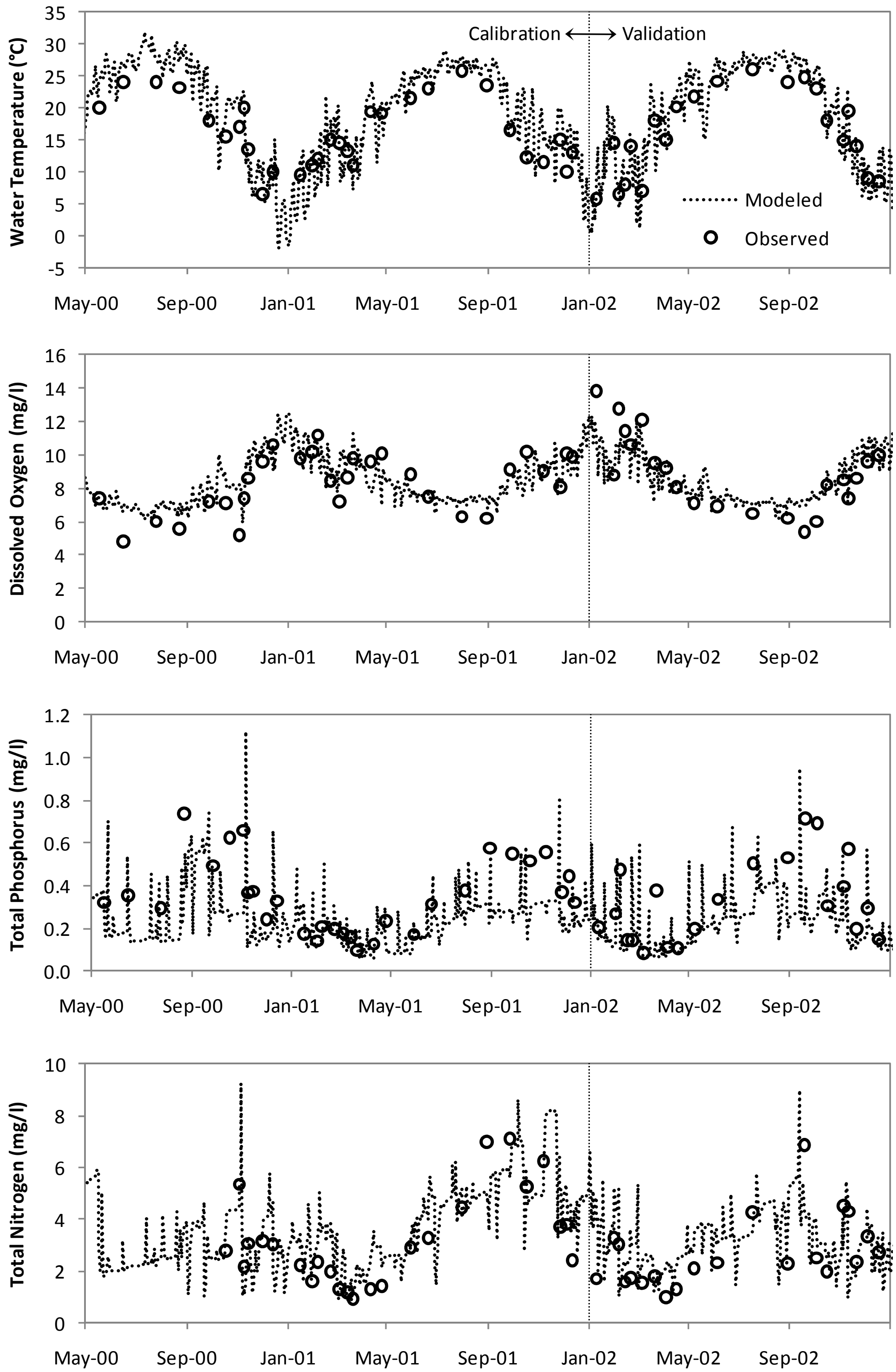

Fig. 3.4 Water quality calibration (2000-01) and validation (2002) at Station-8 near Loachapoka

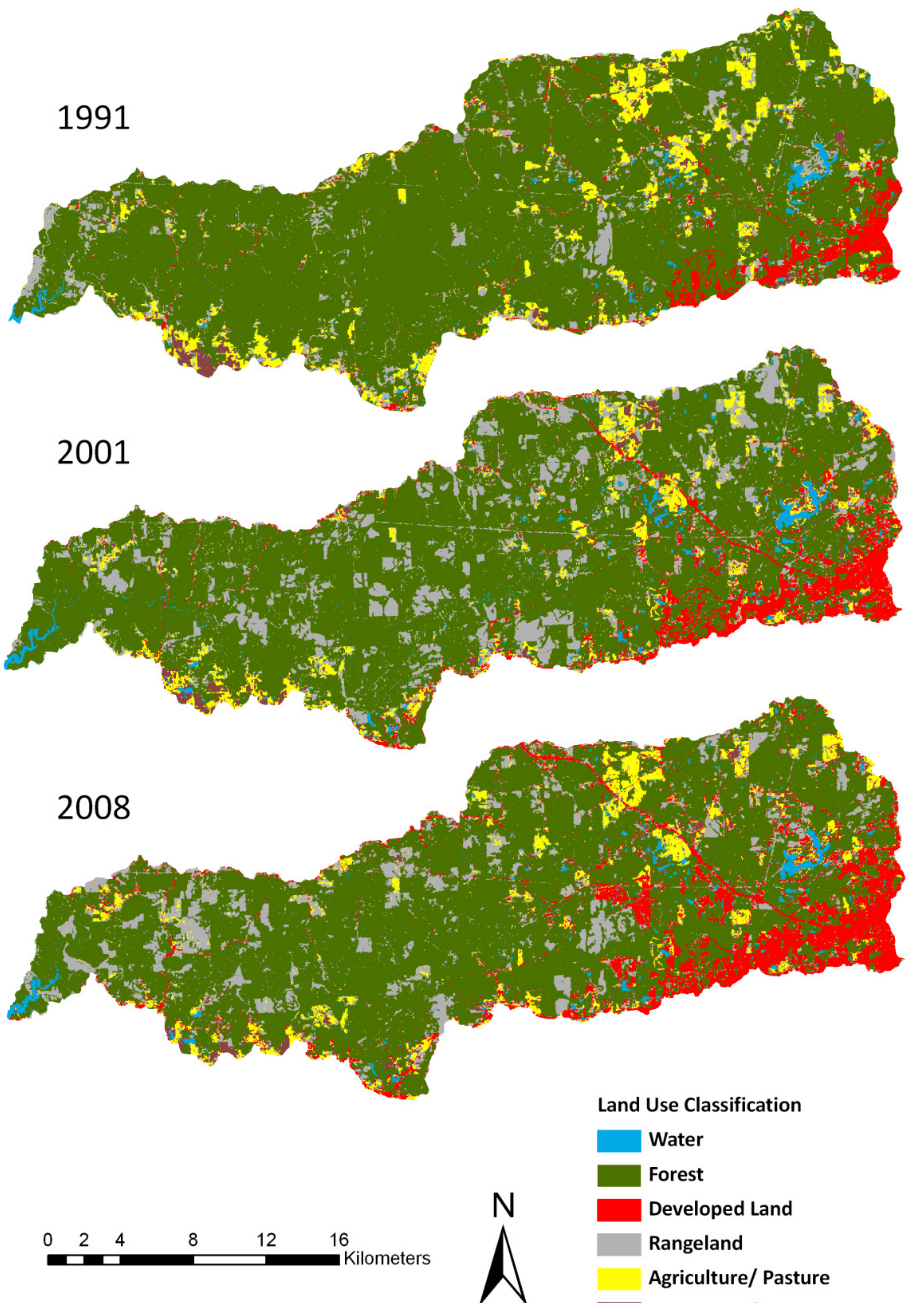

Fig. 3.5 Land use change scenarios for the Saugahatchee Creek Watershed from 1991 to 2008

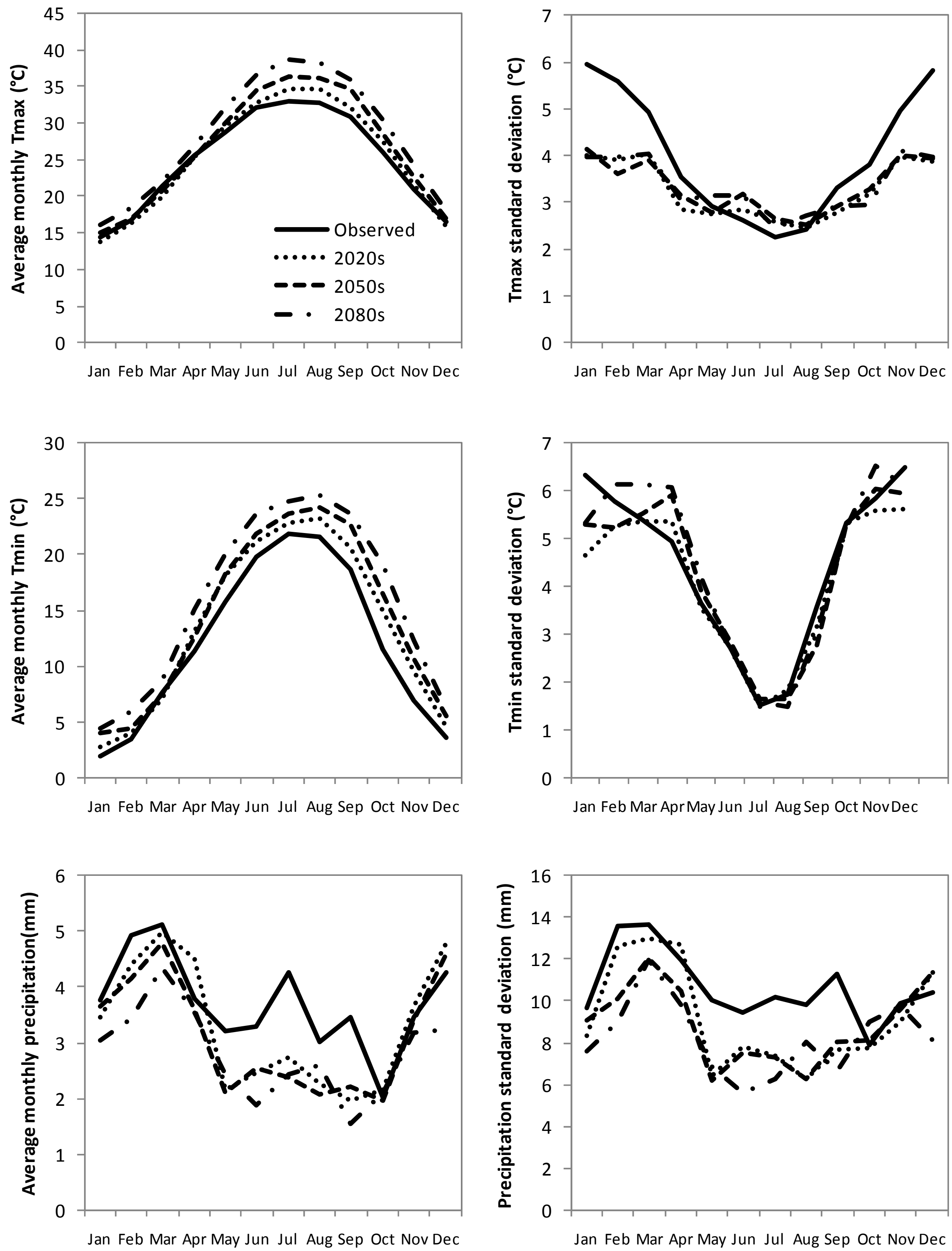

Fig. 3.6 General trend in maximum temperature, minimum temperature, and precipitation corresponding to downscaled climate change scenario based on HadCM3 A2

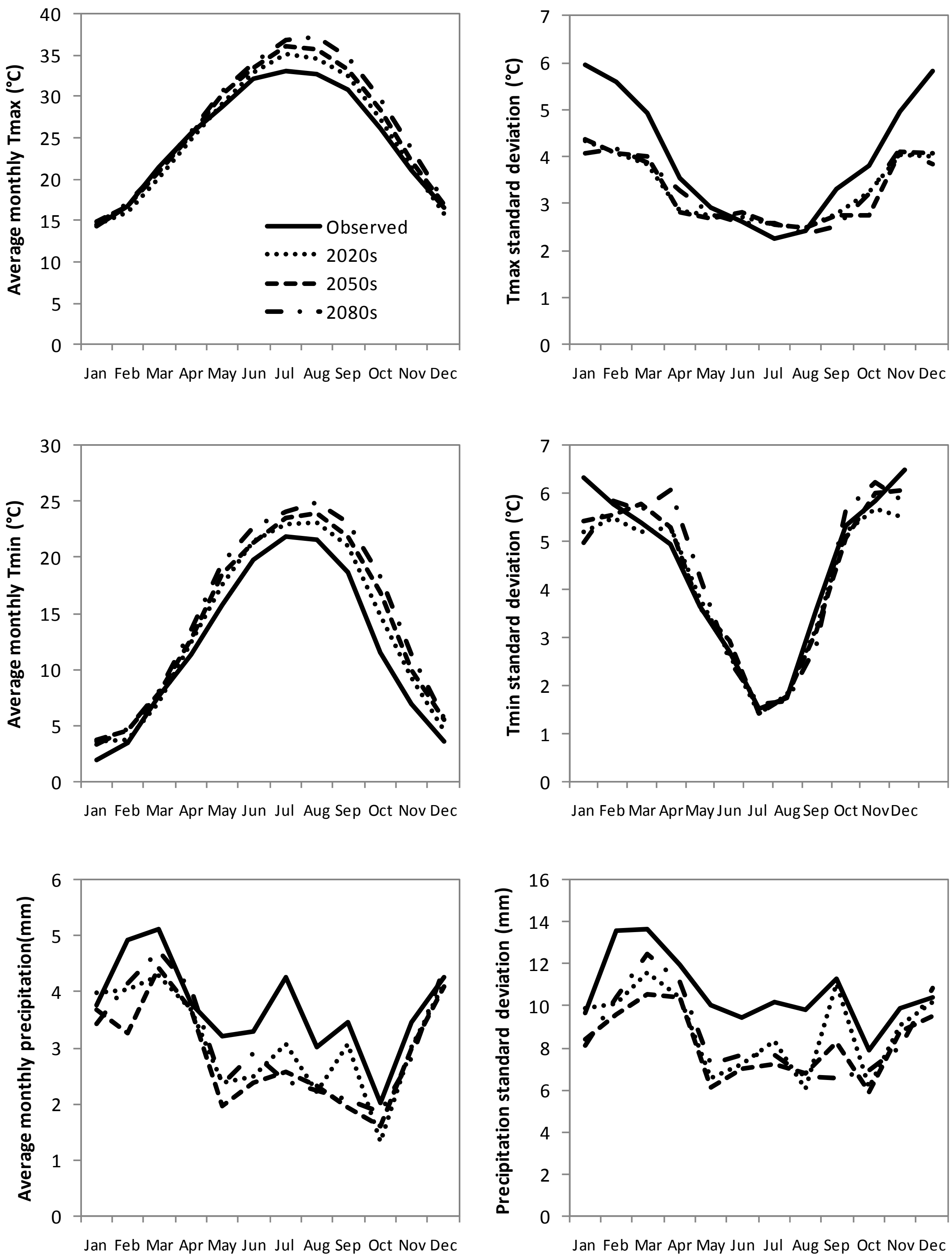

Fig. 3.7 General trend in maximum temperature, minimum temperature, and precipitation corresponding to downscaled climate change scenario based on HadCM3 B2

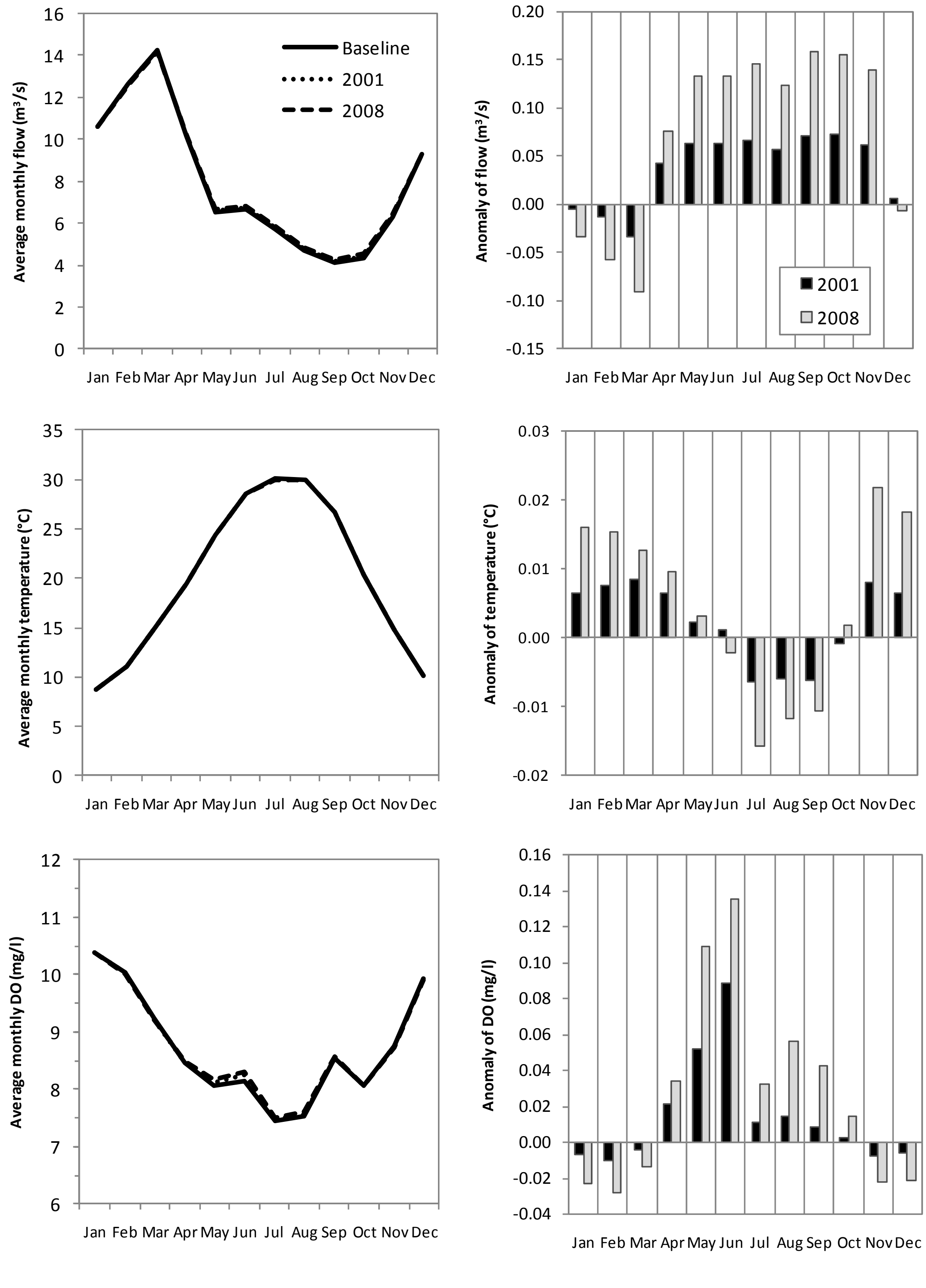

Fig. 3.8 Anomaly of average monthly flow, surface water temperature, and DO oxygen concentration to the baseline corresponding to land use scenarios of 2001 and 2008

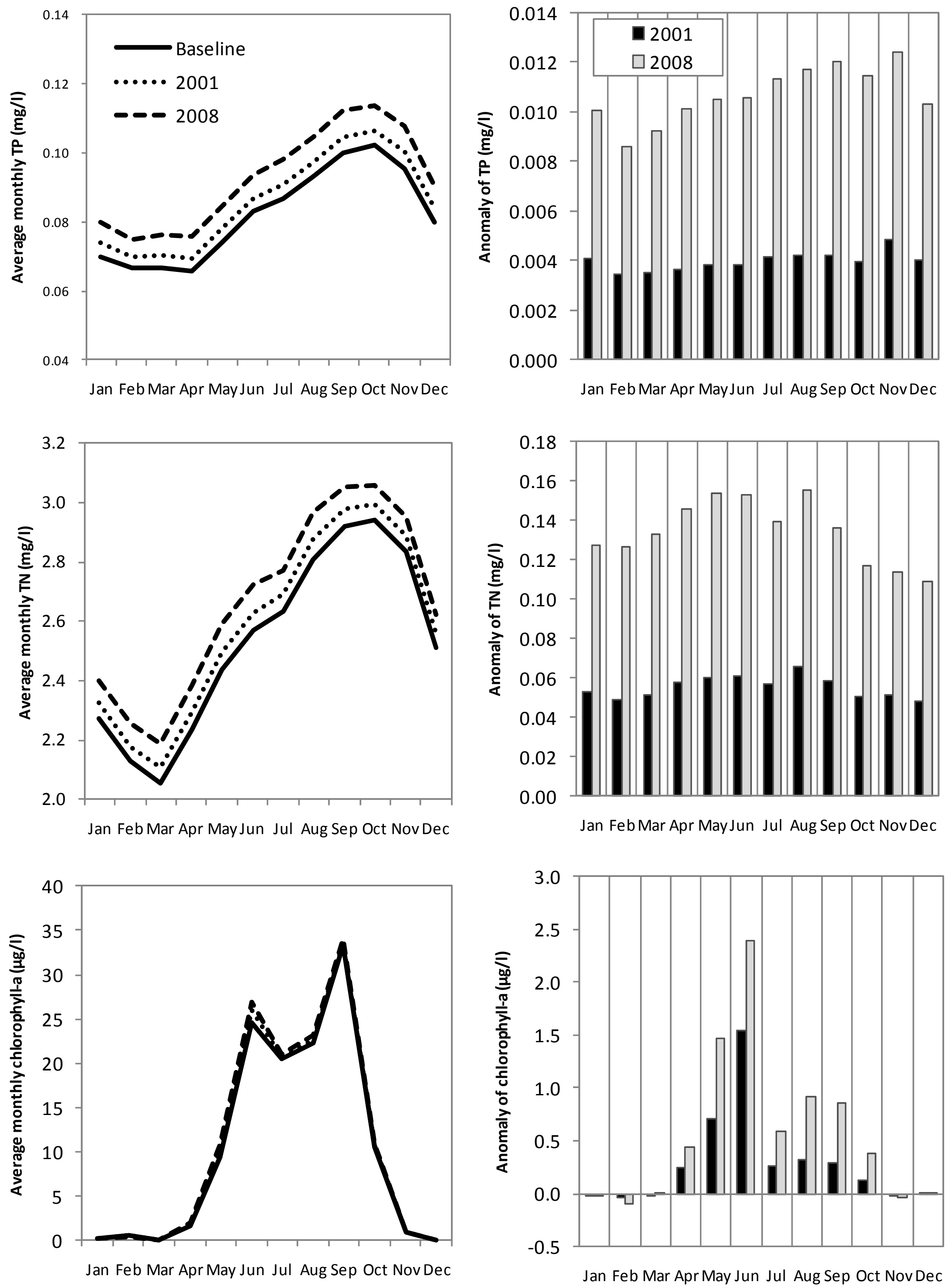

Fig. 3.9 Anomaly of average monthly TP, TN, and chlorophyll-a concentration to the baseline corresponding to land use change scenarios of 2001 and 2008

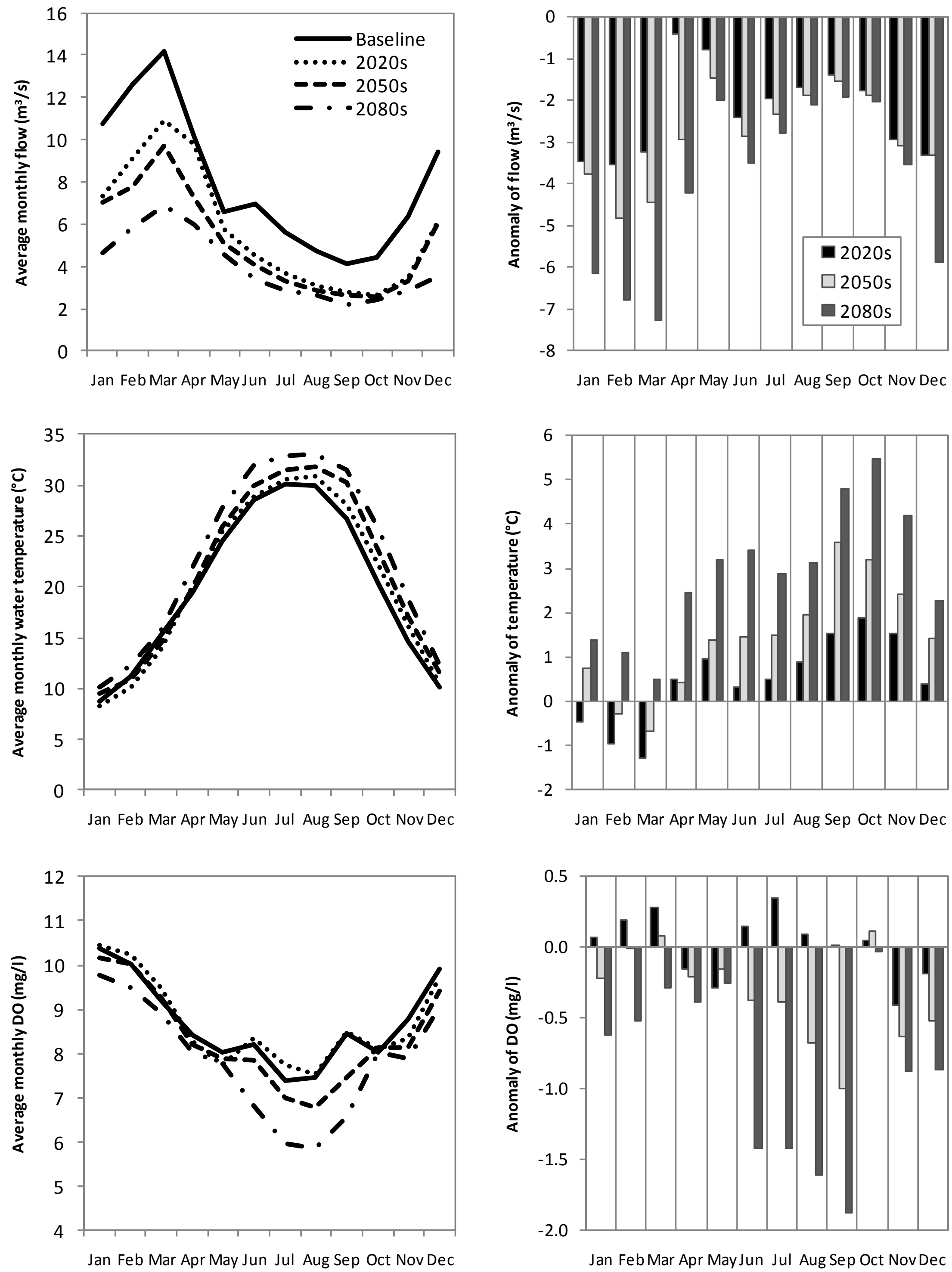

Fig. 3.10 A Anomaly of average monthly flow, surface water temperature and DO concentration to the baseline corresponding to climate change scenarios downscaled with HadCM3 A2

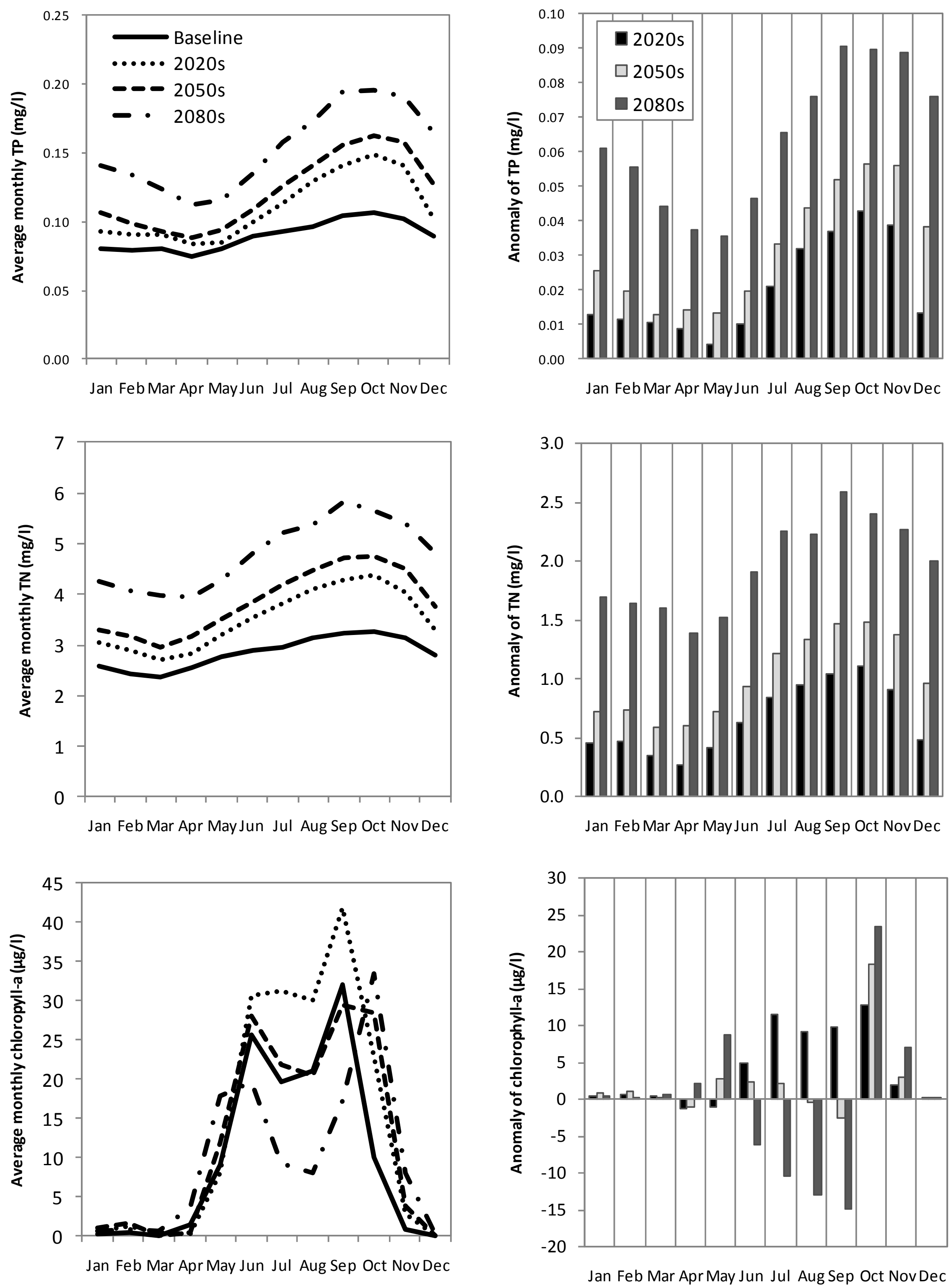

Fig. 3.11 Anomaly of average monthly TP, TN and chlorophyll-a concentration to the baseline corresponding to climate change scenario downscaled with HadCM3 A2

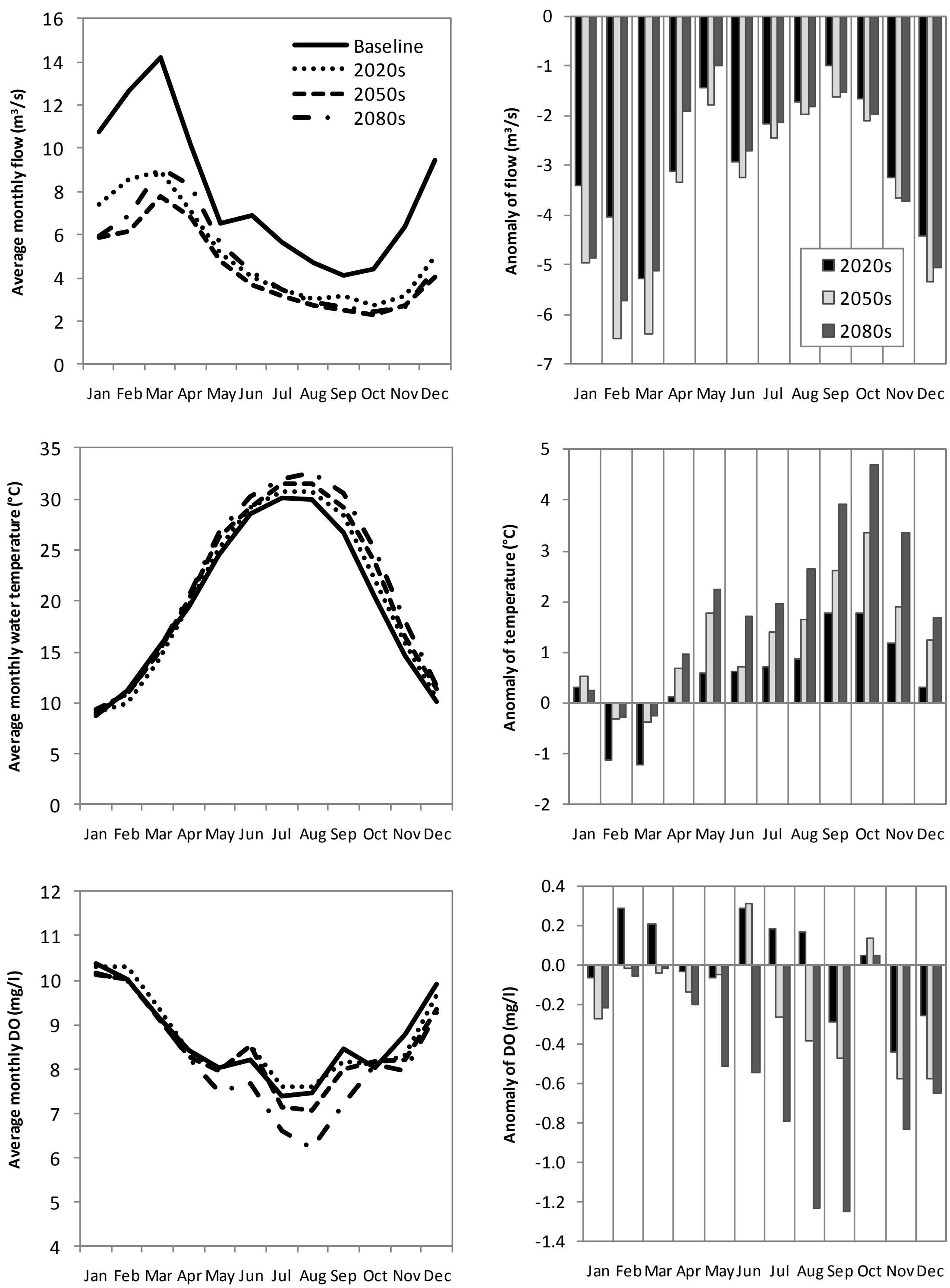

Fig. 3.12 Anomaly of average monthly flow, surface water temperature and DO concentration to the baseline corresponding to climate change scenario downscaled with HadCM3 B2

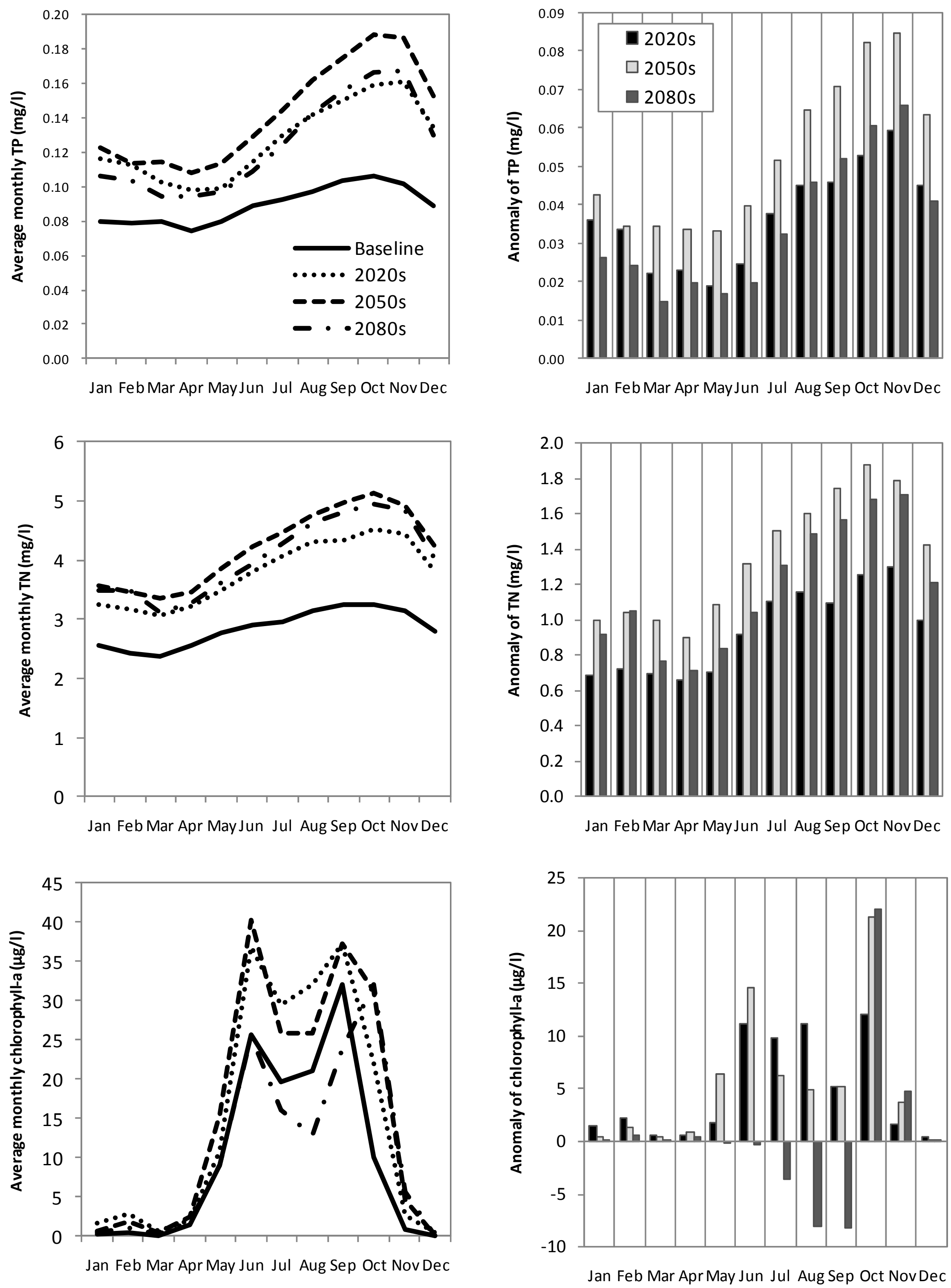

Fig. 3.13 Anomaly of average monthly TP, TN and chlorophyll-a concentration to the baseline corresponding to climate change scenario downscaled with HadCM3 B2

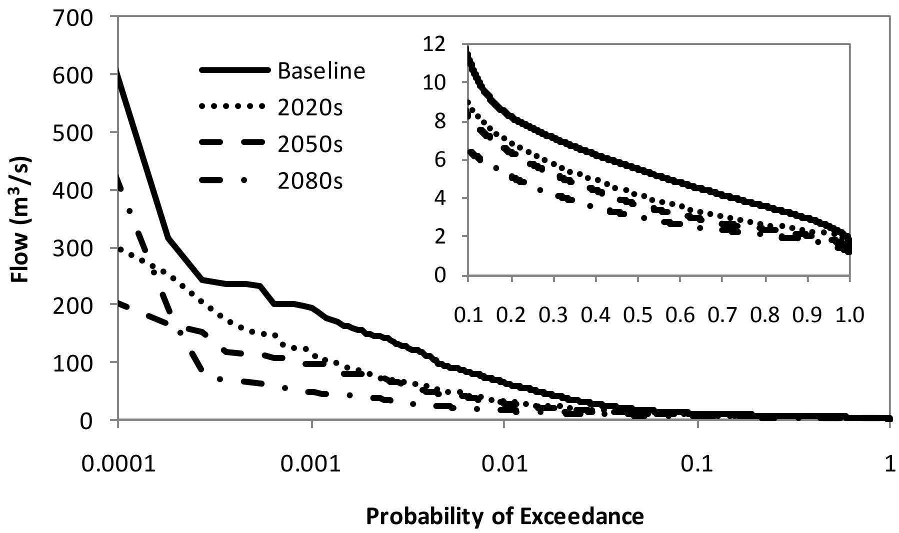

Fig. 3.14 Flow duration curves for baseline and projected HadCM3 A2 future scenarios

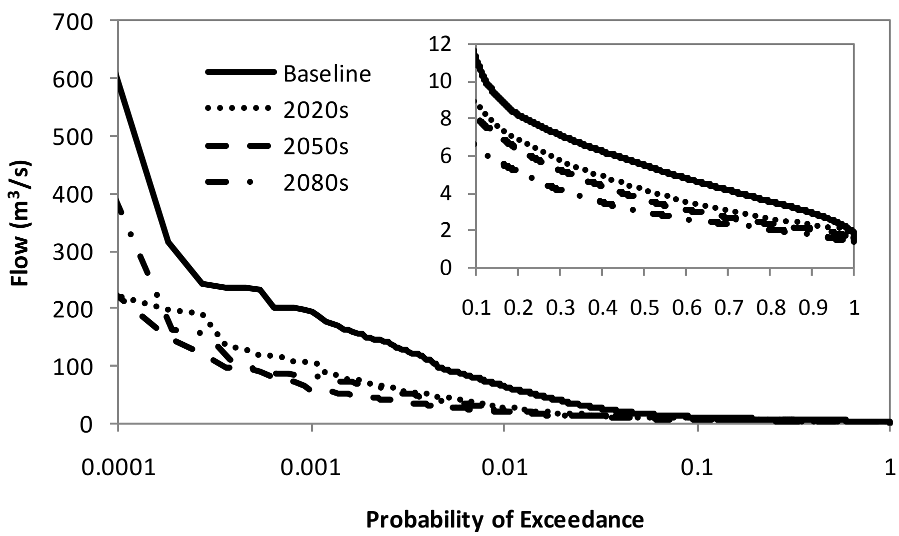

Fig. 3.15 Flow duration curves for baseline and projected HadCM3 B2 future scenarios

Chapter 4. Rainfall Depths of the 95th Percentile Events in the Contiguous U.S.

Preface

Stormwater runoff is the major source of water pollution, mostly in urban and developed areas. Strict stormwater runoff requirements have been enforced by the U.S. Congress for federal projects according to Section 438 of Energy Independence and Security Act (EISA) of 2007, which requires federal agencies to develop and redevelop facilities with a footprint that exceeds 5000 square feet in a manner that maintains or restores the pre-development hydrology to the maximum extent technically feasible. In December 2009, the U.S. Environmental Protection Agency (USEPA) developed and published a technical guidance to help federal agencies in implementing Section 438 of the EISA. Two options listed in the technical guidance are: (1) Retain the 95th percentile rainfall event and (2) Site-specific hydrological analysis. The option 1 is one of the stormwater management practices that manages rainfall onsite and prevents the off-site discharge of the precipitation from all rainfall events less than or equal to the 95th percentile rainfall event.

This chapter is independent of earlier studies in the thesis and is developed with a purpose of developing 95th percentile rainfall isohyetal map for the contiguous US. The 95th percentile 24-hour rainfall depths were computed following the U.S. EPA guidelines at 206 weather stations in the contiguous U.S. The result obtained herein may provide valuable information for engineers and designer to comply with Section 438 of EISA when federal agencies need to design, construct, and maintain stormwater management practices for development and redevelopment projects in the contiguous U.S

Abstract

Based on Section 438 of the Energy Independence and Security Act of 2007, U.S. Environmental Protection Agency (USEPA) published a technical guidance that recommends using the 95th percentile rainfall event for Green Infrastructure/Low Impact Development to preserve or restore the hydrology of the site. The 95th storm rainfall depths for a few selected cities were reported in the technical guidance. In this technical note, the 95th percentile 24-hour rainfall depths were computed following the U.S. EPA guidelines at 206 weather stations/cities in the contiguous U.S. The 95th storm rainfall depths in 18 selected cities were compared with and smaller than those calculated based on hourly rainfall data using the method of L-moments. When compared with NOAA's 1-year 24-hour rainfall depths derived from TP-40 rainfall frequency atlas, the 95th percentile rainfall depths are smaller, and a correlation relation was developed between these two rainfall depths. A table with rainfall depths for 206 U.S. cities was generated for 85th, 90th, and 95th percentiles, and the 85th or 90th percentile rainfall depths are extensively used in many stormwater management manuals in U.S. to determine water quality volume.

Introduction

When lands are developed and urbanized, the hydrologic characteristics of the areas are modified. Urbanization of the land usually results increase in the volume and the peak discharge of runoff. Stormwater runoff in urban and developed areas is one of the leading sources of water pollution in the United States (U.S.) and over the world. In December 2007, U.S. Congress enacted the Energy Independence and Security Act (EISA), and Section 438 of EISA establishes strict stormwater runoff requirements for federal development and redevelopment projects. In December 2009, the U.S. Environmental Protection Agency (USEPA) developed and published a Technical Guidance (USEPA 2009) to help federal agencies in implementing Section 438 of the EISA. The intent of Section 438 is to require federal agencies to develop and redevelop applicable facilities (exceeding 5000 ft^2) in a manner that maintains and restores stormwater runoff to the maximum extent technically feasible (METF) (USEPA 2009). It requires maintaining or restoring the predevelopment site hydrology during the development or redevelopment process (USEPA 2009). U.S. EPA Technical Guidance (USEPA 2009) provides two options for site designers to use and to comply with Section 438: (1) Retain the 95^{th} percentile rainfall event and (2) Site-specific hydrological analysis. The option 1 is one of the stormwater management practices that manages rainfall onsite and prevents the off-site discharge of the precipitation from all rainfall events less than or equal to the 95^{th} percentile rainfall event to METF (USEPA 2009).

U.S. EPA Technical Guidance (USEPA 2009) defines 95^{th} percentile rainfall event as "a precipitation amount which 95 percent of all rainfall events for the period of record do not exceed". U.S. EPA (2009) further defines (page 10 of the Technical Guidance):

"In more technical terms, the 95^{th} percentile rainfall event is defined as the measured precipitation depth accumulated over a 24-hour period for the period of record that ranks as the 95th percentile rainfall depth based on the range of all daily event occurrences during this period."

U.S. EPA Guidance further suggests that implementation of Section 438 can be done by applying Green Infrastructure (GI)/Low Impact Development (LID) management approaches. GI/LID is a stormwater management strategy designed to maintain predevelopment site hydrology by mimicking the natural processes that involve infiltration, evapotranspiration, and reuse of stormwater or runoff. Porous pavements, open drainages, rain barrels, rain gardens, and green roofs are few examples. These on-site design options can be used to manage total volume of rainfall from 95th percentile storms. The 95th percentile was recommended because this storm size appears to best represent the volume that is fully infiltrated in a natural condition and thus should be managed on-site to restore and maintain this pre-development hydrology for duration, rate and volume of stormwater flows (USEPA 2009). The 95th percentile rainfall event was identified because small, frequently-occurring storms produce large proportion of the annual precipitation volume, and the runoff from those storm events significantly alter the discharge frequency, rate and temperature of the runoff.

U.S. EPA Guidance further defines: "The 24-hour period is typically defined as 12:00:00 am to 11:59:59 pm. In general, at least a 20-30 year period of rainfall record is recommended for such an analysis." Storms or rainfall events are defined by a minimum interevent time – a time in which no rainfall occurs. A hourly record of rainfall data may be converted into rainfall events using the specification of a minimum period of no rainfall that defines the separation of storm events (USEPA 1986). Typical minimum interevent time is 4 to 5 hours to separate more or less independent storms (Wanielista and Yousef 1993). The rainfall event or storm depth increases with the increase of the minimum interevent time used to define a storm event. For design of stormwater runoff control structures, e.g., detention ponds, the minimum interevent time to develop rainfall statistics are related to the drawdown time, infiltration time, or treatment time for a given Best Management Practice (BMP) design (Asquith et al. 2006). Therefore, the 24-hour period recommended by U.S. EPA Guidance to organize rainfall data, i.e. using daily rainfall data, is not optimal option, e.g., a rainfall event starting from 10:00 pm and ending at 2:00 am could be reported in two days. The 90th percentile storm depths for minimum interevent times of 6, 8, 12, 18, 24, 48, and 72 hours for 774 weather stations in eastern New Mexico, Oklahoma and Texas were determined using hourly rainfall data and presented by Asquith et al. (2006) in the USGS Professional Paper 1725 (available online at http://pubs.water.usgs.gov/pp1725/). The 90th percentile storm depths increase with the minimum interevent time, for example, it was determined to be 1.92" and 3.34" in Houston, respectively, when the minimum interevent times used to define a storm were 24- and 72-hours (Asquith et al. 2006). Therefore, to specify or determine the 95th percentile rainfall event or depth using daily data recommended by U.S. EPA Guidance (USEPA 2009) would be misleading to engineering community and stormwater management agencies without considering of the drawdown time for detention pond or infiltration time for green infrastructures.

In this technical note, the 95th percentile rainfall depths at 206 cities or weather stations in the contiguous U.S. have been calculated using U.S. EPA recommended procedures. Isohyetal map depicting the patterns of 95th percentile rainfall depths has been constructed using calculated rainfall depths from the 206 stations. The tabulation of the calculated values for all 206 stations is included. The table and isohyetal map provide valuable data for engineers and designer to comply with EISA Section 438 when federal agencies need to design, construct, and maintain stormwater management practices for development and redevelopment projects in the contiguous U.S. A sensitivity analysis was conducted to examine variations of the 95th percentile rainfall depths on the length (e.g., 10, 20, and 30 years) of period of rainfall records used and on specific period of rainfall records chosen by analyst (e.g., 10-year data from 1960's or 1980's). The 95th percentile rainfall depths at 18 selected stations were also calculated using Kappa distribution and L moments that were derived from hourly rainfall data with 24-hour minimum interevent dry period, and were compared with those determined using U.S. EPA Guidance (USEPA 2009). These two 95th rainfall depths were compared and analysed. The 85th and 90th percentile rainfall depths commonly used to determine the water quality volume (WQV) were also computed at the 206 cities and compared with the 95th percentiles.

Calculating the 95th Percentile Rainfall Depths Using U.S. EPA Guidance

A long period of precipitation records, e.g., a minimum of 10 years of data, is recommended by U.S. EPA Guidance to determine the 95th percentile rainfall depths at a location. In this study, the daily rainfall data at 206 weather stations in the contiguous U.S. were obtained from the National Climatic Data Center (NCDC)'s Global Summary of Day (GSOD) product (NCDC 2010). The data inventories for the GSOD product start from as early as 1931 to recent. However, most of the years before 1973 showed discontinuity in rainfall data; with either missing data reported as "99.99" and/or zerorainfall reported as "0" for the whole year. With few exceptions, the rainfall data were available at 206 stations for the period of 1973-2010 (38-year) for our rainfall data analysis.

A computer program was developed to compute n^{th} percentile rainfall depths using long-term precipitation data at 206 stations in the contiguous U.S. The precipitation records for air temperature less than 32 °F were considered as snowfall and were excluded for the analysis. Small rainfall depths that are 2.5 mm (0.1 in.) or less were excluded for the percentile analysis because they generally do not produce any measurable surface runoff due to rainfall loss through interception, depression storage, and infiltration (USEPA 2009; Viessman and Lewis 2003). All the remaining daily rainfall data were sorted in ascending order and the n^{th} percentile was determined using National Institute of Standards and Technology formula (NIST/SEMATECH 2010). For the n^{th} percentile of the data with N records (X_1, X_2… X_N), rank (r) is computed as follows:

$$r = \frac{n}{100}(N-1)+1 \tag{4.1}$$

The rank r was then splitted into its integer component, i and decimal component, d such that $r = i + d$. After the data were arranged in ascending order, the n^{th} percentile value was computed as (NIST/SEMATECH 2010):

$$X_{n}th = \begin{cases} X_1 & for\ i = 0 \\ X_N & for\ i = N \\ X_i + d(X_{i+1} - X_i) & for\ 0 < i < N \end{cases} \tag{4.2}$$

Fig. 4.1 shows daily rainfall frequency spectrum or percentile distributions for Minneapolis, MN and Montgomery, AL. The 95^{th} percentile rainfall depth determined for

Minneapolis is 35.6 mm (1.4 in.) and 53.3 mm (2.1 in.) for Montgomery (Fig. 4.1 and Table 4.1). The 95th percentile rainfall depth determined using U.S. EPA Guidance was based on cumulative probability or occurrence frequency of daily rainfall events, i.e., representing 95% of daily rainfall events. Therefore, the 95% of daily rainfall events in Minneapolis and Montgomery is less than or equal to 35.6 mm and 53.3 mm, respectively.

U.S. EPA Guidance (USEPA 2009) suggests a minimum of 10 years of data and recommends at least a 20-30 year period of rainfall records for the 95th percentile analysis. A sensitivity analysis was conducted to determine the 95th percentile rainfall depths using 10 years, 20 years, and 30 years of data. A moving time window method was used for the sensitivity analysis; the 95th percentile rainfall depths were determined for 10 years of data from 1961 to 1970, 1962 to 1971, and so on, until the end of rainfall record, i.e., 2010 for Minneapolis and Montgomery stations, which have additional rainfall data starting from 1961. Fig. 4.2 shows the 95th percentile rainfall depths determined using moving time window for consecutive 10, 20, and 30 years of daily rainfall data for Minneapolis and Montgomery. When 10 years of data were used, the 95th percentile rainfall depths ranged from 30.5 to 40.6 mm (1.2 to 1.6 in.) with standard deviation of 2.5 mm (0.10 in.) for Minneapolis and 43.2 to 53.4 mm (1.7 to 2.1 in.) with standard deviation of 3.0 mm (0.12 in.) for Montgomery. The variation of the 95th percentile rainfall depths determined using 10 years of data is up to 12.7 mm (0.5 in.) for these two stations, and calculated depths are sensitive to which period of records was used (Fig. 4.2). When 30 years of data were used, the 95th percentile rainfall depths ranged from 33.0 to 38.1 mm (1.3 to 1.5 in.) with standard deviation of 1.3 mm (0.05 in.)

for Minneapolis and 50.8 to 53.3 mm (2.0 to 2.1 in.) with standard deviation of 0.02 for Montgomery (Fig. 4.2). When 20 years of data were used, the ranges of the 95th percentile rainfall depths were about the same (Fig. 4.2) but the standard deviations were slightly larger: 2.0 and 1.0 mm (0.08 and 0.04 in.) for Minneapolis and Montgomery, respectively. These results indicate that the 95th percentile rainfall depths determined using long-term data, e.g., 20 or more years, have smaller variations (< 0.1"); it can be claimed that these values are essential the same regardless the rainfall data used in 1960s or 1990s (Fig. 4.2). Therefore, the 95th percentile rainfall depths determined using 38 years rainfall data from 1973 to 2010 are accurate and representative to historical rainfall conditions. The values of the 95th percentile rainfall depths developed at 206 stations in the contiguous U.S. are listed and reported in Table 4.1 for engineering and stormwater management communities to use.

The 95th percentile rainfall depths determined for 206 stations in the contiguous U.S. ranged from 17.8 mm to 63.5 mm (0.7 in. to 2.5 in.) and was plotted over a U.S. map (Fig. 4.3). Isohyetal map depicting the patterns of 95th percentile rainfall depths was constructed using calculated rainfall depths from the 206 stationsfollowed by isohyetal maps for 90th percentile (Fig. 4.4) and 85th percentile (Fig. 4.5). Gray scale colors in these figures correspond to change or variation of percentile rainfall depths: darker for higher values. For central and eastern U.S., the 95th percentile rainfall depths increase from north to south, e.g., 27.9 mm (1.1 in.) at Sault St. Marie, MI to 63.5 mm (2.5 in.) at Mobile, AL (Fig. 4.3). In the western U.S., there are regions with low rainfall forming decreasing contours. The minimum 95th percentile value is 27.9 mm (0.7 in.) obtained at Rock Springs, WY; Pendleton, OR; Tonopah, NV; Eagle, CO; and Boise, ID (Table 4.1). The low rainfall in the western U.S. is explained by rain shadow effect due to mountain ranges, notably Sierra Nevada and Cascades, which impede the rainfall in the area in the lee of the mountain (Haylock and Nicholls 2000). The southeastern U.S. is relatively wet with higher 95th percentile rainfall depths, as it receives tropical rainstorms from the Gulf of Mexico. The maximum 95th percentile value is 63.5 mm (2.5 in.) obtained at Mobile, AL; Port Arthur, TX, and New Orleans, LA (Table 4.1).

Hirschman and Kosco (2008) reported the 95th percentile rainfall depths for selected stations in U.S. that were also reported by U.S. EPA Guidance (USEPA 2009) and are listed in Table 4.2 for a comparison. The 95th percentile rainfall depths determined in this study are generally in agreement with ones reported by Hirschman and Kosco (2008) except for Seattle in Washington (Table 4.2). For Seattle, the relative difference was 37.5% or 15.2 mm (0.6 in.). In a large city, there are several weather stations in and surrounding the city; and it is possible that rainfall data from different weather stations were used. In the state of Washington, the 95th percentile rainfall depth at Seattle is 25.4 mm (1.0 in.), and at Quillayute, close to the Pacific Ocean, is 50.8 mm (2.0 in.) (Table 4.1). This indicates that there is a large variation of rainfall in that region.

The upper percentiles (e.g., 85th and 90th) of daily (24-hr) rainfall depths have been widely applied to numerous urban stormwater management manuals (Haubner et al. 2001; NYSDEC 2001) and water quality management plans (Riverside County 2004; Williardson and Walden 2004). Therefore, the 85th and 90th percentiles of daily rainfall depths at 206 stations were also computed and reported in Table 4.1. In some states of the contiguous U.S., e.g., Georgia, the upper percentiles are about the same for different stations, but for some other states they are different from station to station, for example, the 90th percentiles in New York ranged from 20.3 to 30.5 mm (0.8 to 1.2 in.) (Table 4.1) and are the same reported by NYSDEC (2001). In Los Angeles County, the 90th percentiles were determined at 90 gaging stations and ranged from 7.6 mm (0.3 in.) to 38.1 mm (1.5 in.) (Williardson and Walden 2004). It is necessary to exercise caution when using the upper percentiles in Table 4.1 for regions with large rainfall variations. For 206 cities in contiguous U.S., the 85th percentiles of daily rainfall depths ranged from 10.2 mm (0.4 in.) to 38.1 mm (1.5 in.) (Table 4.1) with average of 22.9 mm (0.9 in.) and standard deviation of 5.1 mm (0.2 in.); and the 90th percentiles of daily rainfall depths ranged from 12.7 mm (0.5 in.) to 45.7 mm (1.8 in.) (Table 4.1) with average of 27.9 mm (1.1 in.) and standard deviation of 7.6 mm (0.3 in.).

Estimated 95th Percentile Rainfall Depths Using Hourly Data

To analyze storm characteristics, storms or rainfall events are generally defined using a minimum interval of no rainfall, which is known as a minimum interevent time. The U.S. EPA (1986) performed statistical analysis of hourly rainfall in the contiguous U.S. (dividing into six zones) using a minimum interevent dry period of 3 to 4 hours. Driscoll et al. (1989) studied mean rainfall volume and mean duration of runoff-generating events with a minimum interval between rainfall midpoints of 6 hours. Asquith et al. (2006) performed statistical analysis of hourly rainfall data using minimum interevent times of 6, 8, 12, 18, 24, 48, and 72 hours and reported L-moments and percentiles of storm depth and duration for 774 rainfall-gauging stations in Eastern New Mexico, Oklahoma, and Texas. The percentile storm depths depend on the minimum interevent times used, for example, the 90th percentile rainfall depth for Abilene, TX is reported to be 25.9 mm (1.02 in.) for minimum interevent time of 6 hours and 52.1 mm (2.05 in.) for 72 hours (Asquith et al. 2006). Results from Asquith et al. (2006) using the minimum interevent time of 24 hours were used to determine the 95th percentile storm depths that are compared with the 95th percentile rainfall depths using U.S. EPA Guidance developed in the above section.

The data used by Asquith et al. (2006) were National Weather Service hourly rainfall data obtained from Hydrosphere (2003) from 1940-2002 with total of 155 million values of hourly rainfall from 774 stations. For each of the minimum interevent times, the time series of hourly rainfall for each station was separated into sequences of storms for subsequent statistical analysis to develop L-moments and fit Kappa distribution (Asquith et al. 2006).

L-moments are linear combination of the ranked observations ($X_{i:n}$) used for probability distribution fitting. For the *n* sample of data (storm depths) in ascending order, $X_{1:n} \leq X_{2:n} \leq \ldots\ldots \leq X_{n:n}$, L-moments of a probability distribution is defined by Hosking and Wallis (1997) as follows:

Mean:
$$\lambda_1 = \frac{1}{2} E\left(X_{1:1}\right) \tag{4.3}$$

L-scale:
$$\lambda_2 = \frac{1}{2} E\left(X_{2:2} - X_{1:2}\right) \tag{4.4}$$

$$\lambda_3 = \frac{1}{3} E\left(X_{3:3} - 2X_{2:3} + X_{1:3}\right) \tag{4.5}$$

$$\lambda_4 = \frac{1}{4} E\left(X_{4:4} - 3X_{3:4} + 3X_{2:4} - X_{1:4}\right) \tag{4.6}$$

The dimensionless L-moment ratios are

$$L - CV = \frac{\lambda_2}{\lambda_1} \tag{4.7}$$

$$L - skew = \frac{\lambda_3}{\lambda_2} \tag{4.8}$$

$$L - kurtosis = \frac{\lambda_4}{\lambda_2} \tag{4.9}$$

A quantile function is the inverse of a cumulative distribution function for a random variable X, in this case storm depth, and can be defined as:

$$X(F) = \mu \times x(F) \tag{4.10}$$

where X(F) is the variable for non-exceedance probability, F; μ is the arithmetic mean of the variable; and x(F) is the dimensionless quantile function (a dimensionless frequency curve). The dimensionless Kappa distribution as quantile function for storm depth was preferable in terms of quality of distribution fit (Asquith et al. 2006) and is given as (Hosking 1994):

$$x(F) = \xi + \frac{\alpha}{\kappa}\left[1 - \left(\frac{1 - F^h}{h}\right)^{\kappa}\right] \tag{4.11}$$

Where, ξ, α, κ and h are parameters of Kappa distribution. These four parameters can be computed using the mean, L-CV, L-skew and L-kurtosis (Hosking and Wallis 1997). However, Kappa parameter estimation is not manually tractable. Hosking and Wallis (1997) report that there are no simple expressions for the Kappa parameters in terms of the L-moments. Newton-Raphson iteration can be used for parameter estimation, as described by Hosking (1997). Fig. 4.6 shows an example of non-exceedance probability or percentile distribution of daily rainfall depths at Abilene Regional Airport, Texas, and quantile values of rainfall depths computed from Kappa distribution using Kappa parameters derived from 38-year daily rainfall data (1973 to 2010). Fig. 4.6 demonstrates that Kappa distribution describes percentiles of daily rainfall depths well, and Asquith et al. (2006) also showed that Kappa distribution represents well non-exceedance probability distribution of storm depths derived from hourly rainfall data using minimum interevent time of 24 hours.

In this study, the 95th percentile of storm depth using hourly data was calculated using Kappa distribution parameters derived from site-specific L-moment ratios that were calculated by Asquith et al. (2006). L-moment ratios for 18 selected stations in the eastern New Mexico, Oklahoma and Texas were extracted from the USGS Professional Paper 1725 (Asquith et al. 2006) and used to calculate Kappa distribution parameters (Table 4.3) for each station separately using Newton-Raphson iteration. These 18 selected stations have 33 to 63 years of hourly rainfall record to compute L-moment ratios, and mean storm depth with minimum interevent time of 24 hours ranged from 6.4 mm (0.25 in.) to 16.8 mm (0.66 in.). The quantiles of storm depths having minimum interevent time of 24 hours were calculated using Equation (4.10) and (4.11), e.g., using $F = 0.95$ to compute the 95th percentiles of storm depths for 18 stations, results are listed in Table 4.4. The 95th percentile rainfall depths computed from daily rainfall data using U.S. EPA Guidance (USEPA 2009) from these 18 stations were originally given in Table 4.1 as a subset of the 206 stations and listed again in Table 4.4 for easy comparison. Differences of 95th percentile rainfall or storm depths estimated between from daily rainfall data and hourly rainfall data (Kappa distribution) are listed in Table 4.4 and ranged from -22.9 to 2.5 mm (-0.9 to 0.1 in.).

The 95th percentile rainfall depths computed using the daily rainfall data are less than the 95th storm depths calculated using Kappa distribution with parameters derived from hourly rainfall data except El Paso, Texas (dry and desert area). Underestimation of the 95th percentile 24-hr storm depths for the 18 stations was up to 32.0% when daily rainfall data was used. U.S. EPA Guidance (USEPA 2009) states that the 95th percentile rainfall event represents a precipitation amount that 95 percent of all rainfall events for the period of record do not exceed. It is relatively easy to compute the rainfall depth for the 95th percentile rainfall event based on daily rainfall data (e.g., from NOAA). Underestimate of the 95th percentile rainfall depths can be significant in comparison to the 95th percentile of storm depths estimated from hourly data organized as storm events using minimum interevent time of 24 hours. Fig. 4.7 (left) shows regression equation between the 95th percentile daily rainfall depth and the 95th percentile 24-hr storm depths (derived from hourly data) with Pearson's correlation coefficient (R) of 0.89 for 18 selected stations studied at the confidence level of 95% (p-value < 0.05).

Discussions

The U.S. Weather Bureau Technical Paper No. 40 (TP-40) (Hershfield 1963) is a rainfall frequency atlas of the United States that includes 24-hour rainfall depths for return periods from 1 to 100 years. The 1-year 24-hour rainfall depths for the 18 weather stations in Table 4.4 were adopted from TP-40 and listed in the first column of Table 4.5 for comparison. The 1-year 24-hour rainfall depths for the 18 weather stations are on the average 54.0% (ranged from 18.2% to 85.0%) or 25.4 mm (1.0 in.) (ranged from 5.1 to 43.2 mm or 0.2 to 1.7 in.) larger than the 95th percentile of rainfall depths estimated from daily rainfall data. The 95th percentile rainfall depth calculated using U.S. EPA guidance correlated well with NOAA's 1-year 24-hour rainfall (Fig. 4.7) with Pearson's correlation coefficient (R) of 0.93, which implies strong linear correlation between them at the confidence level of 95% (p-value < 0.05).

U.S. EPA suggests that water quality volume (WQV) for BMPs is the storage needed to capture and treat "the runoff from 90% of average annual rainfall" for BMPs in urban watersheds (Clar et al. 2004). The Iowa Stormwater Management Manual (ISU 2009) states "In numerical terms, it is equivalent to the rainfall depth in inches (the 90% cumulative frequency rainfall depth) multiplied by the volumetric runoff coefficient (R_v) for the site, and the site drainage area." The 90% cumulative frequency rainfall depth is the same as 90th percentile rainfall depth based on cumulative probability or occurrence frequency of daily rainfall events, i.e., representing 90% of daily rainfall events. However, "the runoff from 90% of average annual rainfall" suggested by U.S. EPA (Clar et al. 2004) could be interpreted as cumulative percent of average annual rainfall multiplied by the volumetric runoff coefficient. The 90 percent of average annual rainfall can be determined by sorting long-term 24-hr (daily) rainfall data from the lowest to the highest and then computing cumulative rainfall depths and corresponding cumulative percents of average annual rainfall over K years of records.

$$\text{Cumulative percent of rainfall depth, } X_i = Xi = \frac{\sum_{i=1}^{m}\left(X_i/K\right)}{\sum_{i=1}^{N}\left(X_i/K\right)} \tag{4.12}$$

Where, *m* is the number of daily rainfall depths that are less than or equal to the rainfall record X_i from the total number of N records (X_1, X_2, …, X_i, … X_N) at a weather station. The Iowa Stormwater Management Manual (ISU 2009) shows that, using 46-year (1960-2006) rainfall data at Ames, IA, "90.6% of the rainfall events (greater than 0.1 inch) had a depth of 1.25 inches or less", and this is the 90th percentile rainfall depth similar to the depth reported in Table 4.1 for current study. Based on cumulative percent of average annual rainfall, BMP to capture and treat the runoff of 90% of average annual rainfall is 2" rainfall at Ames, IA (ISU 2009), and this is 60% larger than the 90th percentile at Ames. Pan et al. (2009) computed design rainfalls for water quality volume at 31 major cities in China. Design rainfall determined for Beijing, China was 35 mm (1.4 in.) using 90th percentile of daily rainfall events and 70 mm (2.8 in.) using 90% (cumulative percent) of average annual rainfall (Pan et al. 2009).

Using cumulative percent of average annual rainfall as described in Equation (4.12), the rainfall depths for BMP to capture and treat the runoff of 90% of average annual rainfall were determined at 206 U.S. cities. For example, the rainfall depths from 90% of average annual rainfall are 45.7 mm (1.8 in.) in Minneapolis and 66.0 mm (2.6 in.) in Montgomery (Fig. 4.8), which are much larger than the 90th percentile depths determined by frequency of the number of events (Table 4.1). Statistical summary of rainfall depths that can capture 90% of average annual rainfall based on cumulative percent of rainfall depth (not by number of events) at 206 stations in the contiguous U.S. is given in Table 4.6 including statistical summary of 90th and 95th percentile rainfall depths for comparison. The ratio of 90% of average annual rainfall (cumulative percent) and 90th percentile of daily rainfall events was calculated for each of the 206 stations, and the statistical summary of the ratio is given in Table 4.6 (the last column). On the average, 90% of average annual rainfall determined from cumulative percent of daily rainfall depths is about 88% larger than the 90th percentile rainfall depth determined from cumulative occurrence frequency of daily rainfall events. This is similar to the results from Pan et al. (2009) and reported by the Iowa Stormwater Management Manual (ISU 2009). Unfortunately, U.S. EPA (Clar et al. 2004) did not specifically explain how "the runoff from 90% of average annual rainfall" should be quantified. Based on the data analysis at the 206 stations in the contiguous U.S., depending on interpretation on design rainfall, the water quality volume of a BMP can be quite different.

Conclusions

Rainfall percentile statistics is valuable for estimating design storms, e.g., for water quality improvement, low impact development, and green infrastructures. The 95th percentile rainfall, recommended value for design storm by U.S. EPA, was determined and reported at 206 stations/cities in the contiguous U.S. using daily rainfall data from 1973 to 2010. The 95th percentiles ranged from 17.8 mm (0.7 in.) to 63.5 mm (2.5 in.). The sensitivity analysis has indicated that the 95th percentile rainfall depths determined using long-term data, e.g., 20 or more years, have small variations (< 0.1 in.) and are independent of data period used. Comparing with the 95th percentile rainfall depths derived from hourly data at 18 selected stations in eastern New Mexico, Oklahoma and Texas, the 95th percentile rainfall depths derived from daily rainfall record was typically underestimated. The 95th percentile daily rainfall depths are linearly corrected well with NOAA's 1-yr 24-hour rainfall depth reported in TP-40 but 95th percentiles are smaller.

Water quality volume determined using 90% cumulative percent of average annual rainfall is on average 88% larger than one determined using 90^{th} percentiles of daily rainfall.

References

Asquith, W. H., Roussel, M. C., Cleveland, T. G., Fang, X., and Thompson, D. B. (2006). "Statistical characteristics of storm interevent time, depth and duration for eastern new Mexico, Oklahoma, and Texas." *Professional Paper 1725, Rep. No. 5-4194-01-1*, U.S. Geological Survey, Austin, TX.

Clar, M. L., Barfield, B. J., and O'Connor, T. P. (2004). "Stormwater best management practice design guide: Volume 1 general considerations." *Rep. No. EPA/600/R-04/121*, U.S. Environmental Protection Agency, Cincinnati, OH.

Driscoll, E. D., Palhegyi, G. E., Strecker, E. W., and Shelley, P. E. (1989). "Analysis of storm event characteristics for selected rainfall gages throughout the United States." U.S. Environmental Protection Agency, Washington, D.C.

Guo, J. C. Y., and Urbonas, B. (1996). "Maximized detention volume determined by runoff capture tatio." *Journal of Water Resources Planning and Management*, 122(1), 33-39.

Haubner, S., Reese, A., Brown, T., Claytor, R., and Debo, T. (2001). "Unified stormwater sizing criteria." *Georgia Stormwater Management Manual Volume 2 Technical Handbook,* <http://www.georgiastormwater.com/vol2/1-3.pdf> (Nov. 6, 2010)

Haylock, M., and Nicholls, N. (2000). "Trends in extreme rainfall indices for an updated high quality data set for Australia, 1910-1998." *International Journal of Climatology*, 20(13), 1533-1541.

Hershfield, D. M. (1963). "Rainfall frequency atlas of the United States for durations from 30 minutes to 24 hours and return periods from 1 to 100 years." U.S. Weather Bureau, U.S. Department of Commerce, Washington, D.C.

Hirschman, D., and Kosco, J. (2008). "Managing stormwater in your community: A guide for building an effective post-construction program." *EPA Publication No. 833-R-08-001*, Center for Watershed Protection, Ellicott City, MD.

Hosking, J. R. M. (1994). "The four-parameter kappa distribution." *IBM Journal of Research and Development*, 38(3), 251-258.

Hosking, J. R. M. (1997). "Fortran routines for use with the method of L-moments, Version 3.02." *Research Rep. RC-20525,* IBM Research Division, T. C. Watson Research Center, Yorktown Heights, NY.

Hosking, J. R. M., and Wallis, J. R. (1997). *Regional frequency analysis: an approach based on L-moments*, Cambridge Univ Pr., Cambridge, U.K.

Hydrosphere. (2003). "NCDC hourly precipitation - West." (CD-ROM), Hydrosphere Data Products Inc., v. 13.2, Boulder, CO.

Iowa State University (ISU). (2009). "Stormwater hydrology. " *Iowa Stormwater Management Manual*, <http://www.intrans.iastate.edu/pubs/stormwater/ index.cfm> (Mar. 17, 2011).

National Climatic Data Center (NCDC). (2010). "Global summary of day. "*NNDC climate data online,* <http://www.ncdc.noaa.gov/oa/climate/onlineprod/ drought/xmgr.html> (May 18, 2009).

NIST/SEMATECH. (2010). "Product and process comparisons." *e-Handbook of statistical methods,* <http://www.itl.nist.gov/div898/handbook/ > (Aug. 20, 2010).

New York State Department of Environmental Conservation (NYSDEC). (2001). " Unified stormwater sizing criteria." *New York State Stormwater Management Design Manual*. <http://www.dec.ny.gov/chemical/29072.html> (Nov. 6, 2010).

Pan G., Che W., Li J., and Li H.Y. (2008). "Urban runoff pollution control quantity and its design rainfall in China." *China Water & Wastewater*, 24(22), 25-29.

Riverside County. (2004). "Water quality management plan for urban runoff." Storm Water Clean Water Protection Program, Riverside County, CA.

U.S. Environmental Protection Agency (USEPA). (1986). "Methodology for analysis of detention basins for control of urban runoff quality." *EPA 440/5-87-001*, U.S. Environmental Protection Agency, Washington, D.C.

USEPA. (2009). "Technical Guidance on Implementing the Stormwater Runoff Requirements for Federal Projects under Section 438 of the Energy Independence and Security Act." *EPA 841-B-09-001*, U.S. Environmental Protection Agency, Washington, D.C.

Viessman, W., and Lewis, G. L. (2003). *Introduction to hydrology*, Pearson Education, Upper Saddle River, NJ.

Wanielista, M. P., and Yousef, Y. A. (1993). *Stormwater management*, John Wiley & Sons, Inc., New York, NY.

Williardson, B., and Walden, A. (2004). "Analysis of 85th percentile 24-hour rainfall depths within the County of Los Angeles." Water Resources Division/ Hydrology Section, Department of Public Works, County of Los Angeles, CA.

Table 4.1 The 85th. 90th, 95th Percentile, and 90% Cumulative Rainfall Depths (in.) Derived Using Daily Rainfall Data for 206 Weather Stations or Cities in the Contiguous U.S.

State	Station/City	Latitude	Longitude	Percentile Rainfall Depth (in.)			90% Cumulative Rainfall Depth (in.)
				85th	90th	95th	
AL	Birmingham	33.564	-86.754	1.2	1.5	2.0	2.4
AL	Huntsville	34.644	-86.786	1.2	1.4	2.0	2.6
AL	Mobile	30.688	-88.246	1.4	1.8	2.5	3.6
AL	Montgomery	32.301	-86.394	1.3	1.6	2.1	2.6
AR	Fort Smith	35.334	-94.365	1.1	1.4	1.9	2.5
AR	Little Rock	34.916	-92.146	1.3	1.6	2.1	2.6
AZ	Flagstaff	35.140	-111.672	0.7	0.9	1.3	1.4
AZ	Phoenix	33.443	-111.990	0.7	0.8	1.1	1.3
AZ	Prescott	34.652	-112.421	0.6	0.8	1.0	1.1
AZ	Tucson	32.131	-110.955	0.7	0.9	1.2	1.7
CA	Bakersfield	35.434	-119.056	0.5	0.6	0.8	1.8
CA	Fresno	36.780	-119.719	0.6	0.8	0.9	1.0
CA	Los Angeles	33.938	-118.406	1.1	1.3	2.0	4.7
CA	Sacramento	38.513	-121.493	0.8	0.9	1.2	1.5
CA	San Diego	32.735	-117.169	0.9	1.1	1.5	1.7
CA	San Francisco	37.620	-122.398	0.9	1.1	1.5	2.1
CA	Santa Maria	34.916	-120.465	0.9	1.1	1.5	2.3
CO	Buckley	39.702	-104.752	0.7	0.9	1.2	1.6
CO	Colorado Spring	38.812	-104.711	0.6	0.8	1.0	1.3
CO	Denver	39.833	-104.658	0.6	0.8	1.0	1.3
CO	Eagle	39.643	-106.918	0.5	0.6	0.7	0.9
CO	Grand Junction	39.134	-108.538	0.5	0.6	0.8	4.1
CO	Pueblo	38.290	-104.498	0.6	0.6	0.9	1.0
CT	Bridgeport	41.175	-73.146	1.0	1.2	1.6	1.9
CT	Hartford	41.938	-72.683	1.0	1.3	1.7	2.1
DC	Washington	38.865	-77.034	0.9	1.1	1.5	1.7
DE	Wilmington	39.673	-75.601	1.0	1.2	1.6	1.9
FL	Daytona Beach	29.177	-81.060	1.1	1.4	2.0	2.6
FL	Jacksonville	30.494	-81.693	1.1	1.5	2.0	2.6
FL	Miami	25.824	-80.300	1.2	1.5	2.1	2.9
FL	Tallahassee	30.393	-84.353	1.4	1.7	2.4	3.2
FL	Tampa	27.961	-82.540	1.2	1.4	1.9	2.4
FL	West Palm Beach	26.685	-80.099	1.1	1.4	2.1	3.0
GA	Athens	33.948	-83.327	1.1	1.4	1.8	2.4
GA	Atlanta	33.640	-84.427	1.1	1.4	1.8	2.2
GA	Augusta	33.370	-81.965	1.1	1.3	1.7	2.3
GA	Columbus	32.516	-84.942	1.1	1.4	1.9	2.4
GA	Macon	32.688	-83.654	1.1	1.4	1.8	2.3
GA	Savannah	32.119	-81.202	1.1	1.3	1.9	2.7
IA	Des Moines	41.538	-93.666	1.0	1.2	1.7	2.1
IA	Sioux City	42.391	-96.379	0.9	1.1	1.5	2.1
IA	Waterloo	42.554	-92.401	0.9	1.2	1.5	1.9
ID	Boise	43.565	-116.220	0.4	0.5	0.7	1.6
ID	Coeur D'Alene	47.774	-116.817	0.5	0.6	0.8	0.9
ID	Pocatello	42.920	-112.571	0.4	0.6	0.8	1.3
IL	Chicago	41.986	-87.914	0.9	1.1	1.5	2.0
IL	Greater Peoria	40.668	-89.684	0.9	1.1	1.5	1.9
IL	Greater Rockford	42.196	-89.093	0.9	1.1	1.6	1.9
IL	Moline	41.465	-90.523	1.0	1.2	1.6	2.0
IL	Springfield	39.845	-89.684	0.9	1.1	1.5	2.1
IN	Evansville	38.043	-87.537	1.0	1.3	1.8	2.2
IN	Fort Wayne	41.006	-85.206	0.8	1.0	1.4	1.6
IN	Indianapolis	39.710	-86.272	0.9	1.1	1.5	2.0

State	Station/City	Latitude	Longitude	Percentile Rainfall Depth (in.) 85th	90th	95th	90% Cumulative Rainfall Depth (in.)
IN	South Bend	41.707	-86.333	0.8	1.0	1.5	2.0
KS	Dodge City	37.773	-99.970	0.8	1.0	1.5	1.9
KS	Goodland	39.368	-101.693	0.7	1.0	1.4	2.0
KS	Topeka	39.073	-95.626	1.0	1.3	1.8	2.4
KS	Wichita	37.647	-97.429	1.0	1.2	1.7	2.1
KY	Fort Campbell	36.673	-87.492	1.0	1.3	1.8	2.1
KY	Lexington	38.041	-84.606	0.9	1.1	1.5	2.0
KY	Louisville	38.177	-85.730	0.9	1.1	1.5	2.0
LA	Baton Rouge	29.350	-89.408	1.3	1.6	2.2	2.9
LA	Lake Charles	30.125	-93.228	1.4	1.7	2.4	3.4
LA	New Orleans	29.993	-90.251	1.5	1.8	2.5	3.3
LA	Shreveport	32.447	-93.824	1.3	1.6	2.1	2.8
MA	Boston	42.361	-71.011	0.9	1.2	1.6	1.9
MA	Worchester	42.267	-71.876	1.0	1.2	1.6	2.0
MD	Baltimore	39.172	-76.684	1.0	1.2	1.5	1.8
ME	Caribou	46.867	-68.033	0.7	0.8	1.1	1.4
ME	Portland	43.642	-70.304	1.0	1.3	1.8	2.7
MI	Alpena	45.072	-83.581	0.7	0.8	1.1	1.3
MI	Detroit	42.215	-83.349	0.8	0.9	1.3	1.7
MI	Flint	42.967	-83.749	0.8	0.9	1.4	2.2
MI	Grand Rapids	42.882	-85.523	0.9	1.1	1.6	2.2
MI	Houghton	44.368	-84.691	0.7	0.9	1.3	1.9
MI	Lansing	42.780	-84.579	0.7	0.9	1.2	1.6
MI	Muskegon	43.171	-86.237	0.8	0.9	1.3	1.7
MI	Sault St. Marie	46.467	-84.367	0.7	0.8	1.1	1.3
MN	Duluth	46.844	-92.194	0.9	1.1	1.5	1.8
MN	International Falls	48.566	-93.403	0.8	0.9	1.3	1.7
MN	Minneapolis	44.883	-93.229	0.8	1.0	1.4	1.8
MN	Rochester	43.904	-92.492	0.9	1.2	1.6	2.0
MN	St. Cloud	45.545	-94.052	0.9	1.1	1.5	2.0
MO	Columbia	38.817	-92.218	1.0	1.3	1.9	2.4
MO	Kansas City	39.299	-94.718	1.0	1.3	1.8	2.3
MO	Springfield	37.240	-93.390	1.1	1.4	1.9	2.4
MO	St. Louis	38.753	-90.374	1.0	1.2	1.7	2.3
MS	Jackson	32.320	-90.078	1.2	1.5	2.0	2.6
MS	Meridian	32.333	-88.751	1.3	1.6	2.2	2.7
MT	Billings	45.808	-108.543	0.6	0.8	1.2	1.9
MT	Cut Bank	48.608	-112.376	0.6	0.8	1.0	1.7
MT	Glasgow	48.214	-106.621	0.6	0.8	1.2	1.6
MT	Great Falls	47.473	-111.382	0.6	0.8	1.2	2.1
MT	Helena	46.606	-111.964	0.5	0.7	1.0	1.8
MT	Kalispell	48.304	-114.264	0.5	0.5	0.8	1.1
MT	Lewistown	47.049	-109.467	0.5	0.7	0.9	1.1
MT	Miles City	46.428	-105.886	0.6	0.8	1.0	1.3
MT	Missoula	46.921	-114.093	0.4	0.6	0.8	1.7
NC	Asheville	35.432	-82.538	1.0	1.2	1.7	2.1
NC	Charlotte	35.214	-80.944	1.0	1.3	1.7	2.0
NC	Greensboro	36.098	-79.944	1.0	1.2	1.7	2.3
NC	Hatteras	35.232	-75.623	1.2	1.5	2.1	3.2
NC	Raleigh	35.871	-78.786	1.0	1.2	1.6	2.1
NC	Wilmington	34.268	-77.906	1.2	1.5	2.1	2.9
ND	Bismarck	46.774	-100.748	0.7	0.9	1.4	2.1
ND	Fargo	46.925	-96.811	0.8	1.0	1.4	1.7
ND	Minot	48.259	-101.281	0.8	0.9	1.2	1.6
NE	Grand Island	40.958	-98.313	0.9	1.1	1.6	2.0
NE	Norfolk	41.981	-97.437	1.0	1.2	1.7	2.2
NE	North Platte	41.122	-100.668	0.9	1.0	1.4	1.8

State	Station/City	Latitude	Longitude	Percentile Rainfall Depth (in.) 85th	90th	95th	90% Cumulative Rainfall Depth (in.)
NE	Omaha	41.310	-95.899	0.9	1.0	1.3	1.7
NE	Scottsbluff	41.874	-103.595	0.7	0.8	1.1	1.5
NH	Concord	43.195	-71.501	0.9	1.1	1.5	1.7
NJ	Atlantic City	39.458	-74.577	1.0	1.2	1.5	1.9
NJ	Newark	40.683	-74.169	1.0	1.2	1.6	2.0
NM	Albuquerque	35.042	-106.616	0.5	0.6	0.8	0.9
NM	Tucumcari	35.182	-103.603	0.8	0.9	1.3	1.6
NV	Elko	40.825	-115.792	0.4	0.5	0.7	0.8
NV	Ely	39.295	-114.845	0.5	0.6	0.9	2.1
NV	Las Vegas	36.079	-115.155	0.7	0.8	1.4	2.2
NV	Reno	39.484	-119.771	0.5	0.7	1.0	1.9
NV	Tonopah	38.060	-117.087	0.4	0.5	0.7	0.9
NV	Winnemucca	40.902	-117.807	0.4	0.6	0.9	1.8
NY	Albany	42.748	-73.803	0.8	1.0	1.3	1.5
NY	Binghamton	42.208	-75.981	0.8	0.9	1.2	1.5
NY	Greater Buffalo	42.941	-78.736	0.7	0.8	1.1	1.4
NY	Massena	44.936	-74.846	0.7	0.9	1.1	1.4
NY	New York City	40.779	-73.881	1.0	1.2	1.7	2.1
NY	Rochester	43.117	-77.677	0.7	0.8	1.1	1.4
NY	Syracuse	43.109	-76.103	0.8	0.9	1.2	1.6
OH	Akron	40.918	-81.443	0.8	0.9	1.2	1.5
OH	Cincinnati	39.103	-84.419	0.9	1.0	1.4	1.7
OH	Cleveland	41.405	-81.853	0.8	0.9	1.2	1.5
OH	Columbus	39.991	-82.881	0.8	1.0	1.3	1.6
OH	Dayton	39.906	-84.219	0.9	1.1	1.5	1.9
OH	Mansfield	40.820	-82.518	0.9	1.0	1.3	1.6
OH	Toledo	41.589	-83.801	0.8	0.9	1.2	1.6
OH	Youngstown	41.254	-80.674	0.8	0.9	1.2	1.5
OK	Oklahoma City	35.389	-97.600	1.1	1.3	1.8	2.3
OK	Tulsa	36.198	-95.886	1.1	1.4	1.9	2.5
OR	Astoria	46.158	-123.878	0.9	1.0	1.4	1.8
OR	Burns	43.592	-118.954	0.4	0.5	0.8	2.1
OR	Eugene	44.133	-123.214	0.9	1.0	1.4	1.8
OR	Medford	42.389	-122.871	0.6	0.7	1.0	1.4
OR	North Bend	43.417	-124.250	0.9	1.1	1.5	1.9
OR	Pendleton	45.698	-118.834	0.4	0.5	0.7	1.1
OR	Portland	45.591	-122.600	0.6	0.7	1.0	1.1
OR	Salem	44.908	-122.995	0.7	0.8	1.2	1.4
PA	Allentown	40.651	-75.449	0.9	1.1	1.5	1.9
PA	Bradford	41.803	-78.640	0.8	0.9	1.2	1.4
PA	Erie	42.080	-80.183	0.8	0.9	1.2	1.5
PA	Greater Pittsburgh	40.501	-80.231	0.7	0.9	1.2	1.5
PA	Harrisburg	40.194	-76.763	1.0	1.2	1.5	1.8
PA	Philadelphia	39.868	-75.231	1.0	1.2	1.6	2.0
PA	Wilkes-Barre	41.339	-75.727	0.8	0.9	1.3	1.6
PA	Williamsport	41.243	-76.922	0.9	1.1	1.5	1.8
RI	Providence	41.722	-71.433	1.1	1.3	1.8	2.3
SC	Charleston	32.899	-80.041	1.1	1.4	1.9	2.5
SC	Columbia	33.942	-81.118	1.1	1.3	1.8	2.3
SC	Greenville	34.899	-82.219	1.1	1.4	1.8	2.3
SD	Huron	44.385	-98.229	0.9	1.0	1.4	1.9
SD	Rapid City	44.046	-103.054	0.7	0.9	1.2	2.0
SD	Sioux Falls	43.577	-96.754	0.9	1.2	1.6	2.0
TN	Chattanooga	35.033	-85.200	1.1	1.3	1.7	2.3
TN	Dyersburg	36.019	-89.318	1.1	1.4	1.9	2.4
TN	Knoxville	35.818	-83.986	0.9	1.1	1.5	1.9
TN	Memphis	35.061	-89.985	1.3	1.6	2.1	2.7

State	Station/City	Latitude	Longitude	Percentile Rainfall Depth (in.) 85th	90th	95th	90% Cumulative Rainfall Depth (in.)
TN	Nashville	36.119	-86.689	1.1	1.3	1.8	2.4
TX	Abilene	32.411	-99.682	1.1	1.4	1.8	2.2
TX	Amarillo	35.219	-101.706	0.8	1.0	1.4	1.7
TX	Austin	30.179	-97.681	1.2	1.5	1.9	3.3
TX	Brownsville	25.906	-97.426	1.1	1.5	2.2	3.6
TX	Corpus Christi	27.773	-97.513	1.3	1.6	2.4	3.2
TX	El Paso	31.811	-106.376	0.7	0.8	1.1	1.3
TX	Fort Worth	32.769	-97.441	1.2	1.4	1.9	2.4
TX	Houston	29.607	-95.159	1.2	1.5	2.0	2.9
TX	Lubbock	33.668	-101.821	0.9	1.1	1.6	2.2
TX	Port Arthur	29.951	-94.021	1.4	1.8	2.5	3.4
TX	San Angelo	31.351	-100.494	1.0	1.3	1.8	2.1
TX	San Antonio	29.533	-98.464	1.2	1.6	2.1	3.2
TX	Victoria	28.863	-96.930	1.3	1.6	2.3	3.7
TX	Waco	31.611	-97.229	1.2	1.5	2.2	2.9
TX	Wichita Falls	33.979	-98.493	1.0	1.3	1.7	2.2
UT	Salt Lake City	40.787	-111.968	0.5	0.6	0.8	1.0
VA	Lynchburg	37.338	-79.207	0.9	1.1	1.6	1.9
VA	Norfolk	36.904	-76.192	1.0	1.3	1.8	2.5
VA	Richmond	37.511	-77.323	1.0	1.3	1.6	2.0
VA	Roanoke	37.317	-79.974	0.9	1.2	1.6	2.1
VT	Burlington	44.468	-73.150	0.8	0.9	1.2	1.5
WA	Olympia	46.973	-122.903	0.8	0.9	1.2	1.5
WA	Quillayute	47.934	-124.561	1.2	1.5	2.0	2.5
WA	Seattle	47.461	-122.314	0.6	0.8	1.0	1.4
WA	Spokane	47.621	-117.528	0.5	0.6	0.8	1.4
WA	Yakima	46.564	-120.534	0.4	0.6	0.8	3.1
WI	Green Bay	44.513	-88.120	0.8	1.0	1.3	1.5
WI	La Crosse	43.754	-91.256	0.9	1.1	1.4	1.8
WI	Madison	43.141	-89.345	0.9	1.1	1.5	2.2
WI	Milwaukee	42.947	-87.897	0.9	1.1	1.5	2.3
WV	Beckley	37.795	-81.125	0.8	0.9	1.2	1.5
WV	Elkins	38.885	-79.853	0.8	0.9	1.2	1.4
WV	Huntington	38.382	-82.555	0.8	1.0	1.4	1.7
WY	Casper	42.898	-106.473	0.6	0.7	1.0	1.4
WY	Cheyenne	41.158	-104.807	0.6	0.8	1.0	1.2
WY	Lander	42.817	-108.733	0.6	0.8	1.0	1.3
WY	Rock Springs	41.594	-109.065	0.4	0.5	0.7	0.9
WY	Sheridan	44.774	-106.976	0.6	0.7	1.0	1.8

Table 4.2 The 95th Percentile Depths (in.) from This Study and Hirschman and Kosco (2008) and Their Absolute and Relative Differences (%) in 20 U.S. Cities

	95th Percentile Rainfall Depth (in.)		
Station/City	This Study	Hirschman & Kosco (2008)	Difference [1]
Atlanta	1.8	1.8	0.0” (0.0%)
Baltimore	1.5	1.6	-0.1” (-6.3%)
Boston	1.6	1.5	0.1” (6.7%)
Buffalo	1.1	1.1	0.0” (0.0%)
Burlington	1.2	1.1	0.1” (9.1%)
Cincinnati	1.4	1.5	-0.1” (-6.7%)
Coeur D'Alene	0.8	0.7	0.1” (14.3%)
Columbus	1.3	1.3	0.0” (0.0%)
Concord	1.5	1.3	0.2” (15.4%)
Denver	1.0	1.1	-0.1” (-9.1%)
Kansas City	1.8	1.7	0.1” (5.9%)
Knoxville	1.5	1.5	0.0” (0.0%)
Louisville	1.5	1.5	0.0” (0.0%)
Minneapolis	1.4	1.4	0.0” (0.0%)
New York City	1.7	1.7	0.0” (0.0%)
Phoenix	1.1	1.0	0.1” (10.0%)
Portland	1.0	1.0	0.0” (0.0%)
Salt Lake City	0.8	0.8	0.0” (0.0%)
Seattle	1.0	1.6	-0.6” (-37.5%)
Washington DC	1.5	1.7	-0.2” (-11.8%)

[1] Difference was given in inches and in percent that was computed as the difference between the values determined in this study and reported by Hirschman and Kosco (2008) divided by the value reported by Hirschman and Kosco (2008)

Table 4.3 Storm Depth Mean and Kappa Distribution Paramters for 18 Selected Stations in Eastern New Mexico, Oklahoma and Texas

Station name	Storm Depth Mean (in.) [1]	Kappa Distribution Parameters [2]			
		ξ	α	Κ	h
Abilene	0.54951	-1.0166	1.4485	-0.0647	2.0081
Amarillo	0.42832	-1.0425	1.3198	-0.1401	2.1559
Austin	0.62048	-1.2368	1.4770	-0.1012	2.2560
Brownsville	0.55926	-1.5950	1.3479	-0.2258	2.8952
Corpus Christi	0.62332	-1.3302	1.2648	-0.2272	2.6009
El Paso	0.25273	-0.7447	1.1176	-0.1882	1.9348
Fort Worth	0.75086	-0.9257	1.4774	0.0040	2.0053
Houston	0.74602	-0.8873	1.1963	-0.1817	2.0231
Lubbock	0.44280	-0.9854	1.2629	-0.1610	2.1208
Port Arthur	0.86073	-0.7344	1.0967	-0.2099	1.8786
San Angelo	0.46788	-1.2914	1.5072	-0.0936	2.3193
San Antonio	0.59669	-1.1826	1.2911	-0.1884	2.3525
Victoria	0.66368	-1.1389	1.2522	-0.2007	2.3330
Waco	0.63370	-1.0224	1.4888	-0.0444	1.9845
Wichita Falls	0.59963	-0.9523	1.4329	-0.0572	1.9386
Oklahoma City	0.62856	-0.8200	1.3398	-0.0789	1.8246
Tulsa	0.66302	-0.9199	1.4384	-0.0472	1.8874
Tucumcari	0.43087	-0.5830	1.0862	-0.1384	1.8668

[1] extracted from Asquith et al. (2006)

[2] computed station by station using Newton- Raphson method using L-moment ratios extracted from Asquith et al. (2006).

Table 4.4 The 95th Percentile Storm Depths Determined Using Kappa Distribution Parameters Derived from Hourly Rainfall Data and Differences between 95th Percentile Rainfall Depths Estimated from Daily and Hourly Rainfall Data

		95th rainfall depth (in)		
State	Station	From daily rainfall data	From hourly rainfall data	Differences of 95th rainfall depths (in.)
TX	Abilene	1.8	2.1	-0.3
TX	Amarillo	1.4	1.7	-0.3
TX	Austin	1.9	2.5	-0.6
TX	Brownsville	2.2	2.4	-0.2
TX	Corpus Christi	2.4	2.6	-0.2
TX	El Paso	1.1	1.0	0.1
TX	Fort Worth	1.9	2.6	-0.7
TX	Houston	2.0	2.9	-0.9
TX	Lubbock	1.6	1.7	-0.1
TX	Port Arthur	2.5	3.3	-0.8
TX	San Angelo	1.8	1.9	-0.1
TX	San Antonio	2.1	2.4	-0.3
TX	Victoria	2.3	2.7	-0.4
TX	Waco	2.2	2.4	-0.2
TX	Wichita Falls	1.7	2.3	-0.6
OK	Oklahoma City	1.8	2.4	-0.6
OK	Tulsa	1.9	2.5	-0.6
NM	Tucumcari	1.3	1.5	-0.2

Table 4.5 Comparison between NOAA's 1 Year 24-Hour Rainfall and Computed 95th Percentile Rainfall Depth Using Daily Data

State	Station/City	Rainfall Depth (in.) 1 year 24-hr [1]	Rainfall Depth (in.) 95th percentile	Difference (in.)
TX	Abilene	2.7	1.8	-0.9
TX	Amarillo	2.2	1.4	-0.8
TX	Austin	3.2	1.9	-1.3
TX	Brownsville	3.6	2.2	-1.4
TX	Corpus Christi	3.4	2.4	-1.0
TX	El Paso	1.3	1.1	-0.2
TX	Fort Worth	3.2	1.9	-1.3
TX	Houston	3.7	2.0	-1.7
TX	Lubbock	2.2	1.6	-0.6
TX	Port Arthur	4.1	2.5	-1.6
TX	San Angelo	2.6	1.8	-0.8
TX	San Antonio	3.1	2.1	-1.0
TX	Victoria	3.4	2.3	-1.1
TX	Waco	3.2	2.2	-1.0
TX	Wichita Falls	2.8	1.7	-1.1
OK	Oklahoma City	2.9	1.8	-1.1
OK	Tulsa	3.2	1.9	-1.3
NM	Tucumcari	1.8	1.3	-0.5

[1] From U.S. Weather Bureau Technical Paper No. 40 (Hershfield 1963).

Table 4.6 Statistical Summary of 90th and 95th Percentile Daily Rainfall Depths (in.) and the Rainfall Depths that can Capture the Runoff from 90% of Average Annual Rainfall at 206 Weather Stations in the Contiguous U.S.

Statistical distribution parameters	90th percentile	95th percentile	90% of average annual rainfall [1]	Ratio of 90% and 90th rainfall depth
Minimum	0.49	0.67	0.79	1.29
Maximum	1.81	2.50	4.72	7.18
25% Quartile	0.87	1.19	1.56	1.64
Median	1.09	1.47	1.94	1.72
75% Quartile	1.30	1.79	2.28	1.90
Average	1.08	1.48	1.99	1.88
Standard deviation	0.31	0.42	0.62	0.59

[1] To avoid the few very large or extreme events from dominating the annual averages, rainfall depths (events) greater than 99.5 percentiles were excluded from the analysis (Guo and Urbonas, 1996)

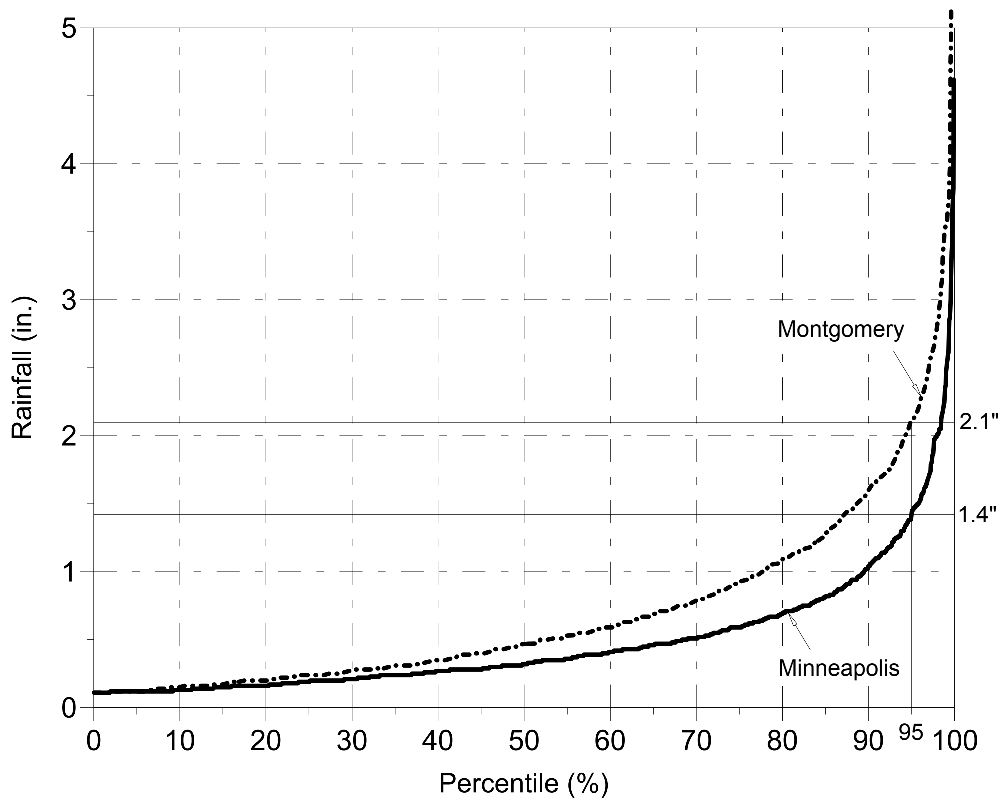

Fig. 4.1. Percentile distribution of daily rainfall depths for Montgomery and Minneapolis weather stations

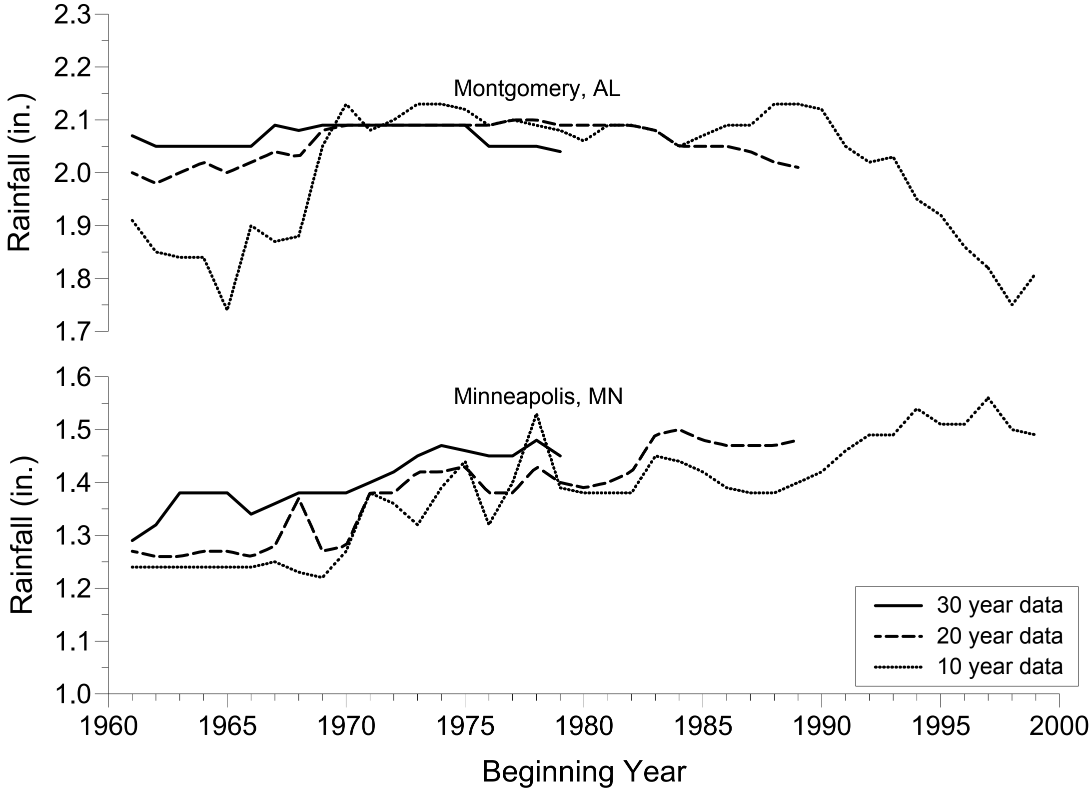

Fig. 4.2. 95th percentile rainfall depths estimated using 10, 20, and 30 years of daily rainfall data at Montgomery, AL (top) and Minneapolis, MN (bottom) for sensitivity analysis

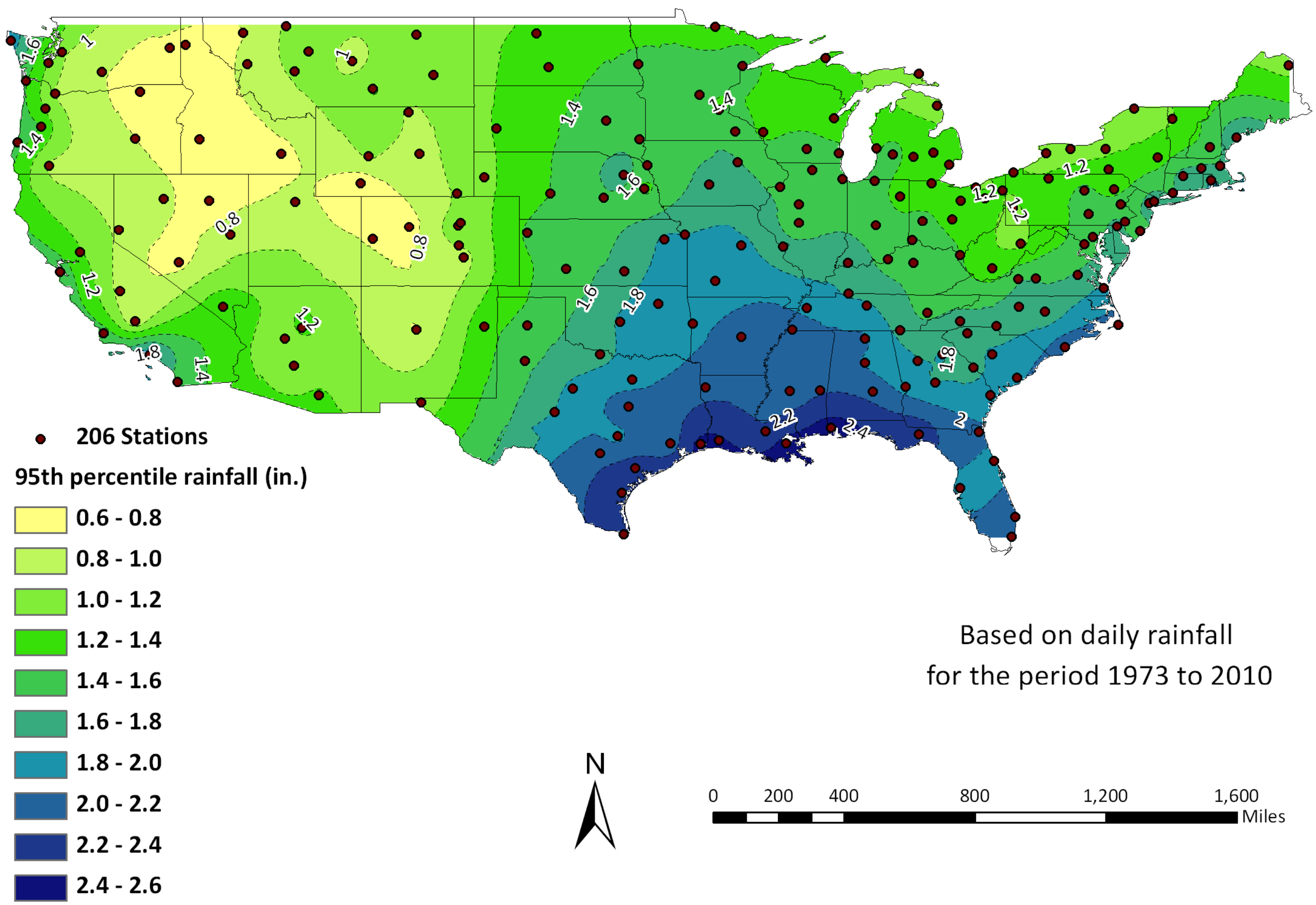

Fig. 4.3. 95th percentile rainfall map for the contiguous U.S.

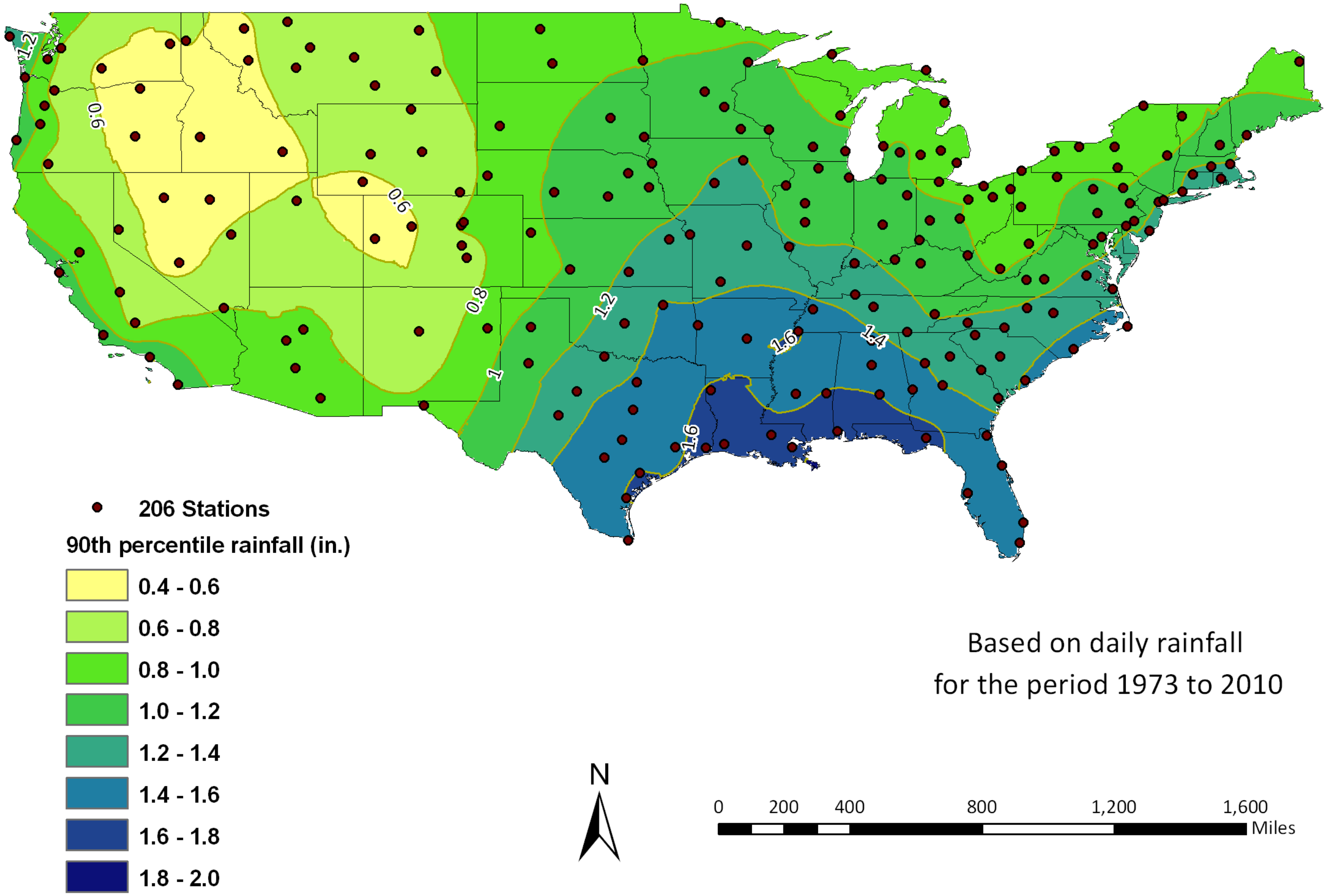

Fig. 4.4. 90th percentile rainfall map for the contiguous U.S.

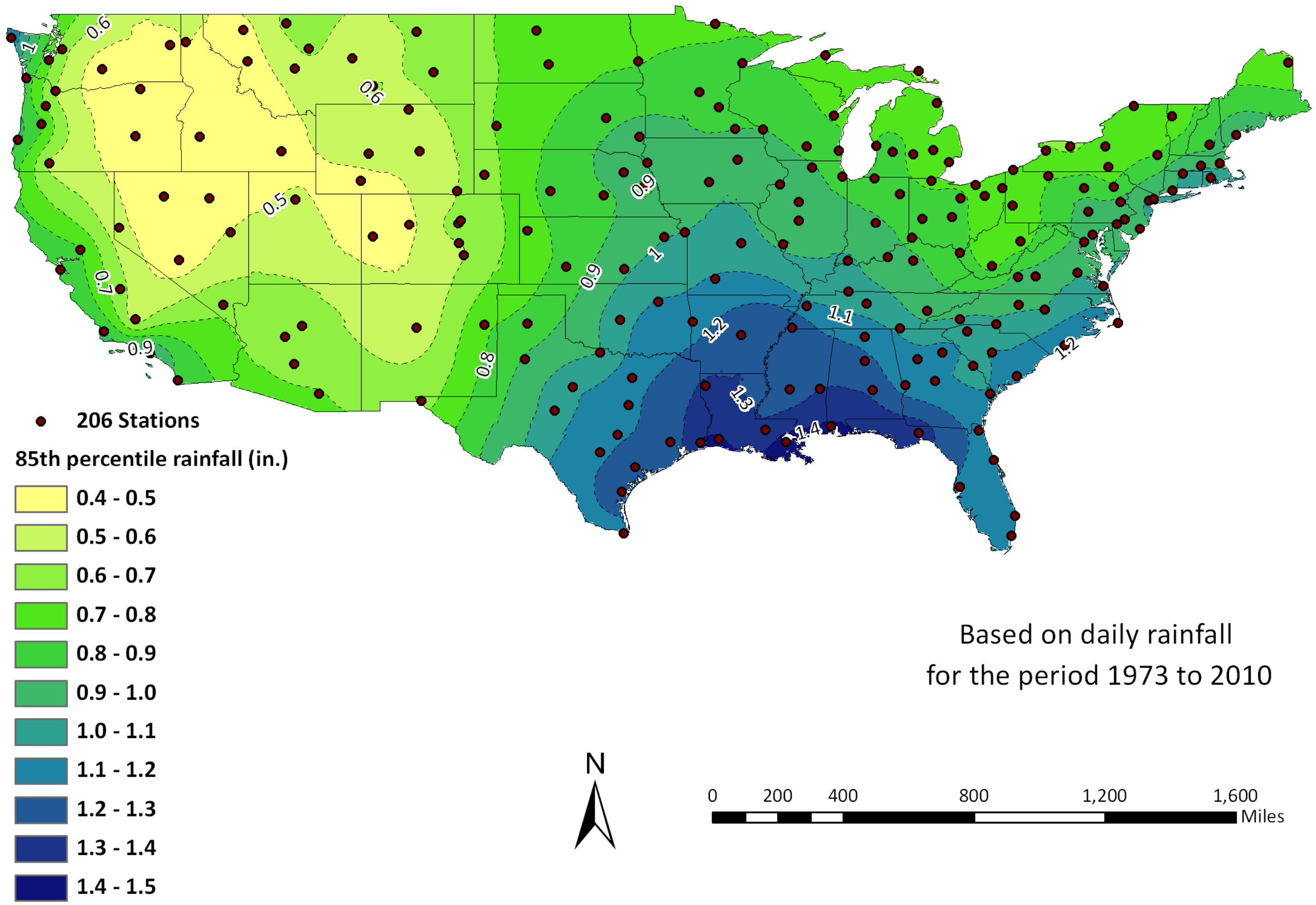

Fig. 4.5. 85th percentile rainfall map for the contiguous U.S.

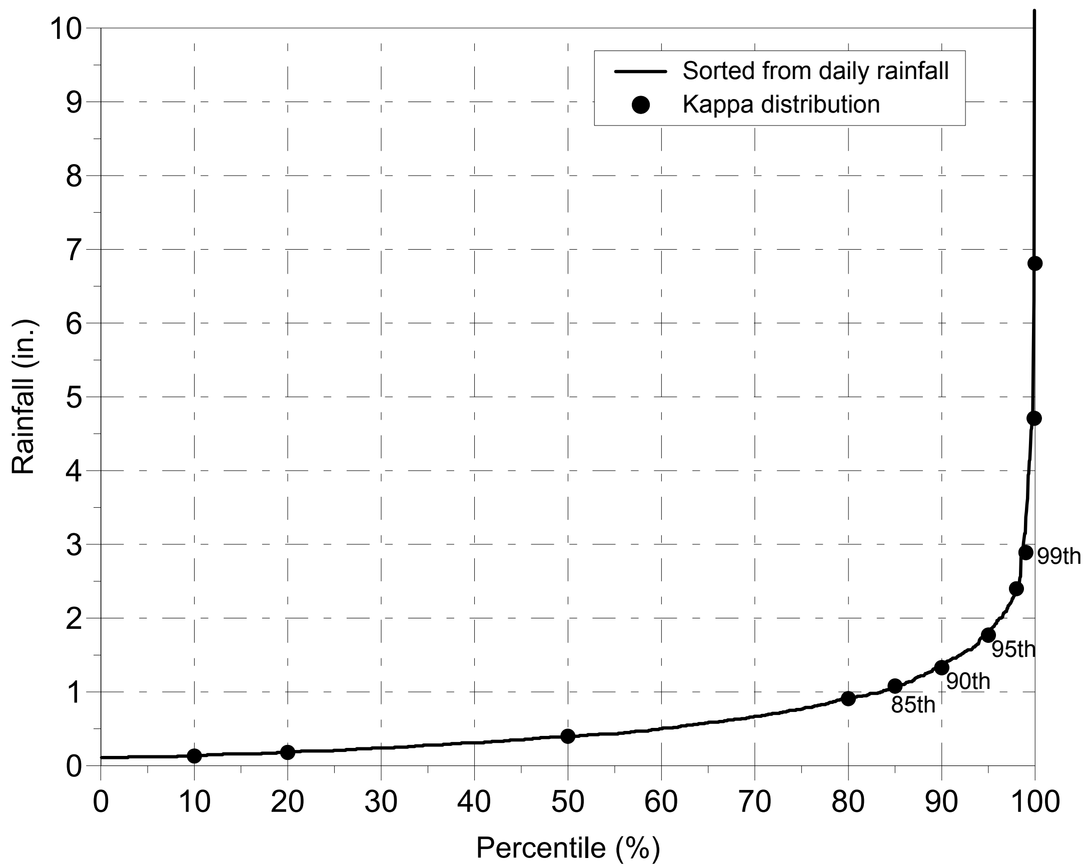

Fig. 4.6. Distribution of daily rainfall depths and quantiles calculated using Kappa distribution with paramters derived from daily data at Abilene Regional Airport, Texas

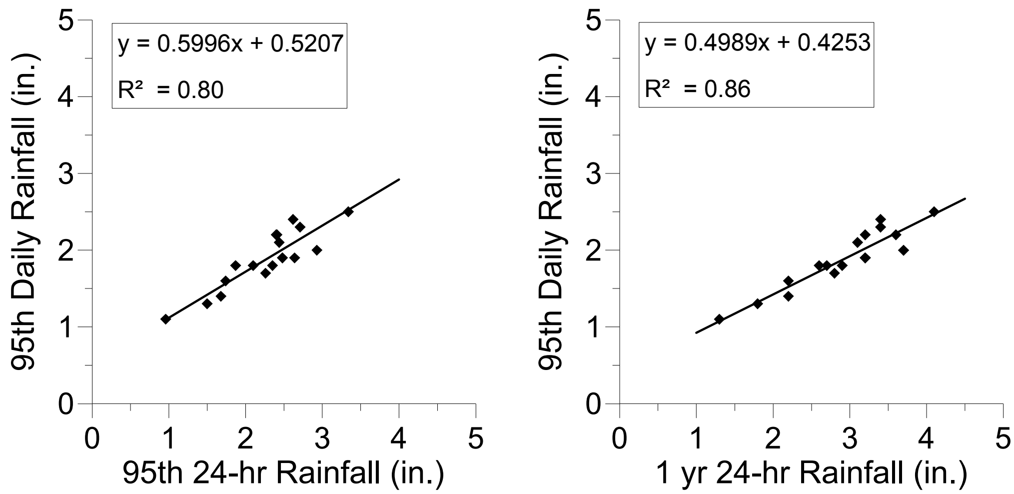

Fig. 4.7. Regression equations between 95th percentile rainfall depth derived from daily rainfall data and 95th percentile rainfall depth derived from hourly rainfall data (left) and NOAA's 1 year 24-hr rainfall (right) for selected 18 stations (Table 4.4 and Table 4.5)

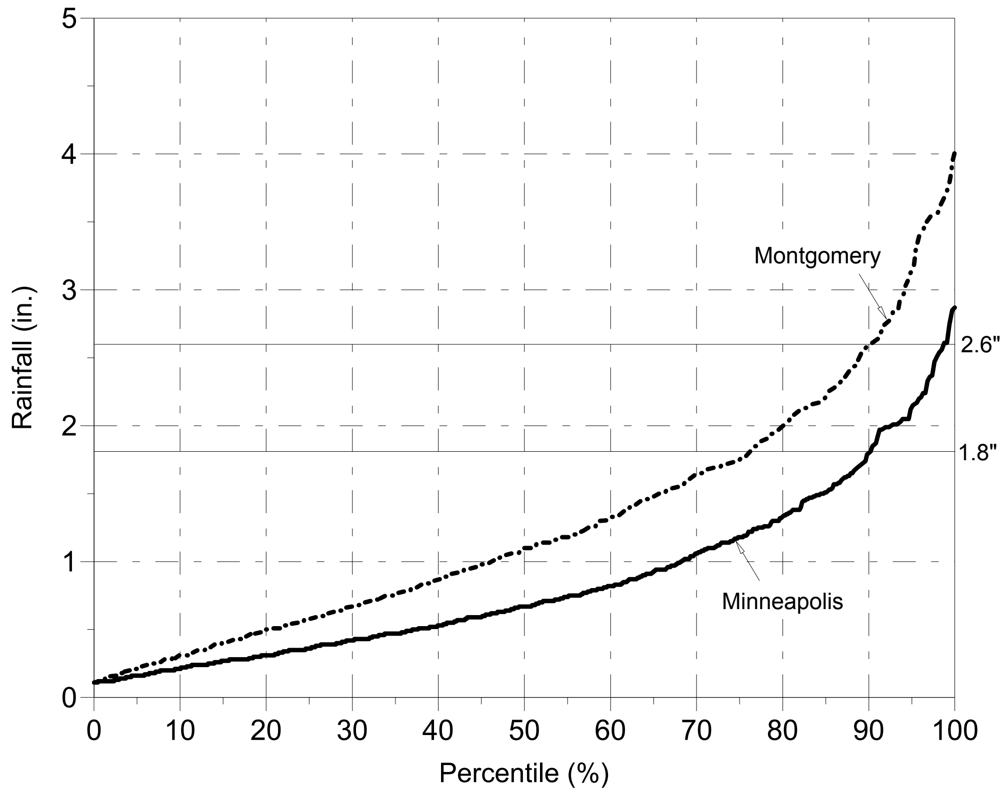

Fig. 4.8 Percentile distribution of cumulative rainfall depths for Montgomery and Minneapolis weather stations

Chapter 5. Conclusions and Recommendation

General Summary and Conclusions

In this study, Watershed Analysis Risk Management Framework (WARMF) model was developed and applied to the Saugahatchee Creek Watershed (SCW) to simulate flow and water quality, which is based on calibration and validation results, supported by quantitative statistics for model evaluation and/or graphical techniques. Flow calibration for the period from 2000 – 2005 and validation for the period from 2006 – 2009 was performed using observed daily flow data at USGS 02418230 station in the Saugahatchee Creek near Loachapoka. The quantitative statistics recommended by Moriasi et al (2007), NSE, RSR, and PBIAS were 0.64, 0.60, and -2.78%, respectively for calibration and 0.56, 0.66, and -9.53%, respectively for validation. These values indicate satisfactory performance of the WARMF model for flow simulation. The simulation of water quality parameters such as water temperature, dissolved oxygen (DO), total phosphorus (TP), total nitrogen (TN), and chlorophyll-a concentration were calibrated to be satisfactorily predicted at various water quality stations in the watershed by the WARMF model based on visual inspection.

WARMF model simulation was run using daily time step. Certain water quality parameter such as DO concentration that vary, especially in an eutrophic system, during a day cannot be featured with daily time step. Shorter time step must be used to simulate diurnal variations.

A portion of the Saugahatchee Creek (Yates Reservoir Embayment) that enters Yates reservoir, when treated as a stream instead of a reservoir in the WARMF model, accounted for significant decrease in chlorophyll-a concentration. Reservoir tends to have calm water, which aids in settling of organic matter and nutrient accumulation. Also, stratification was predicted in reservoir during summer that will cut off oxygen supply to the bottom layer depleting DO concentration. River impounding can possibly be the cause, in addition to excess nutrient, of impairment of Saugahatchee Creek (Yates Reservoir Embayment) for nutrients and organic enrichment/ dissolved oxygen.

Land use scenarios of 1991, 2001, and 2008 for the SCW show the land use transformation from forest areas to cropland and urban areas. The major impact of land use change was predicted to be rise in nutrient levels. The model predicted as much as 15.4% and 27.8% increase in concentrations of TP and TN concentration, respectively in terms of monthly average of daily values for land use change scenarios. Since two portions of the Saugahatchee Creek is already in the list of impaired water for nutrients (ADEM 2009), it is essential to exercise effective best management practices (BMPs) for nutrient runoff.

The outputs derived from Hadley Centre Coupled Model, version 3 (HadCM3) future climate model were downscaled to obtain meteorological variables at local watershed scale for allotted time frames of 2020s (2011-2040), 2050s (2041-2070), and 2080s (2071-2099). Two emission scenarios (A2 and B2) for HadCM3, used in this study, report that the climate in the SCW for the 21st century will likely be warmer and drier. Based on the WARMF model simulation for baseline scenario (1981-2010) and future climate scenarios, the general predicted trend was increase in water temperature, and nutrient concentration; decrease in flow, and DO concentration; and mixed result for chlorophyll-a concentration. The relative decrease in flow, in terms of monthly average of daily values for, ranged from 4.1% to 62.2% for HadCM3 A2 and 15.1% to 56.8% for HadCM3 B2 scenarios. Water temperature increased as high as 5.5°C and 4.7°C for HadCM3 A2 and B2, respectively. DO concentration decreased by 22.1% and 16.5% at most for HadCM3 A2 and B2 respectively. The TP concentration climbed as much as 87.4% and 83.16%; TN concentration climbed as much as 80.0% and 57.5% for HadCM3 A2 and B2 respectively.

Uncertainties involved with future climate scenarios, downscaling, and watershed model outputs should not be discarded while using these results. However, the impact study under different scenarios of land use and climate change, in general, is useful for decision making in watershed management and sustainable development.

Summary of Chapter 4

The 95th percentile rainfall, recommended value for design storm by U.S. Environmental Protection Agency (USEPA), was determined and reported at 206 stations/cities in the contiguous U.S. using daily rainfall data from 1973 to 2010. The 95th percentiles ranged from 17.8 mm (0.7 in.) to 63.5 mm (2.5 in.). Comparing with the 95th percentile rainfall depths derived from hourly data at 18 selected stations in eastern New Mexico, Oklahoma and Texas, the 95th percentile rainfall depths derived from daily rainfall record was typically underestimated. The 95th percentile daily rainfall depths showed good linear correlation with NOAA's 1-yr 24-hour rainfall depth but the later was greater. Water quality volume determined using 90% cumulative percent of average annual rainfall is on average 88% larger than one determined using 90th percentiles of daily rainfall.

The rainfall isohyetal map for 85th, 90th, and 95th percentile rainfall depth, accompanied with values in tabular form, was generated for 206 stations in the contiguous U.S. Rainfall percentile statistics from this study will be valuable for estimating design storms, e.g., for water quality improvement, low impact development, and green infrastructures.

Recommendations for Future Exploration

Simulation at finer temporal scale

For this study, daily time step was used in the WARMF model to simulate flow and other water quality parameters. We learned that some of the features that experience diurnal variations are not observable using daily time steps. For example, DO concentration tends to fluctuate largely in an eutrophic system. With the availability of high temporal resolution data, the simulations of flow and water quality are recommended to be simulated using finer (hourly) time step.

Future land use scenarios

The impact of historical land use scenarios were applied in the WARMF model for this research. This research area can be broadened after the completion of future land use scenarios for the SCW (Rajesh Sawant, personal communication, Jun. 8, 2011). It would be a good suggestion to couple it with the future climate change scenario.

Management scenarios

Alabama Department of Environmental Management (ADEM 2008)'s Total Phosphorus (TP) Total Maximum Daily Load (TMDL) study calls for TP reduction of more than 86% from point sources, and 50% from non point sources. Furthermore, it was determined that DO concentrations would fall below the standard (5mg/l) even if all the point sources are removed during simulation(ADEM 2008). Therefore, reduction in both point and non point source pollution is recommended for the SCW. For cost effective implementation of best management practices, identification of critical source areas was carried out in the SCW (Niraula 2010). Consensus module in WARMF guides the users through different management scenarios to compare alternatives. It is recommended to further explore the application of WARMF's consensus module to identify whether water bodies meet water quality criteria for particular scenarios, how point and nonpoint source affect water quality to evaluate management alternatives. Another unique feature of the WARMF, TMDL module is recommended, which is useful for TMDL calculation.

References

Alabama Department of Environmental Management (ADEM). (2008). "Final total maximum daily load: Nutrients & OE/DO. Pepperell branch AL03150110-0201-700 Nutrients; Sougahatchee Creek Embayment (Yates Reservoir) AL03150110-0204-101 Nutrients & OE/DO.", Alabama Department of Environmental Management, Montgomery, AL.

ADEM. (2009). "2008 Alabama 303(d) List." 303(d) Information and Map. Alabama Department of Environmental Management <http://adem.alabama.gov/programs/water/wquality/2008AL303dList.pdf> (Aug. 12, 2009).

Moriasi, D. N., Arnold, J. G., Van Liew, M. W., Bingner, R. L., Harmel, R. D., and Veith, T. L. (2007). "Model Evaluation Guidelines for Systematic Quantification of Accuracy in Watershed Simulations." *Transactions of the ASABE*, 50(3), 885-900.

Niraula, R. (2010). "Identifying critical source areas of sediment, nitrogen, and phosphorus: A modeling approach." M.S. thesis, Auburn University, Auburn, AL.

Appendix A. Downscaling Precipitation Using SDSM 4.2

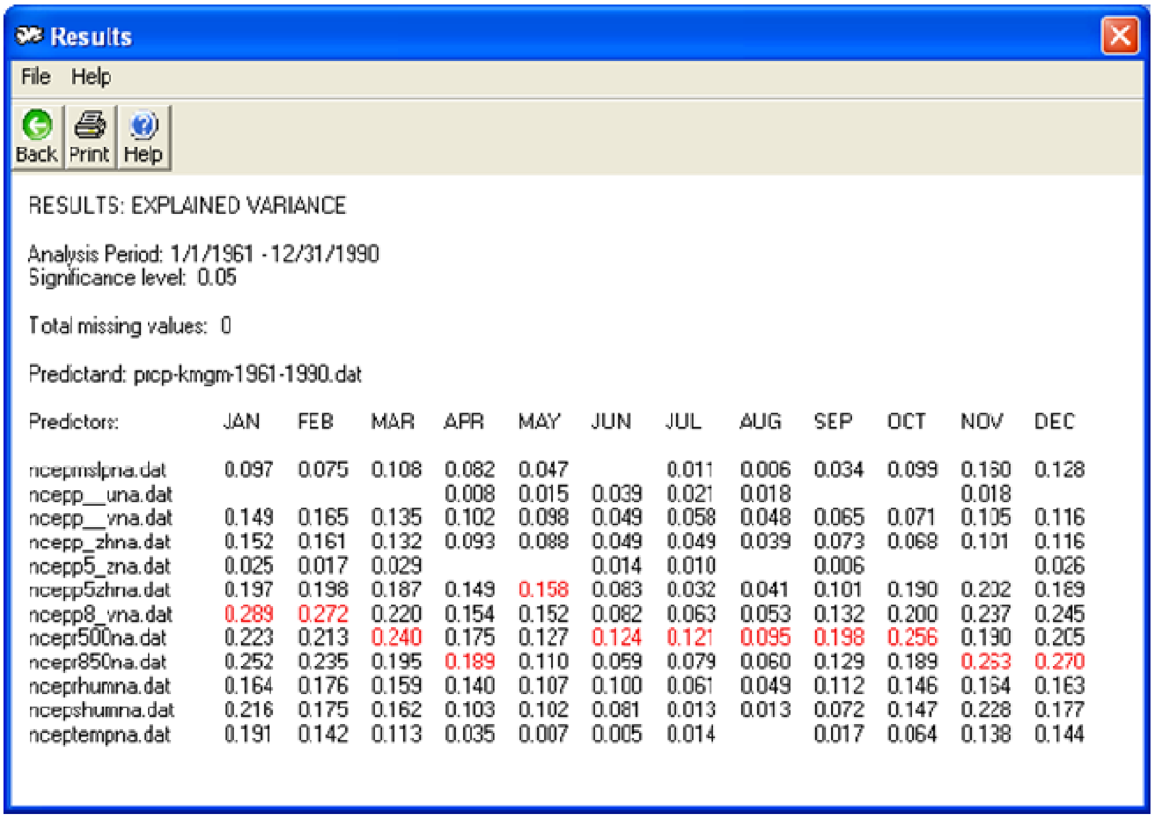

RESULTS: EXPLAINED VARIANCE

Analysis Period: 1/1/1961 - 12/31/1990
Significance level: 0.05

Total missing values: 0

Predictand: prcp-kmgm-1961-1990.dat

Predictors:	JAN	FEB	MAR	APR	MAY	JUN	JUL	AUG	SEP	OCT	NOV	DEC
ncepmslpna.dat	0.097	0.075	0.108	0.082	0.047		0.011	0.006	0.034	0.099	0.160	0.128
ncepp__una.dat				0.008	0.015	0.039	0.021	0.018			0.018	
ncepp__vna.dat	0.149	0.165	0.135	0.102	0.098	0.049	0.058	0.048	0.065	0.071	0.105	0.116
ncepp_zhna.dat	0.152	0.161	0.132	0.093	0.088	0.049	0.049	0.039	0.073	0.068	0.101	0.116
ncepp5_zna.dat	0.025	0.017	0.029			0.014	0.010		0.006			0.026
ncepp5zhna.dat	0.197	0.198	0.187	0.149	0.158	0.083	0.032	0.041	0.101	0.190	0.202	0.169
ncepp8_vna.dat	0.289	0.272	0.220	0.154	0.152	0.082	0.063	0.053	0.132	0.200	0.237	0.245
ncepr500na.dat	0.223	0.213	0.240	0.175	0.127	0.124	0.121	0.095	0.198	0.256	0.190	0.205
ncepr850na.dat	0.252	0.235	0.195	0.189	0.110	0.059	0.079	0.060	0.129	0.189	0.263	0.270
nceprhumna.dat	0.164	0.176	0.159	0.140	0.107	0.100	0.061	0.049	0.112	0.146	0.164	0.163
ncepshumna.dat	0.216	0.175	0.162	0.103	0.102	0.081	0.013	0.013	0.072	0.147	0.228	0.177
nceptempna.dat	0.191	0.142	0.113	0.035	0.007	0.005	0.014		0.017	0.064	0.138	0.144

Fig. A.1 Correlation between observed precipitation and NCEP predictors for each month

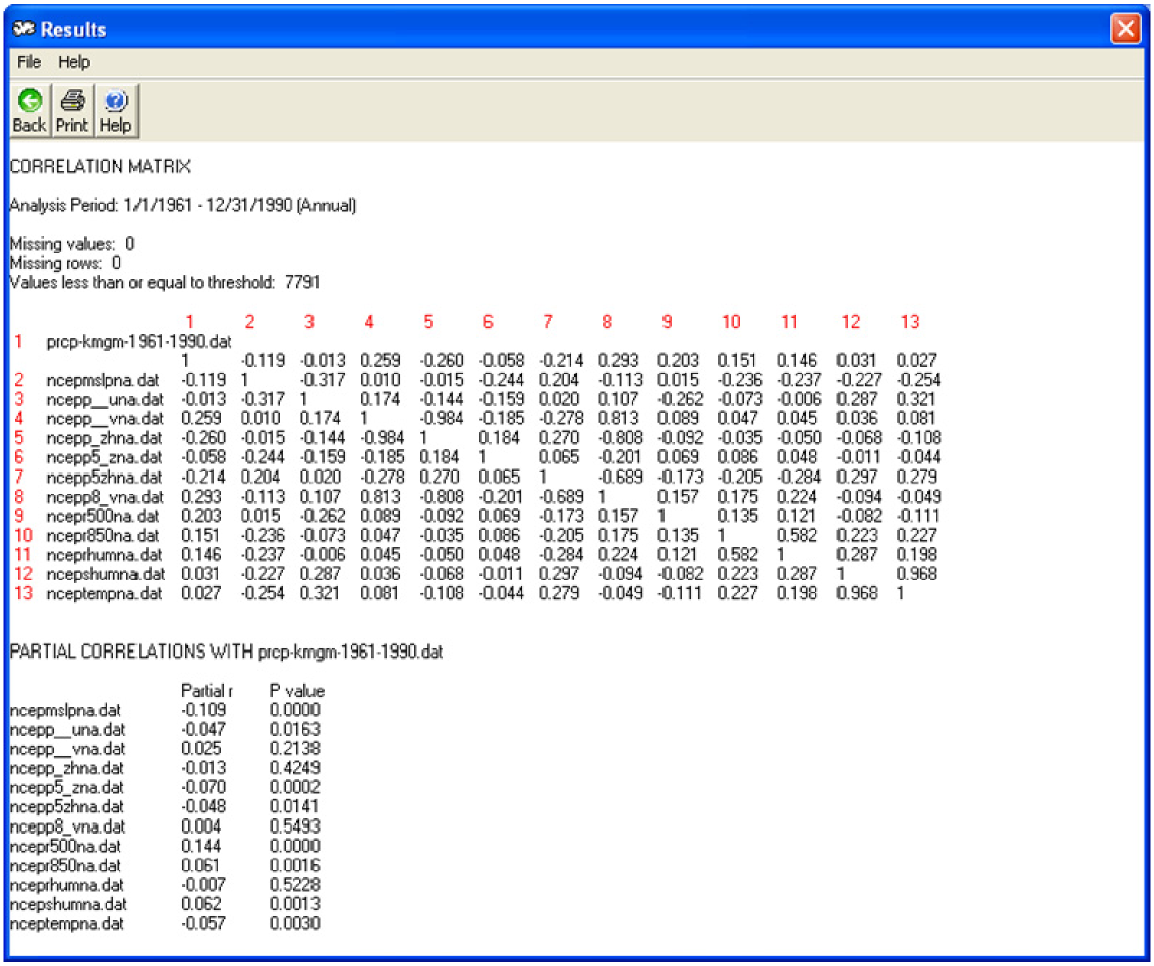

CORRELATION MATRIX

Analysis Period: 1/1/1961 - 12/31/1990 (Annual)

Missing values: 0
Missing rows: 0
Values less than or equal to threshold: 7791

		1	2	3	4	5	6	7	8	9	10	11	12	13
1	prcp-kmgm-1961-1990.dat	1	-0.119	-0.013	0.259	-0.260	-0.058	-0.214	0.293	0.203	0.151	0.146	0.031	0.027
2	ncepmslpna.dat	-0.119	1	-0.317	0.010	-0.015	-0.244	0.204	-0.113	0.015	-0.236	-0.237	-0.227	-0.254
3	ncepp__una.dat	-0.013	-0.317	1	0.174	-0.144	-0.159	0.020	0.107	-0.262	-0.073	-0.006	0.287	0.321
4	ncepp__vna.dat	0.259	0.010	0.174	1	-0.984	-0.185	-0.278	0.813	0.089	0.047	0.045	0.036	0.081
5	ncepp_zhna.dat	-0.260	-0.015	-0.144	-0.984	1	0.184	0.270	-0.808	-0.092	-0.035	-0.050	-0.068	-0.108
6	ncepp5_zna.dat	-0.058	-0.244	-0.159	-0.185	0.184	1	0.065	-0.201	0.069	0.086	0.048	-0.011	-0.044
7	ncepp5zhna.dat	-0.214	0.204	0.020	-0.278	0.270	0.065	1	-0.689	-0.173	-0.205	-0.284	0.297	0.279
8	ncepp8_vna.dat	0.293	-0.113	0.107	0.813	-0.808	-0.201	-0.689	1	0.157	0.175	0.224	-0.094	-0.049
9	ncepr500na.dat	0.203	0.015	-0.262	0.089	-0.092	0.069	-0.173	0.157	1	0.135	0.121	-0.082	-0.111
10	ncepr850na.dat	0.151	-0.236	-0.073	0.047	-0.035	0.086	-0.205	0.175	0.135	1	0.582	0.223	0.227
11	nceprhumna.dat	0.146	-0.237	-0.006	0.045	-0.050	0.048	-0.284	0.224	0.121	0.582	1	0.287	0.198
12	ncepshumna.dat	0.031	-0.227	0.287	0.036	-0.068	-0.011	0.297	-0.094	-0.082	0.223	0.287	1	0.968
13	nceptempna.dat	0.027	-0.254	0.321	0.081	-0.108	-0.044	0.279	-0.049	-0.111	0.227	0.198	0.968	1

PARTIAL CORRELATIONS WITH prcp-kmgm-1961-1990.dat

	Partial r	P value
ncepmslpna.dat	-0.109	0.0000
ncepp__una.dat	-0.047	0.0163
ncepp__vna.dat	0.025	0.2138
ncepp_zhna.dat	-0.013	0.4249
ncepp5_zna.dat	-0.070	0.0002
ncepp5zhna.dat	-0.048	0.0141
ncepp8_vna.dat	0.004	0.5493
ncepr500na.dat	0.144	0.0000
ncepr850na.dat	0.061	0.0016
nceprhumna.dat	-0.007	0.5228
ncepshumna.dat	0.062	0.0013
nceptempna.dat	-0.057	0.0030

Fig. A.2 Correlation matrix and partial correlations between observed precipitation and NCEP predictors

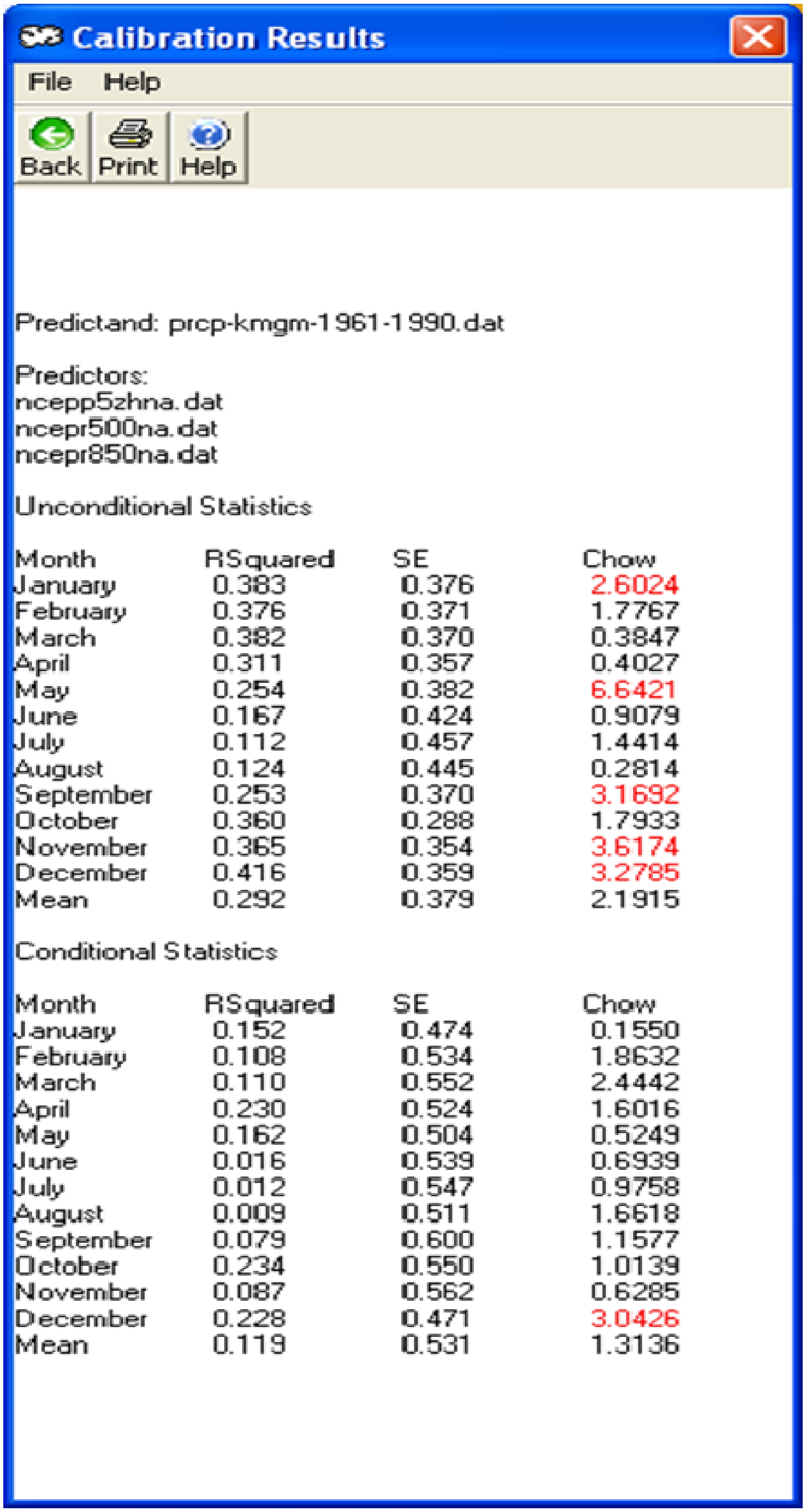
Calibration Results

File Help

Back Print Help

Predictand: prcp-kmgm-1961-1990.dat

Predictors:
ncepp5zhna.dat
ncepr500na.dat
ncepr850na.dat

Unconditional Statistics

Month	RSquared	SE	Chow
January	0.383	0.376	2.6024
February	0.376	0.371	1.7767
March	0.382	0.370	0.3847
April	0.311	0.357	0.4027
May	0.254	0.382	6.6421
June	0.167	0.424	0.9079
July	0.112	0.457	1.4414
August	0.124	0.445	0.2814
September	0.253	0.370	3.1692
October	0.360	0.288	1.7933
November	0.365	0.354	3.6174
December	0.416	0.359	3.2785
Mean	0.292	0.379	2.1915

Conditional Statistics

Month	RSquared	SE	Chow
January	0.152	0.474	0.1550
February	0.108	0.534	1.8632
March	0.110	0.552	2.4442
April	0.230	0.524	1.6016
May	0.162	0.504	0.5249
June	0.016	0.539	0.6939
July	0.012	0.547	0.9758
August	0.009	0.511	1.6618
September	0.079	0.600	1.1577
October	0.234	0.550	1.0139
November	0.087	0.562	0.6285
December	0.228	0.471	3.0426
Mean	0.119	0.531	1.3136

Fig. A.3 Calibration result for precipitation with selected predictors (p5zh, r500, and r850)

PCPN61-75 - WordPad

```
3
 12
 366
1/1/1961
 50769
1/1/1961
 5478
#TRUE#
2
 1
False
prcp-kmgm-1961-1990.dat
ncepp5zhna.dat
nceps500na.dat
nceps850na.dat
0.593     -0.036     0.160     0.271     0.000     0.405
0.561     -0.050     0.200     0.194     0.000     0.384
0.518     -0.037     0.191     0.208     0.000     0.396
0.340     -0.082     0.131     0.154     0.000     0.300
0.290     -0.117     0.132     0.135     0.000     0.240
0.208     -0.160     0.136     0.115     0.000     0.180
0.202     -0.144     0.112     0.104     0.000     0.089
0.064     -0.102     0.099     0.198     0.000     0.120
0.080     -0.127     0.123     0.123     0.000     0.263
0.206     -0.098     0.138     0.063     0.000     0.337
0.426     -0.101     0.116     0.179     0.000     0.372
0.475     -0.066     0.159     0.176     0.000     0.396
1.470     1.000      -0.093    0.174     0.093     0.473
1.608     1.000      -0.082    0.196     0.130     0.519
1.621     1.000      -0.071    0.141     0.156     0.551
1.409     1.000      -0.291    0.166     0.151     0.515
1.317     1.000      -0.165    0.120     0.128     0.508
1.245     1.000      -0.104    -0.041    0.360     0.531
1.538     1.000      -0.039    0.041     -0.006    0.548
1.289     1.000      -0.106    -0.094    0.281     0.504
1.335     1.000      0.026     0.142     0.126     0.600
1.141     1.000      -0.249    0.071     0.275     0.541
1.361     1.000      -0.148    0.082     0.160     0.549
1.555     1.000      -0.075    0.211     0.146     0.462
C:\Documents and Settings\szs0041\My Documents\My Dropbox\Sushban\Downscale\Preci
```

For Help, press F1   NUM

Fig. A.4 Parameter file generated by SDSM for downscaling precipitation

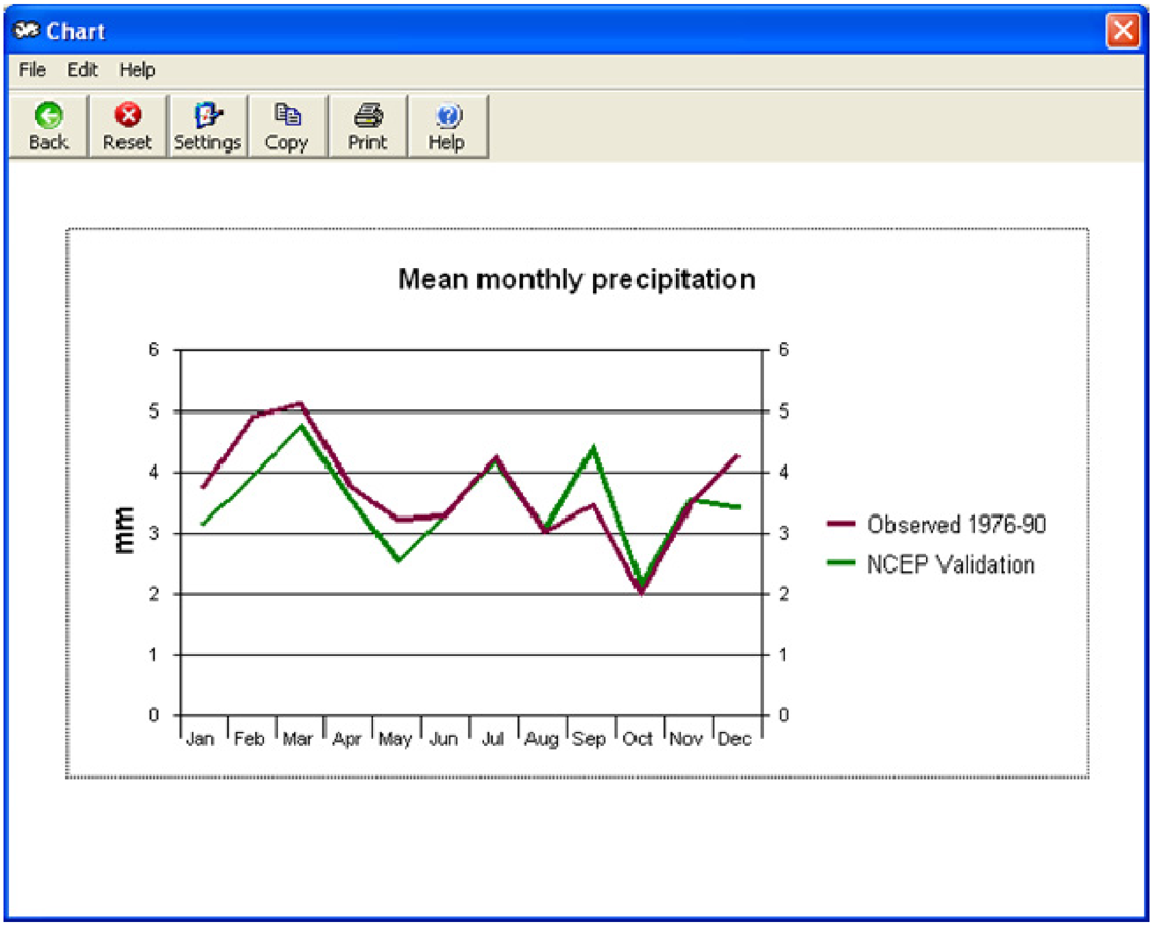

Fig. A.5 Mean monthly precipitation for observed and downscaled results for validation

Appendix B. Land Use Change Impact: Statistical Summary

Table B.1 Monthly Average of Daily Flow and Standard Dev. for Land Use Scenarios

	Average flow (m^3/s)			Standard Deviation (m^3/s)		
	Baseline	2001	2008	1991	2001	2008
Jan	10.64	10.63	10.60	15.59	15.47	15.25
Feb	12.63	12.62	12.57	18.00	17.77	17.44
Mar	14.26	14.23	14.17	30.74	30.57	30.27
Apr	10.15	10.20	10.23	18.76	18.72	18.61
May	6.51	6.58	6.65	5.06	5.06	5.00
Jun	6.68	6.74	6.81	11.21	11.19	11.11
Jul	5.75	5.82	5.89	6.70	6.69	6.67
Aug	4.69	4.74	4.81	3.50	3.60	3.72
Sep	4.08	4.16	4.24	1.88	2.02	2.26
Oct	4.36	4.43	4.52	3.43	3.56	3.72
Nov	6.29	6.35	6.42	8.64	8.53	8.41
Dec	9.27	9.27	9.26	13.89	13.69	13.39

Table B.2 Relative Change in Monthly Average of Daily Flow from the Baseline

	Relative Change (m^3/s)		Relative Change (%)	
	2001	2008	2001	2008
Jan	0.00	-0.03	-0.04	-0.31
Feb	-0.01	-0.06	-0.11	-0.45
Mar	-0.03	-0.09	-0.23	-0.64
Apr	0.04	0.08	0.41	0.76
May	0.06	0.13	0.96	2.05
Jun	0.06	0.13	0.95	2.01
Jul	0.07	0.15	1.17	2.54
Aug	0.06	0.12	1.23	2.64
Sep	0.07	0.16	1.76	3.89
Oct	0.07	0.16	1.66	3.57
Nov	0.06	0.14	0.99	2.21
Dec	0.01	-0.01	0.06	-0.07

Table B.3 Monthly Average of Daily Water Temperature and Standard Deviation for Land Use Scenarios

	Average temperature (°C)			Standard Deviation (°C)		
	Baseline	2001	2008	1991	2001	2008
Jan	8.76	8.76	8.77	3.91	3.91	3.92
Feb	11.11	11.11	11.12	3.53	3.53	3.53
Mar	15.06	15.07	15.07	3.55	3.55	3.55
Apr	19.37	19.38	19.38	3.01	3.01	3.01
May	24.42	24.42	24.42	2.41	2.41	2.41
Jun	28.48	28.48	28.47	1.98	1.98	1.99
Jul	30.02	30.01	30.00	1.42	1.43	1.44
Aug	29.93	29.93	29.92	1.62	1.62	1.63
Sep	26.73	26.72	26.72	2.46	2.47	2.47
Oct	20.42	20.42	20.42	3.24	3.24	3.24
Nov	14.70	14.71	14.73	3.23	3.23	3.23
Dec	10.12	10.12	10.13	3.92	3.92	3.91

Table B.4 Relative Change in Monthly Average of Daily Water Temperature from the Baseline

	Relative Change (°C)		Relative Change (%)	
	2001	2008	2001	2008
Jan	0.01	0.02	0.08	0.18
Feb	0.01	0.02	0.07	0.14
Mar	0.01	0.01	0.06	0.08
Apr	0.01	0.01	0.03	0.05
May	0.00	0.00	0.01	0.01
Jun	0.00	0.00	0.00	-0.01
Jul	-0.01	-0.02	-0.02	-0.05
Aug	-0.01	-0.01	-0.02	-0.04
Sep	-0.01	-0.01	-0.02	-0.04
Oct	0.00	0.00	0.00	0.01
Nov	0.01	0.02	0.06	0.15
Dec	0.01	0.02	0.06	0.18

Table B.5 Monthly Average of Daily Surface DO and Standard Deviation for Land Use Scenarios

	Average DO (mg/l)			Standard Deviation (mg/l)		
	Baseline	2001	2008	1991	2001	2008
Jan	10.39	10.39	10.37	0.92	0.92	0.92
Feb	10.05	10.04	10.02	0.87	0.86	0.85
Mar	9.23	9.22	9.21	0.78	0.78	0.78
Apr	8.45	8.47	8.49	0.70	0.71	0.72
May	8.07	8.12	8.18	1.12	1.15	1.19
Jun	8.16	8.25	8.29	1.21	1.21	1.22
Jul	7.46	7.47	7.49	0.96	0.97	0.97
Aug	7.54	7.56	7.60	1.19	1.20	1.20
Sep	8.53	8.54	8.57	0.99	0.98	0.98
Oct	8.06	8.06	8.07	0.52	0.51	0.51
Nov	8.76	8.75	8.74	0.71	0.70	0.70
Dec	9.92	9.91	9.90	0.97	0.97	0.95

Table B.6 Relative Change in Monthly Average of Daily Surface DO from the Baseline

	Relative Change (mg/l)		Relative Change (%)	
	2001	2008	2001	2008
Jan	-0.01	-0.02	-0.07	-0.22
Feb	-0.01	-0.03	-0.10	-0.28
Mar	0.00	-0.01	-0.04	-0.15
Apr	0.02	0.03	0.25	0.41
May	0.05	0.11	0.64	1.35
Jun	0.09	0.14	1.09	1.66
Jul	0.01	0.03	0.15	0.44
Aug	0.01	0.06	0.19	0.74
Sep	0.01	0.04	0.10	0.50
Oct	0.00	0.01	0.03	0.18
Nov	-0.01	-0.02	-0.09	-0.25
Dec	-0.01	-0.02	-0.06	-0.22

Table B.7 Monthly Average of Daily TP and Standard Deviation for Land Use Scenarios

	Average TP (mg/l)			Standard Deviation (mg/l)		
	Baseline	2001	2008	1991	2001	2008
Jan	0.070	0.074	0.080	0.036	0.039	0.043
Feb	0.066	0.070	0.075	0.031	0.033	0.035
Mar	0.067	0.070	0.076	0.026	0.028	0.031
Apr	0.066	0.070	0.076	0.021	0.022	0.025
May	0.074	0.078	0.085	0.018	0.020	0.023
Jun	0.083	0.087	0.093	0.020	0.022	0.025
Jul	0.087	0.091	0.098	0.026	0.027	0.031
Aug	0.093	0.097	0.105	0.030	0.032	0.036
Sep	0.100	0.104	0.112	0.029	0.030	0.034
Oct	0.102	0.106	0.114	0.033	0.035	0.038
Nov	0.095	0.100	0.108	0.041	0.043	0.048
Dec	0.080	0.084	0.090	0.041	0.043	0.048

Table B.8 Relative Change in Monthly Average of Daily TP from the Baseline

	Relative Change (mg/l)		Relative Change (%)	
	2001	2008	2001	2008
Jan	0.004	0.010	5.87	14.41
Feb	0.003	0.009	5.16	12.98
Mar	0.004	0.009	5.25	13.87
Apr	0.004	0.010	5.58	15.37
May	0.004	0.010	5.17	14.15
Jun	0.004	0.011	4.64	12.73
Jul	0.004	0.011	4.80	13.07
Aug	0.004	0.012	4.56	12.62
Sep	0.004	0.012	4.23	12.00
Oct	0.004	0.011	3.87	11.18
Nov	0.005	0.012	5.11	13.00
Dec	0.004	0.010	5.06	12.96

Table B.9 Monthly Average of Daily TN and Standard Deviation for Land Use Scenarios

	Average TN (mg/l)			Standard Deviation (mg/l)		
	Baseline	2001	2008	1991	2001	2008
Jan	2.28	2.33	2.40	0.74	0.75	0.78
Feb	2.13	2.18	2.26	0.72	0.74	0.77
Mar	2.06	2.11	2.19	0.65	0.66	0.69
Apr	2.24	2.29	2.38	0.66	0.67	0.72
May	2.43	2.50	2.59	0.65	0.66	0.69
Jun	2.57	2.63	2.72	0.70	0.71	0.76
Jul	2.63	2.69	2.77	0.74	0.75	0.79
Aug	2.81	2.88	2.97	0.76	0.78	0.82
Sep	2.92	2.98	3.05	0.70	0.71	0.75
Oct	2.94	2.99	3.06	0.70	0.71	0.75
Nov	2.84	2.89	2.95	0.77	0.79	0.84
Dec	2.51	2.56	2.62	0.83	0.83	0.85

Table B.10 Relative Change in Monthly Average of Daily TN from the Baseline

	Relative Change (mg/l)		Relative Change (%)	
	2001	2008	2001	2008
Jan	0.05	0.13	2.33	5.59
Feb	0.05	0.13	2.30	5.94
Mar	0.05	0.13	2.52	6.47
Apr	0.06	0.15	2.58	6.53
May	0.06	0.15	2.49	6.33
Jun	0.06	0.15	2.38	5.97
Jul	0.06	0.14	2.16	5.28
Aug	0.07	0.16	2.33	5.53
Sep	0.06	0.14	2.02	4.66
Oct	0.05	0.12	1.73	3.98
Nov	0.05	0.11	1.82	4.00
Dec	0.05	0.11	1.92	4.36

Table B.11 Monthly Average of Daily Chlorophyll- a Concentration and Standard Deviation for Land Use Scenarios

	Average Chl-a (µg/l)			Standard Deviation (µg/l)		
	Baseline	2001	2008	1991	2001	2008
Jan	0.26	0.25	0.24	1.82	1.70	1.52
Feb	0.56	0.52	0.47	3.22	2.97	2.57
Mar	0.05	0.05	0.05	0.03	0.03	0.03
Apr	1.60	1.84	2.04	4.72	5.22	5.62
May	9.45	10.15	10.92	11.90	12.29	12.87
Jun	24.56	26.10	26.95	20.19	20.07	20.22
Jul	20.43	20.70	21.03	16.43	16.62	16.60
Aug	22.31	22.64	23.22	16.70	16.88	16.75
Sep	33.21	33.50	34.07	16.49	16.45	16.36
Oct	10.56	10.69	10.94	11.45	11.50	11.71
Nov	1.04	1.01	1.00	3.66	3.61	3.63
Dec	0.05	0.05	0.06	0.10	0.11	0.14

Table B.12 Relative Change in Monthly Average of Daily Chlorophyll-a Concentration from the Baseline

	Relative Change (µg/l)		Relative Change (%)	
	2001	2008	2001	2008
Jan	-0.01	-0.03	-3.71	-10.43
Feb	-0.03	-0.09	-5.79	-16.05
Mar	0.00	0.00	-0.78	0.18
Apr	0.24	0.44	15.04	27.75
May	0.70	1.47	7.46	15.58
Jun	1.54	2.39	6.27	9.74
Jul	0.26	0.60	1.29	2.92
Aug	0.33	0.92	1.47	4.11
Sep	0.28	0.85	0.85	2.57
Oct	0.13	0.38	1.26	3.59
Nov	-0.02	-0.03	-2.16	-3.28
Dec	0.00	0.00	2.46	8.71

Appendix C. Climate Change Impact: Statistical Summary

Table C.1 Monthly Average of Daily Flow (m^3/s)

		HadCM3 A2			HadCM3 B2		
	Baseline	2020s	2050s	2080s	2020s	2050s	2080s
Jan	10.79	7.33	7.03	4.66	7.38	5.83	5.93
Feb	12.63	9.08	7.80	5.86	8.59	6.16	6.91
Mar	14.16	10.93	9.73	6.87	8.90	7.76	9.05
Apr	10.18	9.77	7.24	5.97	7.08	6.84	8.27
May	6.56	5.76	5.10	4.55	5.12	4.78	5.57
Jun	6.92	4.52	4.08	3.41	4.01	3.67	4.23
Jul	5.62	3.66	3.29	2.84	3.46	3.17	3.49
Aug	4.72	3.05	2.83	2.62	3.01	2.75	2.91
Sep	4.14	2.76	2.60	2.21	3.16	2.52	2.62
Oct	4.41	2.67	2.55	2.39	2.76	2.31	2.43
Nov	6.38	3.44	3.30	2.86	3.14	2.73	2.68
Dec	9.42	6.11	6.10	3.56	4.99	4.07	4.38

Table C.2 Standard Deviation of Daily Flow (m^3/s)

		HadCM3 A2			HadCM3 B2		
	Baseline	2020s	2050s	2080s	2020s	2050s	2080s
Jan	16.26	7.00	9.15	4.36	8.14	6.31	5.96
Feb	17.40	11.31	9.46	5.65	12.30	4.01	8.09
Mar	30.71	16.95	13.68	16.24	14.49	10.66	15.98
Apr	18.80	14.52	5.63	4.10	6.78	7.83	10.05
May	5.07	1.82	1.72	2.07	1.73	3.70	3.97
Jun	12.30	2.09	1.41	0.92	1.34	1.08	1.25
Jul	4.50	1.06	0.91	0.76	1.10	0.98	1.31
Aug	3.54	0.74	0.75	0.91	0.93	0.86	0.85
Sep	1.97	0.92	1.20	0.76	2.39	1.09	0.76
Oct	3.51	0.97	1.24	1.37	1.32	0.79	0.87
Nov	8.68	2.13	3.17	2.02	1.92	1.74	1.23
Dec	14.03	5.10	8.50	2.47	4.89	3.35	3.58

Table C.3 Relative Change in Monthly Average of Daily Flow from the Baseline (m^3/s)

	HadCM3 A2			HadCM3 B2		
	2020s	2050s	2080s	2020s	2050s	2080s
Jan	-3.46	-3.76	-6.13	-3.41	-4.96	-4.87
Feb	-3.55	-4.83	-6.77	-4.04	-6.48	-5.73
Mar	-3.22	-4.42	-7.28	-5.26	-6.40	-5.11
Apr	-0.41	-2.95	-4.22	-3.10	-3.35	-1.91
May	-0.79	-1.46	-2.00	-1.44	-1.77	-0.99
Jun	-2.40	-2.85	-3.51	-2.91	-3.25	-2.69
Jul	-1.96	-2.32	-2.78	-2.16	-2.45	-2.13
Aug	-1.67	-1.89	-2.10	-1.72	-1.98	-1.81
Sep	-1.38	-1.54	-1.93	-0.98	-1.62	-1.52
Oct	-1.74	-1.86	-2.02	-1.65	-2.10	-1.98
Nov	-2.94	-3.09	-3.52	-3.24	-3.65	-3.70
Dec	-3.31	-3.33	-5.86	-4.43	-5.35	-5.04

Table C.4 Relative Change in Monthly Average of Daily Flow from the Baseline (%)

	HadCM3 A2			HadCM3 B2		
	2020s	2050s	2080s	2020s	2050s	2080s
Jan	-32.09	-34.87	-56.78	-31.62	-45.94	-45.08
Feb	-28.10	-38.24	-53.62	-32.00	-51.25	-45.33
Mar	-22.77	-31.26	-51.44	-37.15	-45.20	-36.07
Apr	-4.06	-28.94	-41.41	-30.43	-32.88	-18.78
May	-12.11	-22.27	-30.57	-21.93	-27.06	-15.10
Jun	-34.73	-41.13	-50.78	-42.04	-47.00	-38.92
Jul	-34.94	-41.37	-49.41	-38.39	-43.61	-37.89
Aug	-35.34	-40.00	-44.43	-36.33	-41.85	-38.33
Sep	-33.37	-37.13	-46.53	-23.63	-39.09	-36.66
Oct	-39.55	-42.20	-45.82	-37.49	-47.62	-44.89
Nov	-46.12	-48.35	-55.22	-50.79	-57.15	-58.05
Dec	-35.13	-35.30	-62.23	-47.02	-56.76	-53.48

Table C.5 Monthly Average of Daily Water Temperature (°C)

		HadCM3 A2			HadCM3 B2		
	Baseline	2020s	2050s	2080s	2020s	2050s	2080s
Jan	8.77	8.30	9.52	10.16	9.10	9.31	9.01
Feb	11.16	10.20	10.87	12.28	10.04	10.87	10.89
Mar	15.17	13.92	14.52	15.67	13.97	14.80	14.92
Apr	19.49	20.00	19.92	21.93	19.61	20.18	20.46
May	24.51	25.46	25.90	27.72	25.10	26.29	26.75
Jun	28.51	28.85	29.96	31.91	29.12	29.24	30.22
Jul	30.04	30.53	31.53	32.94	30.75	31.45	31.98
Aug	29.91	30.80	31.87	33.03	30.77	31.55	32.55
Sep	26.62	28.15	30.23	31.41	28.40	29.24	30.53
Oct	20.33	22.22	23.53	25.82	22.12	23.67	25.03
Nov	14.63	16.15	17.05	18.82	15.81	16.54	17.99
Dec	10.07	10.48	11.48	12.34	10.40	11.34	11.75

Table C.6 Standard Deviation of Daily Water Temperature (°C)

		HadCM3 A2			HadCM3 B2		
	Baseline	2020s	2050s	2080s	2020s	2050s	2080s
Jan	3.91	2.99	3.33	3.20	3.52	3.49	3.05
Feb	3.53	3.31	3.07	3.50	3.51	3.53	3.72
Mar	3.54	3.52	3.56	3.72	3.30	3.69	3.68
Apr	3.01	3.41	3.60	3.55	3.23	3.15	3.63
May	2.42	2.63	2.75	2.83	2.71	2.50	2.94
Jun	1.98	2.13	2.23	2.00	1.94	2.09	1.90
Jul	1.42	1.30	1.31	1.18	1.23	1.08	1.20
Aug	1.62	1.37	1.29	1.18	1.35	1.28	1.27
Sep	2.48	2.55	2.26	2.46	2.53	2.38	2.15
Oct	3.23	3.45	3.33	3.22	3.25	2.99	3.46
Nov	3.23	3.48	3.51	3.93	3.43	3.78	3.66
Dec	3.90	3.32	3.38	3.62	3.35	3.50	3.25

Table C.7 Relative Change in Monthly Average of Daily Water Temperature (°C)

	HadCM3 A2			HadCM3 B2		
	2020s	2050s	2080s	2020s	2050s	2080s
Jan	-0.47	0.76	1.39	0.33	0.54	0.24
Feb	-0.96	-0.29	1.12	-1.12	-0.30	-0.27
Mar	-1.26	-0.65	0.49	-1.20	-0.38	-0.26
Apr	0.51	0.43	2.45	0.13	0.69	0.98
May	0.95	1.39	3.21	0.59	1.78	2.24
Jun	0.33	1.45	3.40	0.61	0.72	1.71
Jul	0.49	1.49	2.90	0.71	1.41	1.95
Aug	0.89	1.97	3.12	0.86	1.64	2.64
Sep	1.53	3.61	4.79	1.78	2.61	3.91
Oct	1.89	3.20	5.49	1.79	3.35	4.70
Nov	1.52	2.42	4.18	1.18	1.91	3.36
Dec	0.40	1.41	2.26	0.32	1.26	1.68

Table C.8 Relative Change in Monthly Average of Daily Water Temperature (%)

	HadCM3 A2			HadCM3 B2		
	2020s	2050s	2080s	2020s	2050s	2080s
Jan	-5.38	8.63	15.84	3.74	6.16	2.77
Feb	-8.62	-2.57	9.99	-10.01	-2.66	-2.41
Mar	-8.29	-4.31	3.26	-7.92	-2.47	-1.69
Apr	2.63	2.23	12.56	0.64	3.55	5.01
May	3.89	5.67	13.10	2.41	7.25	9.12
Jun	1.17	5.07	11.93	2.14	2.54	6.00
Jul	1.64	4.96	9.64	2.37	4.68	6.48
Aug	2.97	6.57	10.43	2.87	5.48	8.84
Sep	5.74	13.54	18.00	6.69	9.82	14.70
Oct	9.29	15.73	27.00	8.80	16.45	23.12
Nov	10.39	16.54	28.60	8.08	13.02	22.96
Dec	3.99	13.97	22.47	3.21	12.51	16.63

Table C.9 Monthly Average of Daily Surface DO (mg/l)

	Baseline	HadCM3 A2			HadCM3 B2		
		2020s	2050s	2080s	2020s	2050s	2080s
Jan	10.38	10.45	10.16	9.75	10.31	10.11	10.17
Feb	10.02	10.22	10.01	9.50	10.31	10.01	9.97
Mar	9.20	9.49	9.28	8.92	9.41	9.16	9.19
Apr	8.43	8.28	8.22	8.04	8.40	8.30	8.23
May	8.02	7.73	7.87	7.77	7.96	7.97	7.52
Jun	8.22	8.36	7.84	6.81	8.51	8.54	7.68
Jul	7.40	7.75	7.01	5.98	7.59	7.15	6.62
Aug	7.45	7.54	6.77	5.85	7.61	7.06	6.22
Sep	8.46	8.48	7.47	6.59	8.18	7.99	7.22
Oct	8.04	8.09	8.15	8.01	8.09	8.18	8.09
Nov	8.77	8.36	8.14	7.90	8.33	8.20	7.94
Dec	9.93	9.74	9.41	9.06	9.67	9.35	9.28

Table C.10 Standard Deviation of Daily Surface DO (mg/l)

	Baseline	HadCM3 A2			HadCM3 B2		
		2020s	2050s	2080s	2020s	2050s	2080s
Jan	0.91	0.77	0.81	0.72	0.95	0.80	0.69
Feb	0.86	0.83	0.90	0.83	1.16	1.12	0.98
Mar	0.77	0.77	0.72	0.84	0.81	0.78	0.76
Apr	0.70	0.65	0.64	0.91	0.77	0.92	0.79
May	1.10	0.97	1.12	1.30	1.25	1.31	1.00
Jun	1.22	1.13	1.31	1.23	1.21	1.19	1.18
Jul	0.97	0.95	0.94	0.67	0.92	0.81	0.79
Aug	1.19	1.01	0.86	0.52	1.06	0.96	0.71
Sep	1.03	0.96	1.15	1.35	1.03	1.24	1.31
Oct	0.52	0.50	0.54	0.80	0.49	0.54	0.69
Nov	0.71	0.64	0.57	0.54	0.59	0.61	0.53
Dec	0.96	0.77	0.66	0.75	0.85	0.72	0.73

Table C.11 Relative Change in Monthly Average of Daily Surface DO (mg/l)

	HadCM3 A2			HadCM3 B2		
	2020s	2050s	2080s	2020s	2050s	2080s
Jan	0.07	-0.22	-0.62	-0.07	-0.27	-0.21
Feb	0.20	-0.01	-0.52	0.29	-0.01	-0.05
Mar	0.28	0.08	-0.28	0.21	-0.04	-0.01
Apr	-0.15	-0.21	-0.39	-0.03	-0.13	-0.20
May	-0.29	-0.15	-0.25	-0.06	-0.05	-0.51
Jun	0.14	-0.38	-1.41	0.29	0.32	-0.54
Jul	0.35	-0.39	-1.42	0.18	-0.26	-0.79
Aug	0.09	-0.68	-1.60	0.17	-0.39	-1.23
Sep	0.02	-1.00	-1.87	-0.29	-0.47	-1.24
Oct	0.05	0.11	-0.03	0.05	0.14	0.05
Nov	-0.41	-0.63	-0.88	-0.44	-0.57	-0.83
Dec	-0.18	-0.52	-0.87	-0.26	-0.58	-0.64

Table C.12 Relative Change in Monthly Average of Daily Surface DO (%)

	HadCM3 A2			HadCM3 B2		
	2020s	2050s	2080s	2020s	2050s	2080s
Jan	0.66	-2.10	-6.02	-0.63	-2.59	-2.04
Feb	1.95	-0.10	-5.16	2.86	-0.15	-0.53
Mar	3.07	0.85	-3.05	2.25	-0.43	-0.16
Apr	-1.75	-2.46	-4.62	-0.35	-1.57	-2.35
May	-3.60	-1.89	-3.16	-0.79	-0.61	-6.33
Jun	1.74	-4.57	-17.19	3.57	3.85	-6.61
Jul	4.70	-5.27	-19.19	2.49	-3.51	-10.65
Aug	1.26	-9.11	-21.51	2.23	-5.17	-16.49
Sep	0.20	-11.76	-22.12	-3.37	-5.59	-14.71
Oct	0.63	1.34	-0.32	0.58	1.73	0.66
Nov	-4.67	-7.21	-9.98	-5.03	-6.53	-9.43
Dec	-1.84	-5.22	-8.72	-2.60	-5.81	-6.49

Table C.13 Monthly Average of Daily TP concentration (mg/l)

	Baseline	HadCM3 A2			HadCM3 B2		
		2020s	2050s	2080s	2020s	2050s	2080s
Jan	0.080	0.093	0.106	0.141	0.116	0.123	0.106
Feb	0.079	0.090	0.098	0.134	0.112	0.113	0.103
Mar	0.080	0.091	0.093	0.124	0.102	0.114	0.095
Apr	0.075	0.083	0.089	0.112	0.098	0.108	0.094
May	0.080	0.084	0.093	0.116	0.099	0.113	0.097
Jun	0.089	0.100	0.109	0.135	0.114	0.129	0.109
Jul	0.092	0.113	0.126	0.158	0.130	0.144	0.125
Aug	0.097	0.129	0.141	0.173	0.142	0.162	0.143
Sep	0.104	0.141	0.156	0.194	0.150	0.175	0.156
Oct	0.106	0.149	0.163	0.196	0.159	0.188	0.166
Nov	0.102	0.140	0.158	0.190	0.161	0.186	0.167
Dec	0.089	0.102	0.127	0.165	0.134	0.152	0.130

Table C.14 Standard Deviation of Daily TP concentration (mg/l)

	Baseline	HadCM3 A2			HadCM3 B2		
		2020s	2050s	2080s	2020s	2050s	2080s
Jan	0.039	0.030	0.037	0.047	0.037	0.038	0.036
Feb	0.035	0.031	0.037	0.045	0.035	0.033	0.029
Mar	0.037	0.035	0.038	0.042	0.031	0.035	0.029
Apr	0.028	0.026	0.029	0.030	0.024	0.034	0.033
May	0.020	0.019	0.023	0.022	0.019	0.031	0.028
Jun	0.022	0.017	0.025	0.028	0.020	0.028	0.023
Jul	0.026	0.020	0.026	0.028	0.023	0.030	0.024
Aug	0.030	0.020	0.025	0.032	0.024	0.033	0.026
Sep	0.029	0.021	0.025	0.034	0.025	0.038	0.025
Oct	0.034	0.028	0.035	0.041	0.033	0.039	0.028
Nov	0.041	0.035	0.040	0.049	0.039	0.045	0.036
Dec	0.043	0.035	0.051	0.051	0.040	0.044	0.039

Table C.15 Relative Change in Monthly Average of Daily TP concentration (mg/l)

	HadCM3 A2			HadCM3 B2		
	2020s	2050s	2080s	2020s	2050s	2080s
Jan	0.013	0.026	0.061	0.036	0.043	0.026
Feb	0.012	0.020	0.055	0.034	0.034	0.024
Mar	0.011	0.013	0.044	0.022	0.034	0.015
Apr	0.009	0.014	0.037	0.023	0.033	0.020
May	0.004	0.013	0.036	0.019	0.033	0.017
Jun	0.010	0.020	0.046	0.025	0.040	0.020
Jul	0.021	0.033	0.065	0.038	0.052	0.032
Aug	0.032	0.044	0.076	0.045	0.065	0.046
Sep	0.037	0.052	0.090	0.046	0.071	0.052
Oct	0.043	0.057	0.090	0.053	0.082	0.060
Nov	0.039	0.056	0.089	0.059	0.085	0.066
Dec	0.014	0.038	0.076	0.045	0.064	0.041

Table C.16 Relative Change in Monthly Average of Daily TP concentration (%)

	HadCM3 A2			HadCM3 B2		
	2020s	2050s	2080s	2020s	2050s	2080s
Jan	16.30	32.19	76.20	45.09	53.18	32.78
Feb	14.68	24.77	70.16	42.55	43.61	30.66
Mar	13.40	16.05	55.20	27.73	42.92	18.43
Apr	11.85	18.98	50.13	30.94	44.88	26.62
May	5.25	16.62	44.46	23.56	41.62	21.34
Jun	11.66	22.11	51.97	27.82	44.82	22.33
Jul	22.73	35.91	70.89	40.95	56.08	34.88
Aug	33.14	45.43	78.57	46.41	66.97	47.32
Sep	35.50	50.10	87.07	44.41	68.45	50.00
Oct	40.33	53.42	84.66	49.96	77.55	57.07
Nov	37.97	55.23	87.37	58.29	83.16	64.72
Dec	15.21	43.03	85.50	50.76	71.49	46.24

Table C.17 Monthly Average of Daily TN concentration (mg/l)

		HadCM3 A2			HadCM3 B2		
	Baseline	2020s	2050s	2080s	2020s	2050s	2080s
Jan	2.57	3.03	3.29	4.26	3.26	3.57	3.49
Feb	2.43	2.90	3.18	4.07	3.16	3.47	3.48
Mar	2.36	2.71	2.95	3.97	3.06	3.36	3.13
Apr	2.56	2.83	3.17	3.96	3.23	3.46	3.27
May	2.78	3.19	3.50	4.30	3.48	3.86	3.61
Jun	2.90	3.53	3.84	4.82	3.82	4.22	3.94
Jul	2.96	3.81	4.18	5.22	4.07	4.47	4.27
Aug	3.15	4.09	4.48	5.38	4.30	4.75	4.63
Sep	3.24	4.28	4.71	5.83	4.33	4.98	4.81
Oct	3.26	4.37	4.74	5.66	4.51	5.13	4.94
Nov	3.13	4.04	4.52	5.40	4.43	4.92	4.84
Dec	2.80	3.28	3.77	4.80	3.80	4.22	4.01

Table C.18 Standard Deviation of Daily TN concentration (mg/l)

		HadCM3 A2			HadCM3 B2		
	Baseline	2020s	2050s	2080s	2020s	2050s	2080s
Jan	0.80	1.03	1.09	1.28	1.04	0.94	0.92
Feb	0.79	0.91	0.99	1.25	0.92	0.85	0.89
Mar	0.71	0.85	0.90	1.15	0.88	0.90	0.93
Apr	0.73	0.79	0.88	1.07	0.87	0.84	0.90
May	0.71	0.84	0.91	1.10	0.82	0.84	0.87
Jun	0.76	0.87	0.97	1.16	0.85	0.86	0.89
Jul	0.79	0.90	0.94	1.15	0.84	0.83	0.93
Aug	0.81	0.89	1.02	1.23	0.86	0.83	0.94
Sep	0.75	0.94	1.02	1.26	0.92	0.94	0.92
Oct	0.74	0.98	1.08	1.45	0.88	0.91	0.93
Nov	0.83	1.02	1.15	1.50	0.91	1.12	1.04
Dec	0.87	1.06	1.33	1.31	0.96	1.08	1.06

Table C.19 Relative Change in Monthly Average of Daily TN concentration (mg/l)

	HadCM3 A2			HadCM3 B2		
	2020s	2050s	2080s	2020s	2050s	2080s
Jan	0.46	0.72	1.70	0.69	1.00	0.92
Feb	0.47	0.74	1.64	0.73	1.04	1.05
Mar	0.35	0.59	1.60	0.69	1.00	0.77
Apr	0.27	0.61	1.39	0.66	0.90	0.71
May	0.41	0.73	1.52	0.70	1.09	0.84
Jun	0.63	0.94	1.92	0.92	1.32	1.05
Jul	0.85	1.22	2.25	1.11	1.50	1.31
Aug	0.95	1.34	2.23	1.15	1.60	1.48
Sep	1.04	1.48	2.59	1.10	1.75	1.57
Oct	1.11	1.48	2.40	1.26	1.87	1.68
Nov	0.91	1.38	2.27	1.30	1.79	1.71
Dec	0.48	0.97	2.01	1.00	1.42	1.21

Table C.20 Relative Change in Monthly Average of Daily TN concentration (%)

	HadCM3 A2			HadCM3 B2		
	2020s	2050s	2080s	2020s	2050s	2080s
Jan	18.03	28.04	65.97	26.77	38.86	35.69
Feb	19.42	30.63	67.43	29.86	42.81	43.08
Mar	14.92	25.00	67.96	29.38	42.22	32.42
Apr	10.53	23.83	54.43	25.85	35.10	27.75
May	14.85	26.13	54.84	25.36	39.09	30.09
Jun	21.67	32.47	66.10	31.73	45.54	36.07
Jul	28.67	41.05	76.05	37.40	50.67	44.21
Aug	30.14	42.54	70.95	36.70	50.95	47.17
Sep	32.17	45.61	80.01	33.92	53.99	48.50
Oct	34.11	45.42	73.59	38.53	57.49	51.53
Nov	28.92	44.18	72.46	41.53	57.00	54.49
Dec	17.31	34.64	71.75	35.66	50.90	43.25

Table C.21 Monthly Average of Daily Chlorophyll-a (μg/l)

		HadCM3 A2			HadCM3 B2		
	Baseline	2020s	2050s	2080s	2020s	2050s	2080s
Jan	0.25	0.72	1.15	0.63	1.76	0.67	0.39
Feb	0.52	1.25	1.70	0.80	2.81	1.89	1.16
Mar	0.05	0.49	0.07	0.72	0.63	0.50	0.26
Apr	1.52	0.23	0.47	3.73	2.07	2.40	1.90
May	9.15	8.13	11.96	17.97	10.94	15.55	9.01
Jun	25.76	30.66	28.03	19.65	36.88	40.35	25.44
Jul	19.72	31.21	21.89	9.24	29.53	25.97	16.10
Aug	20.98	30.09	20.55	8.06	32.09	25.92	12.89
Sep	32.11	41.92	29.48	17.25	37.34	37.33	23.96
Oct	10.05	22.86	28.42	33.48	22.07	31.33	32.09
Nov	0.95	2.95	3.90	8.08	2.62	4.62	5.76
Dec	0.05	0.08	0.07	0.37	0.43	0.09	0.10

Table C.22 Standard Deviation of Daily Chlorophyll-a (μg/l)

		HadCM3 A2			HadCM3 B2		
	Baseline	2020s	2050s	2080s	2020s	2050s	2080s
Jan	1.73	3.89	3.95	2.75	5.32	2.32	1.47
Feb	3.08	3.84	6.02	3.60	8.20	7.77	4.57
Mar	0.03	2.60	0.18	5.22	3.38	2.47	1.13
Apr	4.85	1.04	1.78	8.71	6.84	8.40	7.77
May	12.02	13.10	14.81	19.19	14.68	17.78	13.09
Jun	20.31	16.50	15.90	15.62	16.57	15.41	15.16
Jul	16.88	12.58	11.93	9.52	12.11	10.94	11.11
Aug	17.27	11.99	10.28	6.73	12.86	12.08	9.14
Sep	17.49	12.51	12.96	16.46	14.54	16.73	15.57
Oct	11.28	14.83	13.95	14.29	14.06	13.79	13.18
Nov	3.59	4.81	4.94	8.50	4.70	6.22	7.01
Dec	0.07	0.27	0.10	1.15	2.48	0.16	0.17

Table C.23 Relative Change in Monthly Average of Daily Chlorophyll-a (μg/l)

	HadCM3 A2			HadCM3 B2		
	2020s	2050s	2080s	2020s	2050s	2080s
Jan	0.48	0.90	0.38	1.51	0.43	0.14
Feb	0.72	1.18	0.28	2.29	1.37	0.64
Mar	0.45	0.03	0.68	0.58	0.46	0.21
Apr	-1.29	-1.05	2.21	0.55	0.88	0.38
May	-1.02	2.80	8.82	1.79	6.40	-0.15
Jun	4.90	2.28	-6.11	11.13	14.60	-0.31
Jul	11.49	2.17	-10.48	9.80	6.25	-3.62
Aug	9.11	-0.44	-12.93	11.10	4.94	-8.10
Sep	9.81	-2.63	-14.85	5.24	5.23	-8.14
Oct	12.80	18.37	23.43	12.02	21.28	22.04
Nov	1.99	2.95	7.12	1.67	3.66	4.80
Dec	0.03	0.02	0.32	0.38	0.04	0.05

Table C.24 Relative Change in Monthly Average of Daily Chlorophyll-a (%)

	HadCM3 A2			HadCM3 B2		
	2020s	2050s	2080s	2020s	2050s	2080s
Jan	194.22	367.35	156.13	613.95	173.13	57.78
Feb	139.37	226.62	54.54	440.17	263.90	122.23
Mar	963.61	58.83	1455.49	1250.46	985.46	450.85
Apr	-84.55	-68.82	145.18	36.14	57.82	24.75
May	-11.17	30.62	96.34	19.54	69.91	-1.63
Jun	19.03	8.85	-23.71	43.21	56.68	-1.22
Jul	58.23	11.00	-53.14	49.71	31.66	-18.38
Aug	43.39	-2.09	-61.59	52.90	23.52	-38.60
Sep	30.56	-8.20	-46.26	16.31	16.28	-25.37
Oct	127.40	182.76	233.13	119.55	211.76	219.32
Nov	209.10	309.06	747.33	174.73	384.29	504.08
Dec	62.59	36.13	644.11	765.99	74.22	91.00